Aspects of non-Fermi-liquid metals

Thesis by

Eugene Pivovarov

In Partial Fulfillment of the Requirements

for the Degree of

Doctor of Philosophy

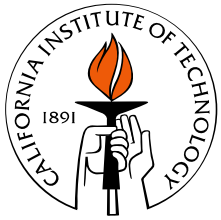

California Institute of Technology

Pasadena, California

2002

(Defended May 22, 2002)

© 2002

Eugene Pivovarov

All Rights Reserved

Acknowledgments

I would like to express my gratitude to Chetan Nayak for his invaluable insight, enthusiasm, and guidance. Special thanks to my advisor John Preskill, Sudip Chakravarty, Steven Kivelson, and Elihu Abrahams for discussions.

I would like to dedicate this thesis to my parents, Simon and Raisa. Thank you for your love and support throughout my years at Caltech.

This work has been supported in part by the U. S. Department of Energy under grant DE-FG03-92-ER 40701.

Abstract

We consider several examples of metallic systems that exhibit non-Fermi-liquid behavior. In these examples the system is not a Fermi liquid due to the presence of a "hidden" order. The primary models are density waves with an odd-frequency-dependent order parameter and density waves with d-wave symmetry. In the first model, the same-time correlation functions vanish and there is a conventional Fermi surface. In the second model, the gap vanishes at the nodes. We derive the phase diagrams and study the thermodynamic and kinetic properties. We also consider the effects of competing orders on the phase diagram when the underlying microscopic interaction has a high symmetry.

Adviser: Prof. John Preskill

Contents

Acknowledgments iii

Abstract iv

Summary 1

1 Introduction 3

1.1 Fermi liquids . . . 3

1.2 Luttinger's theorem . . . 6

1.3 Bose-Einstein condensation and fluctuational superconductivity . . . 9

1.4 Kondo effect . . . 14

1.5 Luttinger liquid . . . 20

1.6 Ginzburg-Landau theory . . . 27

2 Odd-Frequency Density Waves 37

2.1 Introduction . . . 37

2.2 Order parameters and symmetries . . . 38

2.3 Model interaction . . . 40

2.4 Gap equation . . . 45

2.5 Experimental signatures . . . 49

2.6 Discussion . . . 51

3 Competing orders 55

3.1 Model . . . 58

3.2 Critical temperature in mean-field theory . . . 65

3.3 Discussion 70

4 $d_{x^2-y^2}$ Density Wave Order **72**

4.1 Introduction 72

4.2 Model Hamiltonian 78

4.3 Phase diagram 84

4.4 Conclusion 87

5 Conclusion **90**

A Third-order phase transition **93**

B Odd-frequency superconductivity **97**

C Integral evaluation **100**

D Computation of the phase diagram in the $SU(4)$-symmetric model **102**

List of Figures

1.1 Kondo effect. 14
1.2 Self-energy for Kondo effect in Born approximation. 15

2.1 Feynman diagram that induces odd-frequency density wave. 42
2.2 Phase diagram of odd-frequency density wave. 48
2.3 Odd-frequency order parameter. 49
2.4 Condensation energy. 51
2.5 Resistivity in odd-frequency density wave phase. 52

3.1 Two-dimensional bilayer lattice. 56
3.2 Phase diagram in the $SU(4)$-symmetric model. 68
3.3 Temperature dependence of chemical potential. 69

4.1 Phase diagram of the High-T_c cuprates. 72
4.2 Orbital currents in $d_{x^2-y^2}$-density-wave phase. 74
4.3 Phase diagram including $d_{x^2-y^2}$-density wave phase. (I) 84
4.4 Phase diagram including $d_{x^2-y^2}$-density wave phase. (II) 85
4.5 Phase diagram for the model that shows absence of DDW phase. . . . 86

A.1 Condensation energy for third-order phase transition. 96

List of Tables

3.1 Classification of the eigenstates of $\hat{\mathcal{H}}_{\text{int}}$. 64

Summary

The development of the Fermi-liquid theory in the late 50's – early 60's was a major advance in physics, which essentially created a new area of research, the modern theory of condensed matter. Fermi-liquid theory successfully described the properties of a vast majority of metals and metallic alloys. Its development was closely related to the investigation into the properties of materials that had non-Fermi-liquid behavior, such as superconductors and charge-density-wave phases.

Recently, experiments in certain metals and alloys showed peculiar behavior that did not agree with Fermi-liquid theory. These materials include "heavy-fermion" alloys that exhibit Kondo effect, two-dimensional electron gas materials, quantum Hall systems, quantum wires, and high-temperature superconductors.

In Chapter 1, we will review the foundations of the Fermi-liquid theory and the basic models that exhibit non-Fermi-liquid behavior in the metallic state, such as Luttinger liquid. We will also review the technique of the derivation of the mean-field theory (or Ginzburg-Landau theory) from the microscopic models, since this technique is extensively used in the subsequent chapters.

In Chapter 2, we will propose a model in which the order parameter depends on frequency. The odd-frequency dependence allows the system to have a normal Fermi surface, while the presence of order leads to the non-Fermi-liquid behavior.

In Chapter 3, we will consider the case when the underlying interaction has a high symmetry. The phase diagrams of such models are usually complicated due to the proximity of several possible phases. In two dimensions, the part of phase diagrams that is above (in temperature) superconducting or antiferromagnetic phases often has a local order that is coupled to strong quantum fluctuations.

Finally, in Chapter 4, we will study the properties of the 'pseudogap' phase in high-T_c cuprates. According to the model, it is described by a density-wave phase with $d_{x^2-y^2}$-wave symmetry, which is metallic, but breaks several discrete symmetries and is not a Fermi liquid.

The appendices include the discussion of the theory of phase transitions of third-order for long-ranged interactions and the FORTRAN code that was extensively used to obtain the phase diagrams in the studied models.

Chapter 1 Introduction

1.1 Fermi liquids

The theoretical models of the interacting electrons that are studied in condensed matter theory include strong interactions between very large (practically infinite) number of particles. However, what is usually measured are the quantities that are macroscopic and vary slowly across the system. One can imagine starting the investigation into the properties of the model with "zooming" into system to the maximum allowed limit (typically, until we can "see" the lattice) and then slowly zooming out, coming to more and more macroscopic description of the model. This is the basic idea of *scaling*. Under scaling the constants characterizing the original microscopic interactions dramatically change so that some of them disappear (these are called *irrelevant*) and some of them get amplified or appear (these are called *relevant*). Obviously, the macroscopic properties of the system depend mostly on relevant interactions. The behavior of the constants under scaling is akin to a mechanical motion in a potential field: there are points of equilibrium which do not change. These points are called *fixed* points. Since the microscopic models change under scaling in such a way that they reach one of the (stable) fixed points at the macroscopic level, the fixed points describe the actual macroscopic behavior of the system that is generic to a large class of microscopic models.

There is a special case, though, namely, interactions which are finite deviations from the fixed points, but which do not change under scaling. These are called *marginal* perturbations and in some cases they simply correspond to different fixed points. In this case the fixed points merge into a fixed line, along which one can move

by varying the marginal coupling.

An example of marginal interactions is forward scattering, in which the initial and final directions of the particles are the same. Another example is the renormalized mass, which, by definition, is the apparent macroscopic mass of the particles. There are also nonforward scattering processes, in which the total momentum of incoming (and hence, outgoing) particles is zero, but the directions of incoming and outgoing particles are different. The nonforward scattering corresponds to the Cooper channel, and it is marginal at the tree level of renormalization group analysis. However, it becomes relevant or irrelevant at higher orders for attractive or repulsive interactions, respectively.

As the forward scattering interactions become fixed points, the physics that they describe becomes Landau's *Fermi liquid theory* [1, 2]. While the original particles in the microscopic models may be strongly interacting, the elementary fermionic excitations of the Fermi liquid are interacting only weakly and most of their properties resemble those of the degenerated Fermi gas (at temperature $T = 0$). The terms that would lead to the finite lifetime of these quasiparticles turn out to be irrelevant, therefore, the quasiparticles have essentially infinite lifetime. As Landau was describing his theory himself, if you very slowly ("adiabatically") turn off the strong interactions in the original model, you will arrive at the description that still correctly predicts many of the macroscopic properties of the system. The nonforward scattering interactions have to be small and irrelevant in Landau's theory and they are being ignored. The forward scattering interaction is called Landau parameter and it is the only interaction in the Fermi liquid theory.

The picture that Fermi-liquid theory is a fixed point for marginal interactions of the model (excluding nonforward ones) is very descriptive. An alternative way to see this theory is that it is a saddle-point of the theory, in which each particle field is duplicated N times and $N \to \infty$ [3]. This allows one to regard Landau's theory as

a quasi-classical limit. Apart from Fermi liquid state, other possible infrared fixed points that have spin rotation and translational symmetries are insulator, superconductor, and (in one dimension) Luttinger liquid.

The Fermi-liquid theory is characterized by a few important features [4, 5]. The ground state corresponds to the occupation by Fermi quasiparticles of all the states below the Fermi surface. The distribution of real particles of the liquid is not Fermi-like, but there is still discontinuity in this distribution at Fermi surface as well. For a system with rotational invariance, it implies that the number of particles and the Fermi momentum do not depend on the interactions in the model. However, most of these particles are not observable and the only meaningful quasiparticles are those near the Fermi surface, i.e., for which $|p - p_F| \lesssim T$, where p is the momentum of the quasiparticles and p_F is the Fermi momentum. The lifetime of the quasiparticles depends on temperature as $\tau \propto T^{-2}$ for $T \ll \varepsilon_F$, where ε_F is the Fermi energy. The entropy and the specific heat are those of an ideal gas of particles with effective mass $m^* = p_F/v_F$, where Fermi velocity is $v_F = [\partial\varepsilon/\partial p]_{p_F}$. The compressibility $(N/m)\,(\partial\mu/\partial N)$ and the magnetic susceptibility χ are always positive. (μ is chemical potential and N is particle number.) Interactions induce the oscillations in the Fermi liquid, which are called *zero sound* modes and which are associated with a pole in the density-density correlation function at $\omega = u_{zs}k$, where u_{zs} is the zero sound velocity.

Fermi-liquid behavior can be destroyed by attractive interactions, leading to to superconducting instability, or by strong repulsive interactions, leading to density-wave instability. Another possibility for a non-Fermi-liquid behavior is that the system is a marginal Fermi liquid [6], such as models with singular bare interaction vertices. In the latter case, the physics is no longer a continuation of the noninteracting problem, but it still retains a lot of Fermi-liquid features. The Kondo problem, discussed in the following section, shows non-Fermi-liquid behavior due to enhanced scattering of the fermion quasiparticles. The presence of bosonic fields can destroy the Fermi

liquid state as well, such as the gauge bosons [7] or Tomonaga-Luttinger bosons, also discussed later in this chapter.

1.2 Luttinger's theorem

In a Fermi liquid, the number of particles per unit volume is related to Fermi energy by the same formula as for a noninteracting gas of Fermi particles:

$$N = \int_{G(0,\mathbf{k})\geq 0} \frac{2d^d\mathbf{k}}{(2\pi)^d}, \tag{1.1}$$

where $G(\omega,\mathbf{k})$ is the Green function. This constitutes *Luttinger's theorem* [8], which can actually be derived from more basic assumptions with respect to the behavior of the Green function [4]. It is valid when, first, at large frequencies the Green function behaves as $G(\omega)\sim\omega^{-1}$, $\omega\to\infty$, second, the poles of $G(\omega,\mathbf{k})$ on the complex frequency plane satisfy the condition $(\mathrm{Re}\,\omega)(\mathrm{Im}\,\omega)<0$, and third, at the Fermi surface (defined as a boundary of the region $G(0,\mathbf{k})\geq 0$) the self-energy has no singularity. In particular, for a noninteracting Fermi gas, $G_0(\omega,\mathbf{k}) = [\omega-\varepsilon(\mathbf{k})+\mu]^{-1}$. When these conditions are satisfied, one can replace the right-hand side in the definition of the particle density

$$N = -2i\lim_{t\to-0}\int \frac{d^{d+1}k}{(2\pi)^{d+1}}\,G(k)\,e^{-i\omega t}, \qquad k=(\omega,\mathbf{k}) \tag{1.2}$$

$$= 2i\int \frac{d^{d+1}k}{(2\pi)^{d+1}}\left(\frac{\partial\ln G}{\partial\omega}+\Sigma\frac{\partial G}{\partial\omega}\right) \tag{1.3}$$

with only first term in Eq. (1.3),

$$2i\int \frac{d^{d+1}k}{(2\pi)^{d+1}}\frac{\partial\ln G}{\partial\omega}, \tag{1.4}$$

so that further integration by parts leads to Eq. (1.1). Here Σ is self-energy.

A different proof of Luttinger's theorem is based on the analysis of density-density correlation function. In this case the Fermi surface is determined as the region where the presence of low-energy particle-hole excitations induces a singularity in the Green function. This approach turns out to be particularly useful in one-dimensional systems, such as Tomonaga-Luttinger liquid [9, 10, 11, 12]. In this case one such low-energy excitation can be constructed explicitly [13] as $\exp\left[(2\pi i/L)\int dx\, xn\,(x)\right]|G\rangle$, where $|G\rangle$ is the ground state, L is the size of the system and $n\,(x)$ is the particle density at coordinate x. Evidently, this state has wavevector $2\pi N/L$ relative to the ground state and this wavevector has to be $2k_F$ because of the associated singularity in the density-density correlation function. This establishes the relation between the Fermi momentum and particle density, which proves the theorem.

However, neither of the proofs above are valid when $G\,(\omega)^{-1}$ has a singularity at Fermi surface. In particular, in a BCS superconductor self-energy is

$$\Sigma = \frac{\Delta^2}{\omega + \xi\,(\mathbf{k}) - i\delta\,\mathrm{sign}\,\xi\,(\mathbf{k})}, \quad \xi = \varepsilon\,(\mathbf{k}) - \mu, \tag{1.5}$$

where Δ is the superconducting gap and $\delta \to +0$, therefore, $G\,(\omega)^{-1} \sim -\Delta^2/\omega$ at $\xi = 0$. Thus, the correct formula for the particle number should include both terms in Eq. (1.3). The second term in this formula becomes a correction to Luttinger's theorem

$$\begin{aligned} N' &= 2i\int \frac{d^{d+1}k}{(2\pi)^{d+1}}\,(G_0 - G) \\ &= -2i\int \frac{d^{d+1}k}{(2\pi)^{d+1}}\,\Sigma G_0 G. \end{aligned} \tag{1.6}$$

Note the importance of the fact that the pole in Eq. (1.5) is in the upper half-plane of the complex plane for $\varepsilon\,(\mathbf{k}) < \mu$. This causes the second term in Eq. (1.3) to make a nonzero contribution. On the contrary, in the case of a charge-density wave,

$\Sigma = \Phi^2/\left[\omega + \xi\left(\mathbf{k}\right) + 2\mu + i\delta \mathrm{sign}\,\xi\left(\mathbf{k}\right)\right]$, where Φ is the charge gap, therefore, the pole has $\mathrm{Im}\,\omega < 0$ for $\xi\left(\mathbf{k}\right) < 0$ and there is no correction to the theorem. As for a BCS superconductor, there *is* such a correction to the right-hand side of Luttinger's theorem Eq. (1.1):

$$\begin{aligned} N' &= \int \frac{d^d\mathbf{k}}{\left(2\pi\right)^d}\left[\mathrm{sign}\,\xi\left(\mathbf{k}\right) - \frac{\xi\left(\mathbf{k}\right)}{\sqrt{\xi\left(\mathbf{k}\right)^2 + \Delta^2}}\right], \\ &= -\int \frac{d^d\mathbf{k}}{\left(2\pi\right)^d}\,\mathrm{sign}\,\xi\left(\mathbf{k}\right)\frac{1}{2}\left[\frac{\Delta}{\xi\left(\mathbf{k}\right)}\right]^2 + \mathcal{O}\left\{\left[\frac{\Delta}{\xi\left(\mathbf{k}\right)}\right]^4\right\}. \end{aligned} \tag{1.7}$$

The expression in the square brackets in the first line of the formula above is just the difference between the occupation numbers in the BCS state and in the normal state, $2\left|v_{\mathbf{k}}\right|^2 - 2\theta_H\left(-\xi\right)$, where θ_H is the Heaviside unit step function and $v_{\mathbf{k}}$ has a usual definition [14]. If the chemical potential is fixed at the center of the band $\mu = 0$, then $N' = 0$ and Luttinger's theorem is exact. If we fix the number of particles instead, then μ will be shifted in the superconducting state and there will be small correction even at half-filling. This correction is also related to the condensation energy at zero temperature $\Delta F\left(\mu\right) = F_s - F_n$, where F_s is free energy in superconducting state and F_n and the normal state:

$$N' = -\frac{\partial}{\partial\mu}\Delta F. \tag{1.8}$$

This means that the correction to the theorem will be largest away from half-filling, in the region where the condensation energy varies most rapidly with chemical potential, which is usually near the bottom of the band or near the quantum critical point.

In a certain aspect this situation is similar to Bose-Einstein condensation. Below the critical temperature the total number of bosons becomes the sum of the number of particles at nonzero momenta and the number of particles at zero momentum, i.e., in the condensate. The fraction of bosons in the condensate is macroscopically large and does not depend directly on the total number of the particles in the system. In our

case, the off-diagonal long range order [15] implies that in the thermodynamic limit the anomalous correlation function $iF^{*}(1,2) = \left\langle N+2 \left| \psi^{\dagger}(1)\,\psi^{\dagger}(2) \right| N \right\rangle \neq 0$, which means that when we add a pair of electrons to the system, there is a finite probability that they will settle in the condensate as a Cooper pair. The condensate amplitude is $\Phi(x) = iF(x,x) = \Delta/g$, where g is the strength of mean-field superconducting coupling constant, and the condensate fraction is [16] $(1/N)\int dx_1 dx_2 \left|F(1,2)\right|^2 \sim \rho(\varepsilon_F)\,\Delta$, where $\rho(\varepsilon)$ is density of states. Therefore, both of them become macroscopic quantities, which leads to the violation of Eq. (1.1). Just like in Bose-Einstein condensate, each Cooper pair has a total momentum zero. However, for the case of a particle-hole condensate, the total momentum of a particle-hole pair is $\mathbf{Q} \neq 0$, which preserves the symmetry of occupation with respect to the center of the band and there is no violation of the theorem.

1.3 Bose-Einstein condensation and fluctuational superconductivity

The fact that BCS ground state is not a Fermi liquid prompts a question: perhaps, it could actually be described as a Bose liquid? Indeed, being a subsystem of two fermions, each Cooper pair has statistical properties of a boson, therefore, it is possible to describe the superconductor at $T = 0$ in terms of a condensed Bose gas of nonoverlapping particles, resemble to diatomic molecules [17]. For most of the known superconductors, it seems like the critical temperature T_c is much lower than the temperature of the Bose-Einstein condensation of the Cooper pairs, which explains why the pairs condense immediately at T_c and always have total momentum zero.

However, one can imagine that electrons bind together into pairs at a higher temperature T_b, but the momentum of the pairs has initially a wide distribution, for example, due to the presence of incoherent pair excitations. These pair excitations

have a usual Bose distribution, but they block the sites available to fermions. Thus, the system may have composite bosons (Cooper pairs) and a gap in the single-fermion excitation spectrum, but the bosons may remain uncondensed. At T_{BEC} a macroscopic fraction of the Cooper pairs undergoes Bose-Einstein condensation and the system becomes superconducting. Hence, for temperatures $T_{BEC} < T < T_b$, the presence of incoherent thermal pair excitations leads to finite resistivity and the system is metallic in this aspect, although it is almost a Bose liquid. The main difference of this state from real Bose liquids is that the composite bosons have a hard core. However, they do not interact much with each other and their hard cores reveal themselves mostly in the collective mode spectrum [18].

In order to have such an intermediate metallic phase, one has to have a sufficiently strong attractive interaction, since for weak attractive interactions there will be only the conventional superconducting phase of BCS type. This is related to the Bose-Einstein condensate (BEC) – BCS crossover [17, 19]. Several authors proposed this crossover as a key to the explanation of the enigmatic properties of the pseudogap [20, 21, 22] and some aspects of bosonic character (such as reduced superfluid density in a microscopic phase separation [23]) in the high-T_c superconductors. Recently it has been argued that the bosons may remain uncondensed at any finite temperature and this has been applied to the model of the pseudogap as well [24].

To understand how Bose-Einstein condensation occurs, let us first consider a simple model of attractive interaction between two free fermions via a delta-function-like potential [19]. The Schrödinger equation in reduced coordinates is

$$\left[-\frac{1}{m}\nabla^2 - V\delta\left(\mathbf{x}\right)\right]\psi\left(\mathbf{x}\right) = -\varepsilon_b\psi\left(\mathbf{x}\right), \tag{1.9}$$

where V is the coupling constant, $\delta\left(\mathbf{x}\right)$ is the delta-function and ε_b is the binding energy. Note that this is *not* a Cooper problem of the pairing of two electrons on

top of the Fermi sea. The solution of this equation can be written for the Fourier-transform of $\psi(\mathbf{x})$:

$$\bar{\psi}(\mathbf{k}) = \frac{V}{2\varepsilon(\mathbf{k}) + \varepsilon_b}\psi(\mathbf{0}). \tag{1.10}$$

Since $\psi(\mathbf{0}) = \int_k \bar{\psi}(\mathbf{k})$, we can express the coupling constant V in terms of binding energy ε_b:

$$\frac{1}{V} = \int \frac{d^d k}{(2\pi)^d} \frac{1}{2\varepsilon(\mathbf{k}) + \varepsilon_b}. \tag{1.11}$$

It is assumed that the bandwidth is finite so that there is no ultraviolet divergence in the integral. If we substitute the latter expression into the gap equation from the BCS theory, we find that

$$\int \frac{d^d k}{(2\pi)^d} \frac{1}{2\varepsilon(\mathbf{k}) + \varepsilon_b} = \frac{1}{2}\int \frac{d^d k}{(2\pi)^d} \frac{1}{\sqrt{[\varepsilon(\mathbf{k}) - \mu]^2 + \Delta^2}}. \tag{1.12}$$

In the limit of strong interaction ($V \to \infty$) both integrals must be small, which is satisfied when

$$\Delta \to 0, \quad \mu \to -\varepsilon_b/2, \quad \varepsilon_b \to \infty. \tag{1.13}$$

This constitutes the strong-coupling BEC limit, in which the fermions are bound together. The fact that the chemical potential μ becomes negative is of significant importance, because it means that the system is substantially far from the Fermi-liquid state. We can regard the fermion pairs as composite bosons, whose spectrum is $E(k) = \varepsilon(\mathbf{k})/2 - \varepsilon_b - 2\mu = \varepsilon(\mathbf{k})/2$. As we can see, the chemical potential for the composite bosons vanishes, which is the condition for their Bose-Einstein condensation in the $\mathbf{k} = 0$ state.

Below the Bose-Einstein condensation temperature the Cooper pairs condense. However, the superconductivity will develop only when ordering occurs globally. It is possible that the superconducting order will develop only locally at first, though. This may happen because the thermal fluctuations may cause the phase of the order

parameter to slip through an integer multiple of 2π, which will cause the dc current to attain a finite value for a finite driving voltage across the sample, i.e., it will result in finite resistivity [25]. The phase slips occur in an area of order of coherence length, where the system becomes almost normal.

In two-dimensional (2-D) case, the normal regions are the cores of the vortices, similar to the vortices in type-II superconductors. In zero magnetic field, the vortices appear in vortex — antivortex pairs so that total flux remains zero. The energy of the attractive interaction within the pair is $E_v(r) = (\kappa\Phi_0^2/8\pi^2\lambda)\ln(r/\xi)$, where $\Phi_0 = hc/2e$, λ is 2-D penetration depth, r is the distance between the vortices, ξ is coherence length and κ is a correction factor of order of one. Hence, the average distance between the vortices is

$$\begin{aligned}\left\langle R^2\right\rangle &\propto \int d^2r\, r^2 e^{-E_v(r)/T} \\ &= \int_\xi^\infty dr\, r^{3-\left(\kappa\Phi_0^2/8\pi^2\lambda\right)/T}.\end{aligned} \tag{1.14}$$

Thus, at temperature

$$T_{KT} = \kappa\frac{\Phi_0^2}{32\pi^2\lambda} \tag{1.15}$$

the vortices become bound, which constitutes Kosterlitz-Thouless transition [26]. Above T_{KT}, the vortices are unbound and can prolifirate. When an unbound vortex passes through the edge of the sample, the phase of the superconducting order parameter slips by 2π there, which leads to finite resistivity.

The existence of finite resistivity for temperatures $T_{KT} < T < T_b$ implies that the superconducting pairing has local amplitude, but the thermal fluctuations of the phase of the order parameter destroy the long-range order completely. In reality, the transition at T_c is not strictly Kosterlitz-Thouless due to the role of third dimension (3-D), which exists in real systems. Weak coupling between the 2-D planes leads to correlated motion of vortices in adjacent planes that form 3-D vortex loops near T_c.

Below T_c these loops are restricted in size and they become arbitrary large at T_c [27]. In Refs. [28, 29, 30, 31] the properties of this intermediate phase with fluctuating superconductivity were studied in the context of the pseudogap regime of high-T_c cuprates.

In the fluctuating superconductivity phase the total vorticity is zero, but the system is full of fluctuating vortex-antivortex pairs. Each of the pairs is surrounded by supercurrents with associated quasiparticle excitation spectrum of BCS type, $\left[\left(\epsilon\left(\mathbf{k}\right)-\mu\right)^2+\Delta\left(\mathbf{k}\right)^2\right]^{1/2}$. These spectra are shifted due to the superfluid motion around the vortices by $\hbar\mathbf{k}\cdot\mathbf{v}_s\left(r\right)$, where r is the distance from the vortex core. The superfluid velocity $\mathbf{v}_s$ decays as $1/r$ away from the core.

The presence of fluctuating superconductivity phase is possible for usual BCS-like interaction, but it is not inevitable. However, it does become inevitable if the system is essentially 2-D and the superconducting transition is associated with spontaneous breaking of a continuous symmetry. According to Mermin-Wagner-Coleman theorem, no such transition is possible at any finite temperature, however, this theorem is applicable neither to Kosterlitz-Thouless type of transition nor to the systems with weak interlayer coupling. One can introduce various symmetry-breaking terms into the Hamiltonian, but generally they will only reduce the symmetry of the model, which still has to be broken spontaneously. For such systems, it should be possible to study the model within mean-field approximation, which will produce the correct estimates for the local (short length-scale) physics, such as the temperature T_b at which the local pairing appears. The spectral properties, being essentially local, should also reveal non-Fermi-liquid features of the state. In particular, Luttinger's theorem appears to be violated due to the presence of the excitation gap in the short scale. The long-range order develops at lower temperature $T_c = T_{KT}$, for which the interlayer coupling plays significant role as well, so that the transition actually belongs to the universality class of 3-D XY rather than of Kosterlitz-Thouless.

1.4 Kondo effect

One of the most important problems in condensed-matter physics that has signatures of non-Fermi-liquid metallic behavior is Kondo effect. This effect is observed in dilute magnetic alloys that consist of a few magnetic impurity atoms, such as Fe or Ni, dissolved in a nonmagnetic metal, such as Cu or Al. In normal Fermi-liquid metals, resistivity slowly decreases with temperature as $1+aT^2$ attaining a finite value at $T = 0$. The Kondo effect is anomalous increase in electrical resistance at low temperatures, which is approximately $\ln(1/T)$ in intermediate regime and $1 - aT^2$ near $T = 0$ (Fig. 1.1). As Kondo [32] proposed, this increase is due to the scattering enhanced by exchange between the conduction electrons and the magnetic impurity atoms.

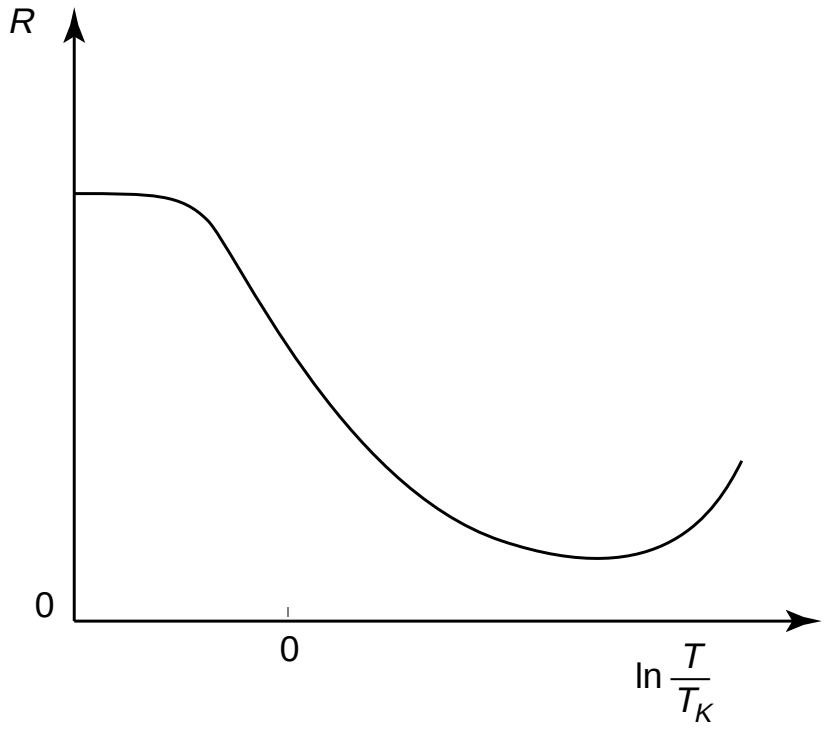

Figure 1.1: Kondo effect.

The Hamiltonian describing such interaction with a single impurity is

$$H = \sum_{\mathbf{k},\alpha} \varepsilon\left(\mathbf{k}\right) c^{\dagger}_{\mathbf{k}\alpha} c_{\mathbf{k}\alpha} + J \sum_{\mathbf{k},\mathbf{k}',\alpha,\alpha'} \left(c^{\dagger}_{\mathbf{k}'\alpha'} \boldsymbol{\sigma}_{\alpha,\alpha'} c_{\mathbf{k}\alpha} \right) \cdot \mathbf{S}, \tag{1.16}$$

where the first term describes the conduction (s) electrons and the second term is the exchange interaction, $\boldsymbol{\sigma}$ are Pauli matrices, $\mathbf{S}$ is the impurity spin 1/2 operator, and $J > 0$ is antiferromagnetic coupling constant. However, it is hard to see why this is actually interaction term, since usually the interactions involve four fermion operators. A naive expectation would be that the interaction term should be regarded as interaction with an external field, which becomes the four-fermion one in second order of perturbation theory, after which it can be treated as usually. However, this is not the case in this problem, as the impurity has an internal degree of freedom (spin), which can flip. As a result, the ordinary "bubble" and three-fermion diagrams do not exhibit any anomaly. The correct treatment is to represent the impurity as a localized fermion by introducing the pseudofermion operators $d^{\dagger}_{\beta}$ and d_{β}. Thus, one should add a "kinetic" term $\sum_{\beta} 0\, d^{\dagger}_{\beta} d_{\beta}$ to the Hamiltoninan and in the interaction term replace $c^{\dagger}_{\mathbf{k}'\alpha'} c_{\mathbf{k}\alpha}$ with $d^{\dagger}_{\beta'} c^{\dagger}_{\mathbf{k}'\alpha'} c_{\mathbf{k}\alpha} d_{\beta}$. If we represent the conducting electrons with solid lines and impurity with dashed lines, then the leading contribution to the self-energy appears to be second order in the interaction vertex (Born approximation), shown on figure 1.2.

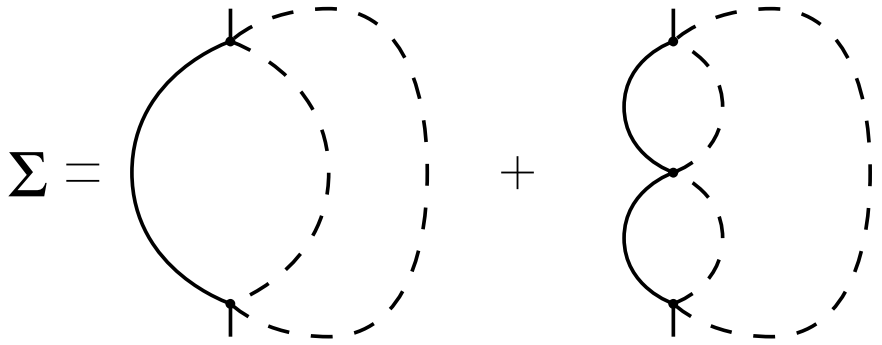

Figure 1.2: Self-energy for Kondo effect in Born approximation.

The physical origin of self-energy can be explained as follows. The incoming s-electron interacts with the impurity spin, as a result of which both the impurity and the electron get flipped. Later, the flipped spin interacts again with the electron, restoring its original spin state. The net effect is that the s-electron is scattered out of its original state, which gives it finite lifetime. If we assume that the density of states is a Lorentzian of width $2W$ with ρ_F being density of states at Fermi level, then for half-filled band we discover a logarithmic contribution to the vertex

$$J\rho_F \ln\left(\frac{W}{2\pi T}\right). \tag{1.17}$$

This contribution correctly predicts the temperature behavior in the "Kondo effect" regime. However, it diverges at $T = 0$ instead of explaining the $1 - aT^2$ behavior at lower temperatures. Abrikosov et al. [4] showed that the leading contribution to the self-energy is given by the "parquet" diagrams, which are obtained from those on Fig. 1.2 by inserting more and more fermion-pseudofermion bubbles into the vertex, and summing over them gives

$$\frac{J}{1 - 2J\rho_F \ln\left(\frac{W}{2\pi T}\right)}. \tag{1.18}$$

The latter formula diverges at finite *Kondo temperature*

$$T_K = \frac{W}{2} e^{-1/2\rho_F J}. \tag{1.19}$$

This means that at T_K the perturbation theory breaks down. The region $T < T_K$ is commonly called a "Kondo problem."

Unlike in the case of phase transitions, when the breakdown of perturbation theory is a signature of the transition, the temperature T_K is critical in a different sense. Below T_K the physics is dominated by the quantum behavior at $T = 0$ so that

the problem simply can no longer be treated perturbatively. However, the "phase transition" occurs only at $T = 0$, at which the conduction electrons screen the local magnetic moments and form the bound singlet states with impurities [33]. At the same time the low energy excitations of the system can be described by a local ("phase shift") Fermi liquid with Fermi temperature of order of T_K [34].

The latter can be seen from the fact that duality transformation permits us to map the strong-coupling regime of the Kondo model onto an Anderson model [35] at weak coupling with renormalized parameters [36]. The Anderson model describes and impurity with on-site interaction, hybridized to a band of conduction electrons:

$$H = \sum_{\alpha} \varepsilon_d d_\alpha^\dagger d_\alpha + U n_{d\uparrow} n_{d\downarrow} + \sum_{\mathbf{k},\alpha} \varepsilon(\mathbf{k})\, c_{\mathbf{k}\alpha}^\dagger c_{\mathbf{k}\alpha} + \sum_{\mathbf{k},\alpha} \left(V_{\mathbf{k}} d_\alpha^\dagger c_{\mathbf{k}\alpha} + V_{\mathbf{k}}^* c_{\mathbf{k}\alpha}^\dagger d_\alpha \right). \quad (1.20)$$

This model is integrable and there is an exact solution [37]. The strong coupling regime of the Kondo model corresponds to Anderson model with

$$U = \frac{3}{4}\frac{t^3}{J^2}, \quad (1.21a)$$

$$\Delta = \frac{3}{8}\frac{t^3}{J}, \quad (1.21b)$$

where hopping $t = W/4$ for one-dimensional case and $\pi \sum_{\mathbf{k}} |V_k|^2 \delta(\omega - \varepsilon_{\mathbf{k}}) \simeq \Delta =$ const is a parameter which controls the width of the virtual bound state resonance at ε_d in the noninteracting ($U = 0$) limit. Similarly, the strong coupling regime ($U \gg \pi\Delta$, $\varepsilon_d < 0$) of Anderson model corresponds to the Kondo model with temperature

$$T_K = U \left(\frac{\Delta}{2U} \right)^{1/2} e^{-(\pi U/8\Delta)+(\pi\Delta/2U)}. \quad (1.22)$$

In the strong coupling regime at $T = 0$, there is scale invariance so that the vertex and the spectral functions of the fermions and localized electrons (pseudofermions) become homogeneous. (The homogeneous functions have a property that $f(x_1, x_2, \ldots) =$

$a^{\gamma} f\left(x_1/a, x_2/a, \ldots\right)$, where the scaling factor a is an arbitrary real number and γ is a scaling exponent.) The pseudofermion propagator is $G\left(\omega\right) \propto \Delta^{-\gamma}\left(\alpha T - i\omega\right)^{\gamma-1}$ for $\omega \ll T \ll \Delta$, where $\gamma > 0$, $\Delta\left(T\right)$ is temperature-dependent and α is a constant. Therefore, the real-time propagator would decay exponentially when $\gamma = 1$ and as a power low when $\gamma \neq 1$. Consequently, the vertex containing $2m$ pseudofermion legs and $2n$ fermion legs becomes $\Gamma_{m,n} \propto \Delta^{m\gamma}\left(\alpha T - i\omega\right)^{1-n-m\gamma}$ and the magnetic susceptibility is $\chi \sim T^{\gamma-1}/\Delta^{\gamma}$. The exact numerical [38] and analytical [39] calculations show that χ remains finite at $T = 0$, since the impurity spins are quenched, so that $\gamma = 1$ and the spin state decays exponentially with finite lifetime Δ^{-1}. The self-consistent evaluation of the pseudofermion self-energy $i\Delta$ determines this quantity, $\Delta\left(T\right) \simeq T_K + \left(\pi\sqrt{3}/4\right)T$ for $T \ll T_K$. This finally leads to Curie-Weiss behavior of magnetic susceptibility

$$\chi \sim \left(T_K + \frac{\pi\sqrt{3}}{4}T\right)^{-1} \tag{1.23}$$

and the correct dependence of resistance on temperature:

$$R \sim 1 - \frac{\pi^2}{4}\frac{T^2}{T_K^2}, \quad T \ll T_K. \tag{1.24}$$

For temperatures above T_K, the resistance remains

$$R \sim \frac{3\pi^2}{16}\ln^{-2}\left(\frac{T}{T_K}\right), \tag{1.25}$$

which should be understood as a crossover from the weak-coupling regime at high temperatures to the strong coupling at low temperatures.

While the original Kondo problem is well understood now, the exact behavior of the lattice model, i.e., the system containing several impurities, remains unknown. One of the reasons for that is the interaction between the localized spins. In the second order of perturbation theory, the spin-spin interaction is described by Ruderman-

Kittel-Kasuya-Yosida (RKKY) Hamiltonian [40],

$$H_{RKKY} = -\frac{9\pi}{8} n_c \frac{J^2}{\varepsilon_F} \sum_{\langle ij \rangle} \frac{\mathbf{S}_i \cdot \mathbf{S}_j}{r_{ij}^3} \left[2k_F \cos\left(2k_F r_{ij}\right) - \frac{1}{r_{ij}} \sin\left(2k_F r_{ij}\right) \right], \qquad (1.26)$$

where n_c is the conduction electron density. This interaction oscillates with distance between the spins due to Friedel oscillations of the spin polarization of conduction electrons induced by a localized spin. To understand which ground state will be favored, it is convenient to study the Fourier transform of the RKKY interaction, which is essentially the susceptibility. If the maximum of the susceptibility is achieved at zero wave vector, the interaction favors ferromagnetic ground state. If it is achieved at wave vector $\mathbf{Q} = (\pi/a, \pi/a)$ (for a two-dimensional lattice with lattice spacing a), the interaction favors antiferromagnetic ground state. In either case, ordering suppresses the Kondo effect. Indeed, the characteristic energy scale of RKKY interaction is $T_{RKKY} = J^2/\varepsilon_F$, which usually dominates over the Kondo temperature, at least in the weak-coupling regime. For example, if we consider just two impurities with antiferromagnetic RKKY coupling, in the ground state they will form a singlet state and will hardly interact with conduction electrons at all.

However, the formation of local singlets between the conduction band electrons and the localized spins in the strong-coupling regime induces quenching of the local moments, which makes the derivation of RKKY Hamiltonian invalid. Thus, the exact behavior of the system becomes dependent on the dimensionality, the strength of the exchange coupling, and the conduction electron density. One of the important questions is whether the change between the regime $T_{RKKY} \ll T_K$ and the regime $T_{RKKY} \gg T_K$ is a transition or a crossover. The recent study of the two-impurity Kondo problem has shown that in the presence of small asymmetry between the channels there is only a crossover between Kondo and RKKY regimes [41].

The electron-electron interaction can induce the opening of several spin-exchange

channels between the local moments and the conduction electrons [42]. In the model that considers a single impurity atom the Kondo effect develops exclusively in the strongest screening channel due to the local symmetry that preserves the channel quantum number of the scattered electrons. However, in a lattice the conduction electrons are allowed to change the channels as they propagate between the impurity sites. This means that the Kondo effect develops coherently in several channels, which is described by the multichannel Kondo problem on a lattice [43]:

$$H = -t \sum_{\lambda=1}^{M} \sum_{\langle ij \rangle} c_{i\alpha}^{(\lambda)\dagger} c_{j\alpha}^{(\lambda)} - \mu \sum_{i} c_{i\alpha}^{(\lambda)\dagger} c_{i\alpha}^{(\lambda)} + J \sum_{\mathbf{k},\mathbf{k}',\alpha,\alpha'} \left(c_{i\alpha}^{(\lambda)\dagger} \boldsymbol{\sigma}_{\alpha,\beta} c_{i\beta}^{(\lambda)} \right) \cdot \mathbf{S}_i. \qquad (1.27)$$

Unlike in a single-channel problem, which exhibits Fermi-liquid behavior in the asymptotic regime when length scales are long compared to v_F/T and time scales are long compared to $1/T_K$, the ground state of the two-channel model has certain non-Fermi-liquid features in the Kondo regime related to the spin excitations [44]. In particular, the spin susceptibility diverges in the limit of large time scales and finite distances [45]. More generally, the non-Fermi-liquid behavior is observed when the number of channels M is larger than $2S$, where S is the spin of the impurity.

1.5 Luttinger liquid

A Luttinger liquid [9, 10, 11, 12] is an important metallic phase that is not a Fermi liquid due to the absence of quasiparticles at Fermi level. Its existence has been proved in one dimension (1-D), but there is still little experimental evidence for Luttinger-liquid behavior in higher-dimensional systems.

Luttinger liquid is a well-known example when renormalization-group approach gives a solution that is qualitatively different from mean-field one. Unlike in Fermi-liquid case, the Luttinger liquid is a fixed point of any repulsive quartic interaction,

which is related to the fact that the number of left- and right-moving fermions is separately conserved. If we compute a correction to the vertex at one-loop level in higher dimensions and discover that so called BCS diagram gives a siginificant contribution, chances are that this contribution is relevant and the ground state of the system is superconducting. The mean-field theory would concentrate on this single type of the diagrams and would estimate the energy of the ground state. In 1-D case, this diagram is precisely cancelled out by "cross-zero-sound" (charge-density wave) one, as a result, the interaction is marginal rather than relevant and the mean-field theory makes totally incorrect predictions, in fact, it breaks down. In higher dimensions the BCS and charge-density-wave instabilities do not cancel each other precisely, therefore, one of them dominates and mean-field theory can concentrate on the leading diagram while neglecting the other.

In 1-D systems the Fermi-liquid state can only correspond to noninteracting fermions. Any *metallic* state with interacting fermions must be Luttinger liquid, therefore, for the general analysis of the properties of the system it is sufficient to consider only weak interactions. The Fermi surface reduces to just two Fermi points, near which there are low energy excitations. Following our experience with Fermi liquids, we should expect that most important physical properties are determined by quasiparticles that exist near the Fermi surface. Since there are only two possible directions for the motion of these excitations, it is convenient to represent electrons near Fermi points as sums of right-moving and left-moving particles. Then the free-electron Hamiltonian for spinless electrons is

$$H_0 = \pi v_F \int dx \left(J_R^2 + J_L^2 \right), \tag{1.28}$$

where the currents for left- and right-moving particles are

$$J_{L,R}(k) = \sqrt{L} \int dx\, e^{-ikx} \psi^{\dagger}_{L,R}(x)\, \psi_{L,R}(x)\,. \tag{1.29}$$

It is clear that the ground state described by such a model is a perfect conductor, since one can move a particle from just below the Fermi surface to just above it at tiny energy cost. A remarkable feature of this Hamiltonian is that it appears to represent the right- and left-moving fermions as totally separate particles. Note that momentum k can be arbitrary, even though the model has been linearized near the Fermi points. The free electron propagators are

$$\left\langle T\psi_{L,R}(t,x)\, \psi^{\dagger}_{L,R}(0) \right\rangle \propto (x \pm v_F t)^{-1}\,, \tag{1.30}$$

whose Fourier transforms are $(\omega \pm v_F k)^{-1}$.

With interaction included, the Hamiltonian becomes

$$H = \int dx \left[\pi v_F \left(J_R^2 + J_L^2\right) + \lambda J_L J_R\right] \tag{1.31}$$

$$= \int dx\, \pi v \left(j_R^2 + j_L^2\right), \tag{1.32}$$

where $j_{L,R} = \cosh(\theta)\, J_{L,R} + \sinh(\theta)\, J_{R,L}$, $\tanh(2\theta) = \lambda/2\pi v_F$, $v = \sqrt{v_F^2 - (\lambda/2\pi)^2}$. The interaction term is actually special, since some of the terms that include different quasiparticles are missing. These terms typically oscillate rapidly with wave vectors of order k_F or involve the derivatives that arise from Taylor expansion of nonlocal interactions. In fact, this model is closely related to the massless Thirring model in quantum field theory, in which the replacement of the fermion field by a boson field leads to a free field theory. It is also exactly soluble [11] by using the bosonization technique.

The bosonization method is based on the idea that in 1-D the correlation func-

tions involving the fermion operators can be represented in terms of the boson operators [46]. Consider the action for the free fermions:

$$S = \int d^2 z \left(\psi_R^\dagger \partial_z \psi_R + \psi_L^\dagger \partial_{\bar{z}} \psi_L \right), \tag{1.33}$$

where $\psi_L(\bar{z})$ and $\psi_R(z)$ are the operators for left- and right-moving particles, $z = x + i\tau$ and τ is imaginary time. A $4N$-point correlation function is

$$\left\langle \psi_R^\dagger(z_1)\,\psi_L(\bar{z}_1)\ldots\psi_R^\dagger(z_N)\,\psi_L(\bar{z}_N)\,\psi_R(z_1')\,\psi_L^\dagger(\bar{z}_1')\ldots\psi_R(z_N')\,\psi_L^\dagger(\bar{z}_N') \right\rangle = \left|\det\left(z_i - z_j'\right)\right|^{-2}, \tag{1.34a}$$

which coinsides with a correlation function involving a bosonic field $\varphi(z)$

$$\left\langle e^{i\varphi(z_1)}\ldots e^{i\varphi(z_N)} e^{-i\varphi\left(z_1'\right)}\ldots e^{-i\varphi\left(z_N'\right)} \right\rangle, \tag{1.34b}$$

where it is assumed that the operators are normal-ordered. The bosons, of course, have a hard core, due to their underlying fermionic nature. Thus, we can define $\psi_{L,R} = \exp(\pm\varphi_{L,R})$, consequently, the density operators for left- and right-movers are

$$j_L = -\frac{1}{2\pi}\partial_{\bar{z}}\varphi_L, \tag{1.35a}$$

$$j_R = -\frac{1}{2\pi}\partial_z\varphi_R. \tag{1.35b}$$

The latter expressions will be valid for the interacting case as well, if one introduces the bosonic fields $\varphi_{L,R}$ as

$$\psi_{L,R} = e^{i\left[\cosh(\theta)\varphi_{L,R} - \sinh(\theta)\varphi_{R,L}\right]}. \tag{1.36}$$

The subsequent computation is straightforward. We find that the low-lying excitations have velocities $\pm v$ and the propagators are

$$\left\langle T\psi_{L,R}\left(t,x\right)\psi_{L,R}^{\dagger}\left(0\right)\right\rangle =\frac{e^{\pm ik_{F}x}}{\left(x\pm vt\right)\left(x^{2}-v^{2}t^{2}\right)^{\gamma}}, \tag{1.37}$$

where $\gamma=\sinh\left(\theta\right)^{2}$ is the anomalous dimension. It can be represented in the form $\gamma=\left(1/4\right)\left(K+K^{-1}-2\right)$, where $K=\exp\left(-2\theta\right)$, so that

$$\frac{v_{F}}{v}=\frac{1}{2}\left(K+\frac{1}{K}\right), \tag{1.38a}$$

$$\frac{\lambda}{2\pi}=\frac{1-K^{2}}{1+K^{2}}. \tag{1.38b}$$

The Fourier transform of the propagators is

$$G\left(\omega,k\right)=\frac{1}{\omega_{0}^{2\gamma}}\frac{\left(v^{2}k^{2}-\omega^{2}\right)^{\gamma}}{\omega\pm vk}. \tag{1.39}$$

From the latter expression it is clear that the Green functions contain no single-particle poles, which means that in the proximity of Fermi points there are no quasi-paticles. The behavior of the system remains qualitatively different from the free-fermion case $\gamma=0$ even in the limit $\gamma\to0$. Apparently, this result would be difficult to prove in conventional perturbation theory.

The occupation number is

$$n\left(k\right)=\frac{1}{2}\mathrm{sign}\ \left(k_{F}-k\right)\left|\frac{k-k_{F}}{k_{0}}\right|^{2\gamma}+\frac{1}{2}\mathrm{sign}\ \left(k_{F}+k\right)\left|\frac{k+k_{F}}{k_{0}}\right|^{2\gamma}, \tag{1.40}$$

where k_0 is a constant. This expression is continuous through the Fermi points for a nonzero interaction constant λ. Note, however, that its derivatives diverge at Fermi points. Consequently, the density of states is $\rho\left(\varepsilon\right)\propto\left(\mu-\varepsilon\right)^{2\gamma}$, which means that the spectral weight near the chemical potential μ is suppressed by the same power law be-

havior as in $n(k) - 1/2$. This power law suppression can be revealed in photoemission and tunneling experiments.

The density-density correlation function has a form

$$\langle \rho(x,t)\,\rho(0)\rangle = \frac{1}{K}\left[\frac{1}{(x-vt)^2} + \frac{1}{(x+vt)^2}\right] + \text{const} \times \frac{\cos(2k_F x)}{(x^2 - v^2t^2)^{(1/K)}}, \tag{1.41}$$

As we can see, for repulsive interactions, the contribution to the density-density correlation funcion at $\pm 2k_F$ falls off slowly due to the modified exponent. For noninteracting electrons $K = 1$.

If we take into account the spins of the fermions, we will discover that the physics remains essentially the same, but spin currents $J_s = J_\uparrow - J_\downarrow$ and charge currents $J_c = J_\uparrow + J_\downarrow$ separate and must be included independently in the Hamiltonian. For free excitations, the correlation function in each sector is $(x \pm v_F t)^{1/2}$, so that the total expression remains Eq. (1.30). Treating interactions becomes more complicated, though. When interactions couple only charge currents, it is somewhat easier to do the calculations, but the charge and spin velocities are no longer the same. In particular, for spin-independent interaction the spin velociy $v_s = v_F$. The bosonization procedure is the same and leads to spinless bosons that have charge and neutral bosons that have spin. The Green function is

$$G_{L,R}(t,x) \propto e^{\mp i k_F x}\left[\frac{1}{(x \pm v_c t)(x \pm v_s t)}\right]^{1/2} \frac{1}{(x^2 - v_c^2 t^2)^\gamma}. \tag{1.42}$$

Let us mention now a few expressions for experimentally observable quantities. The specific heat in 1-D is linear in temperature $\hat{\gamma}T$, where the constant $\hat{\gamma}$ is inversely proportional to the sound velocity. This is the 1-D version of the Debye's law. The ratio of $\hat{\gamma}$ to the corresponding value $\hat{\gamma}_0$ for the noninteracting fermions is

$$\frac{\hat{\gamma}}{\hat{\gamma}_0} = \frac{1}{2}\left(\frac{v_F}{v_c} + \frac{v_F}{v_s}\right). \tag{1.43}$$

The compressibility and spin susceptibility at zero temperature are $\kappa/\kappa_0 = K_c v_F/v_c$ and $\chi/\chi_0 = K_s v_F/v_s$. As we can see, the constants that determine the anomalous dimension in the Green functions also enter the low temperature thermodynamics.

The constant K has generally a physical meaning of conductance. If we imagine that the chemical potential for the right-moving particles has shifted by a small amount $\delta\mu_R$, the system will adjust so that the Hamiltonian will be minimized at new density $n_R + \delta n_R$, where $\delta n_R = (Ke/2\pi v)\,\delta\mu_R$. This extra density carries current δI_R to the right, which corresponds to conductance $G = \delta I_R/\delta\mu_R = Ke^2/h$. For non-interacting fermions, we recover the perfect conductance of the Landauer transport theory, e^2/h per channel. As we can see, interactions in 1-D modify G, since for repulsive interactions $K < 1$. In practice, the applied voltage is coupled to both left and right-moving modes.[1] However, if the piece of 1-D wire is infinitely large, one obtains the same expression for conductance G as given above. For a finite piece of wire of length L between the two Fermi-liquid leads, this expression is valid only for ac conductance with frequency $\omega > v/L$. Evidently, these expressions assume the total absence of impurities. In fact, even a weak impurity potential causes complete backscattering so that the conductance vanishes at zero temperature [47]. Basically, electrons cannot tunnel through the barrier from one semi-infinite Luttinger liquid to another due to vanishing density of states.

Apparently, for 2-D systems the model that is described by interaction that has zero range in y direction and zero hopping in the same direction will be essentially a 1-D Luttinger liquid along x direction and therefore, it will have Luttinger liquid ground state. What if we turn on small hopping along y direction? It turns out that for $\gamma > 1/2$ this perturbation is irrelevant and scales to zero in infrared limit, therefore, the ground state will still be Luttinger liquid [48]. The situation with interactions is more complicated [49]. If interactions merely couple currents along

[1] In some systems, such as those with fractional quantum Hall effect, one can couple to the chiral modes at the edges selectively.

x so that the Hamiltonian can be exactly diagonalized, then such interactions are marginal and still describe a Luttinger liquid. However, so far there have been no convincing evidence that more general interactions between spinful fermions can lead to Luttinger-liquid behavior in two or more dimensions.

1.6 Ginzburg-Landau theory

In the understanding of the mechanism of superconductivity, two theories have played major roles, one suggested by Ginzburg and Landau [50] (GL) and the other by Bardeen, Cooper, and Schrieffer [51] (BCS). The former is a macroscopic model, where the system is described by free energy, which is a function of temperature and chemical potential (or particle number). The latter is a microscopic model, defined by a reduced Hamiltonian at zero temperature. These two models are consistent with each other, as it was shown by Gor'kov [52], who derived the GL theory from BCS.

Unfortunately, his computation is very complicated, therefore, it is rarely reproduced in textbooks. However, the relationship between these two models is of significant importance, since it explains how the same phenomenon can be described at different scales. The technique that is used to derive the macroscopic GL theory from the microscopic BCS model is fundamental and will be used extensively in the following chapters. The goal of this section is to provide a straightforward derivation of the phenomenological GL theory form the microscopic BCS model. We will first derive the GL for a constant order parameter, then find the corrections for space- and time-dependent order parameter, which include the derivatives. Finally, we will consider only these corrections and represent them in terms of vortex currents.

The Hamiltonain in the BCS model is

$$\mathcal{H} = \int \frac{d^d k}{(2\pi)^d} \epsilon(k)\, c^{\alpha\dagger}(k)\, c_\alpha(k) + \int_k \int_{k'} c_\uparrow^\dagger(k)\, c_\downarrow^\dagger(-k)\, V_{kk'} c_\downarrow(-k')\, c_\uparrow(k'), \quad (1.44)$$

where $V_{kk'} = -V$ in a narrow band near the Fermi surface and is zero otherwise. The corresponding action is

$$S = \int d\tau \left\{ \int \frac{d^d k}{(2\pi)^d} \bar{\psi}^\alpha(k) (\partial_\tau + \mu) \psi_\alpha(k) - \mathcal{H}\left[\psi_\alpha, \bar{\psi}_\alpha\right] \right\}. \quad (1.45)$$

We will assume that the interaction is short-ranged in real space, i.e., that it is varying over the region much smaller than $\hbar v_F/V$. The opposite case of a long-ranged interaction is considered in Appendix A and it leads to a third-order phase transition.

Since we are interested in the mean-field theory, the first step is the Hubbard-Stratonovich transformation. Simply speaking, we introduce a new bosonic field $\phi(k)$ such that its equations of motion are

$$\phi = \int \frac{d^d k}{(2\pi)^d} V \psi_\uparrow(k)\, \psi_\downarrow(-k), \quad (1.46a)$$

$$\phi^* = \int \frac{d^d k}{(2\pi)^d} V \bar{\psi}_\downarrow(-k)\, \bar{\psi}_\uparrow(k). \quad (1.46b)$$

The corresponding action,

$$S = \int d\tau \int \frac{d^d k}{(2\pi)^d} \left\{ \bar{\psi}^\alpha(k) (\partial_\tau - \xi(k)) \psi_\alpha(k) - \frac{|\phi|^2}{V} + \int \frac{d^d k'}{(2\pi)^d} \phi(k)\, \bar{\psi}_\uparrow(k')\, \bar{\psi}_\downarrow(-k') + \phi^*(k)\, \psi_\downarrow(-k')\, \psi_\uparrow(k') \right\}, \quad (1.47)$$

is equivalent to the original action of the BCS theory Eq. (1.45). Here $\xi(k) = \epsilon(k) - \mu$. The next step is to integrate out the fermions and to derive the thermodynamic

potential as a function of ϕ. In order to do that, we need to modify Eq. (1.47) so that it will appear bilinear in Fermi fields. Let us define a two-component Fermi field $\Psi_\alpha(k)$:

$$\Psi_\uparrow(k) = \begin{pmatrix} \psi_\uparrow(k) \\ \bar{\psi}_\downarrow(-k) \end{pmatrix}, \ \Psi_\downarrow(-k) = \begin{pmatrix} \psi_\downarrow(-k) \\ \bar{\psi}_\uparrow(k) \end{pmatrix} \tag{1.48}$$

Then, after replacing the time integral with the sum over Matsubara frequencies $\omega_n = (2n+1)\pi T$,

$$S = T\sum_{\omega_n}\int \frac{d^dk}{(2\pi)^d}\Big\{-\frac{|\phi|^2}{V}\frac{\delta_{n,0}}{T^2}+ \int_{k'}(2\pi)^d\bar{\Psi}_\alpha(k',\omega_n)\left(i\omega_n - M(\phi)\right)\Psi_\alpha(k',\omega_n)\Big\}, \tag{1.49}$$

where

$$M(\phi) = \begin{pmatrix} -\xi(k)\,\delta_{kk'} & \phi^*(k) \\ \phi(k) & \xi(k)\,\delta_{kk'} \end{pmatrix}. \tag{1.50}$$

The thermodynamic Gibbs potential is, by definition,

$$F(T,\mu) = -T\ln\int \mathcal{D}\psi\mathcal{D}\bar{\psi}\, e^{S[\psi,\bar{\psi}]}. \tag{1.51}$$

With the help of the Gaussian identity for the fermions, we obtain the expression

$$F = \int \frac{d^dk}{(2\pi)^d}\frac{|\phi|^2}{V} - T\ln\mathrm{Det}\,\left(i\omega_n - M(\phi)\right). \tag{1.52}$$

To evaluate this expression, we substitute Eq. (1.46), i.e., the saddle-point solution. This is equivalent to Hartree-Fock decoupling and represents a mean-field approximation. The eigenvalues of the matrix $i\omega_n - M(\phi)$ are $i\omega_n \pm E(k)$, where $E(k) = \left[\xi(k)^2 + |\phi|^2\right]^{1/2}$. For constant field ϕ, the trace can be calculated in the closed form. Using the identity $\ln\mathrm{Det}\,A = \mathrm{Tr}\ln A$, we derive the thermodynamic

potential per unit volume

$$f = f_0 + \frac{|\phi|^2}{V} - T\sum_{\omega_n}\int \frac{d^dk}{(2\pi)^d}\ln\left(1 + \frac{|\phi|^2}{\omega_n^2 + \xi\left(k\right)^2}\right), \tag{1.53}$$

where f_0 is the value of f for $\phi = 0$,

$$f_0 = -2T\int_k \ln\left\{1 + \exp\left(-\frac{\xi(k)}{T}\right)\right\}. \tag{1.54}$$

Here the factor of two comes from the trace over spins. The frequency sum in Eq. (1.53) can be evaluated, which produces the expression for the free energy in BCS model:

$$f = \frac{|\phi|^2}{V} + \int_k \left\{\xi(k) - 2T\ln\left[2\cosh\left(\frac{E(k)}{2T}\right)\right]\right\}. \tag{1.55}$$

The mean-field solution corresponds to the minimum of free energy so that $\partial f/\partial\phi = 0$. This yields the BCS equation

$$\frac{1}{V} = \int \frac{d^dk}{(2\pi)^d}\frac{1}{2E\left(k\right)}\tanh\left(\frac{E\left(k\right)}{2T}\right). \tag{1.56}$$

Finally, we expand the logarithm in Eq. (1.55). This immediately leads to the expression for the constant part of GL free energy:

$$f = f_0 + a\left|\phi\right|^2 + b\left|\phi\right|^4, \tag{1.57}$$

where

$$a = \frac{1}{V} - \int \frac{d^dk}{(2\pi)^d}\frac{1}{2\xi\left(k\right)}\tanh\left(\frac{\xi\left(k\right)}{2T}\right), \tag{1.58a}$$

$$b = -\int \frac{d^dk}{(2\pi)^d}\frac{1}{2\xi\left(k\right)}\frac{\partial}{\partial\xi}\left[\frac{1}{4\xi\left(k\right)}\tanh\left(\frac{\xi\left(k\right)}{2T}\right)\right]. \tag{1.58b}$$

The parameter $V_{eff} = 1/a$ is sometimes called the "renormalized" coupling constant,

in a sense that expanding Eq. (1.56) in terms of ϕ to the second order leaves the equation with ultraviolet divergence, which can be regularized by introducing a momentum cutoff.

In presence of the electromagnetic field $(\varphi, \mathbf{A})$, the order parameter can no longer be treated as spatially uniform or time-independent. This results in corrections to Eq. (1.57), known as gradient terms in GL theory [53]. In order to find them, we need to expand the logarithm in Eq. (1.53) in terms of the perturbation. If ϕ is finite and the perturbation is $\delta\phi$, this leads to the collective modes in the nonlinear sigma model. However, we are interested in the expansion around $\phi = 0$ when ϕ becomes a function of small frequency and small momentum, $\phi = \phi(\Omega, \mathbf{K})$. In this case the expansion is almost the same as one leading to Eq. (1.57). Let us observe that the second term in Eq. (1.58a) is

$$T\sum_n \int \frac{d^d k}{(2\pi)^d} \frac{1}{i\omega_n + \xi(\mathbf{k})} \frac{1}{i\omega_n - \xi(\mathbf{k})} \tag{1.59}$$

Apparently, in order to take into account the dependence on $(\Omega, \mathbf{K})$, we should replace this expression with

$$T\sum_n \int \frac{d^d k}{(2\pi)^d} \frac{1}{i\omega_n + \xi(\mathbf{k})} \frac{1}{i\omega_n - \Omega - \xi(\mathbf{k}+\mathbf{K})}. \tag{1.60}$$

The latter formula can be expanded in terms of $(\Omega, \mathbf{K})$ and evaluated. Finally, we take into account the presence of electromagnetic field by replacing $\mathbf{K} \to -i\nabla - (2e/c)\mathbf{A}$ and $\Omega \to i\partial_t - 2e\varphi$. Thus, the correction to Eq. (1.57) is

$$f_{\text{grad}} = \frac{1}{2m}\left|\left(\nabla - i\frac{2e}{c}\mathbf{A}\right)^2 \phi\right|^2 + \frac{1}{D}\phi^*\left(\partial_t + 2ie\varphi\right)\phi, \tag{1.61}$$

where

$$\frac{1}{m} = -\int \frac{d^d k}{(2\pi)^d} \frac{\partial^2 \xi}{\partial k^2} \frac{\partial}{\partial \xi} \left[\frac{1}{4\xi(k)} \tanh\left(\frac{\xi(k)}{2T} \right) \right], \tag{1.62}$$

$$\frac{1}{D} = -\int \frac{d^d k}{(2\pi)^d} \frac{\partial}{\partial \xi} \left[\frac{1}{4\xi(k)} \tanh\left(\frac{\xi(k)}{2T} \right) \right]. \tag{1.63}$$

Note that the expansion in frequency is only valid in the limit $\Omega \ll |\phi|$, which means that this model describes slow variations of the order parameter in space and time.

Finally, we will derive the vortex version of the gradient term. The motivation for this calculations stems from the idea of duality in electrodynamics. The dual Lagrangian in electrodynamics contains an additional term describing magnetic monopole currents $\tilde{j}^\mu$, which looks exactly as the usual electrical current term, except that matter fields are coupled to the "dual" vector-potential $\tilde{A}^\mu$ rather than to the electromagnetic vector-potential A^μ and that this term enters Lagrangian with the opposite sign. The definitions of the electromagnetic field tensor $F_{\mu\nu}$ and its dual $\tilde{F}_{\mu\nu} = (1/2)\,\epsilon_{\mu\nu\sigma\rho} F^{\sigma\rho}$ need to be modified so that varying the action by $\tilde{A}^\mu$ will give us the Maxwell's equations that take into account the magnetic monopoles:

$$F_{\mu\nu} = \partial_\mu A_\nu - \partial_\nu A_\mu + \frac{1}{2}\epsilon_{\mu\nu\sigma\rho}\left(\partial^\sigma \tilde{A}^\rho - \partial^\rho \tilde{A}^\sigma \right), \tag{1.64a}$$

$$\tilde{F}_{\mu\nu} = \partial_\mu \tilde{A}_\nu - \partial_\nu \tilde{A}_\mu + \frac{1}{2}\epsilon_{\mu\nu\sigma\rho}\left(\partial^\sigma A^\rho - \partial^\rho A^\sigma \right). \tag{1.64b}$$

In this case the term in action that describes free electromagnetic field does not need to be changed, since $F_{\mu\nu}F^{\mu\nu} = -\tilde{F}_{\mu\nu}\tilde{F}^{\mu\nu}$. Thus, the Maxwell's equations become

$$\partial_\mu F^{\mu\nu} = \frac{4\pi}{c} j^\nu, \tag{1.65a}$$

$$\frac{1}{2}\epsilon_{\mu\nu\sigma\rho}\partial_\mu F^{\sigma\rho} = \frac{4\pi}{c}\tilde{j}^\nu. \tag{1.65b}$$

In absence of magnetic monopoles, $\tilde{j}^\mu = 0$ and Eq. (1.65b) takes its usual form,

$\nabla \times \mathbf{E} + (1/c)\,\partial\mathbf{H}/\partial t = 0$ and $\nabla \cdot \mathbf{H} = 0$. Note that in classical Maxwell's theory of electromagnetism, this equation follows from the symmetry properties of the tensor $F^{\mu\nu}$ rather than from action.

In Eq. (1.65a), the contribution of $F_{\mu\nu}$ containing the tensor $\epsilon_{\mu\nu\sigma\rho}$ vanishes if $\tilde{A}^{\mu}$ is single-valued. The only way it can make a finite contribution is when $\tilde{A}^{\mu}$ is multiple-valued, which will make this term singular at the location of the monopole. The same is true, of course, for Eq. (1.65b) and A^{μ} as well. What is important that the dual part of the Lagrangian has opposite signs compared to the "normal" part, which causes the monopole currents and the associated gauge fields $\tilde{A}^{\mu}$ to become unstable and which leads to their disappearance.

This picture is analogous to two-dimensional vortices in superconductors, when the phase of the order parameter is no longer a single-valued quantity. Another analogy is that the absence of magnetic monopoles in our world can be regarded as a characteristic feature of a certain phase. An alternative phase would be the dual world with magnetic monopoles and no electrical charges. If one of these phases corresponds to an "order," then the other, with the opposite signs in the Lagrangian, should be naturally associated with "disorder."

In the context of superconductivity in $2+1$ dimensions, the gradient term in the "normal" model represents fluctuations of the phase of the order parameter. Hence, the dual model should represent these fluctuations in terms of the vortex current. Thus, we consider a superconducting state in which the absolute value of the order parameter $|\phi|$ is finite and fixed, but its phase η is varying. In presence of an electromagnetic field, these phase fluctuations can be described by a bosonic Lagrangian

$$\mathcal{L} = \frac{|\phi|^2}{2m^*}\left(\partial^{\mu}\eta - \frac{e^*}{c}A^{\mu}\right)\left(\partial_{\mu}\eta - \frac{e^*}{c}A_{\mu}\right) - \frac{1}{16\pi}F_{\mu\nu}F^{\mu\nu}. \tag{1.66}$$

The electromagnetic field tensor $F^{\mu\nu}$ is assumed to be re-defined in the formula above. Even if we start with its usual definition, we will have to introduce additional terms at the end to keep the theory self-consistent, as we will see below. Thus, the tensor $F^{\mu\nu}$ is

$$F_{\mu\nu} = \partial_\mu A_\nu - \partial_\nu A_\mu + \epsilon_{\mu\nu\lambda} j_\lambda. \tag{1.67}$$

Here j_λ is the *vortex current*. As we have already mentioned, we will choose such a definition of the vortex current so that the Lagrangian will describe the self-consistent theory. This definition is

$$j_\mu = \frac{c}{e^*} \epsilon_{\mu\nu\lambda} \partial^\nu \partial^\lambda \eta. \tag{1.68}$$

The vortex current vanishes for a single-valued function η, but it becomes singular when η is multivalued.

The electrical current is

$$J^\mu = \frac{|\phi|^2 e^*}{m^*} \left(\partial^\mu \eta - \frac{e^*}{c} A^\mu \right) \tag{1.69}$$

and it is trivially related to the electromagnetic field tensor:

$$F^{\mu\nu} = \frac{m^* c}{e^{*2} |\phi|^2} \left(\partial^\nu J^\mu - \partial^\mu J^\nu \right). \tag{1.70}$$

Note that the vortex current is precisely canceled out by the singular part in the derivatives of the electrical current. The charge conservation law $\partial_\mu J^\mu = 0$ implies that the current J^μ can be represented in terms of another (*dual*) vector field a^μ so that

$$J^\mu = -\epsilon^{\mu\nu\lambda} \partial_\nu a_\lambda. \tag{1.71}$$

The dual field a^μ is defined up to a gradient of a single-valued scalar field $\partial^\mu \theta$. The

Maxwell's equation Eq. (1.65a) becomes

$$\begin{aligned} J^{\mu} &= -\frac{c}{4\pi}\partial_{\nu}\left(\partial^{\mu}A^{\nu} - \partial^{\nu}A^{\mu}\right) \\ &= \frac{m^{*}c^{2}}{4\pi e^{*2}\left|\phi\right|^{2}}\partial_{\nu}\left(\partial^{\mu}J^{\nu} - \partial^{\nu}J^{\mu}\right) \\ &= \frac{m^{*}c^{2}}{4\pi e^{*2}\left|\phi\right|^{2}}\epsilon^{\mu\nu\lambda}\epsilon_{\sigma\rho\lambda}\partial_{\nu}\partial^{\sigma}J^{\rho}. \end{aligned} \tag{1.72}$$

Comparing the latter formula with Eq. (1.71), we find that

$$F^{\mu\nu} = \frac{4\pi}{c}\epsilon^{\mu\nu\lambda}\left(a_{\lambda} - \partial_{\lambda}\theta\right) \tag{1.73}$$

and that

$$a_{\lambda} = \frac{m^{*}c^{2}}{4\pi e^{*2}\left|\phi\right|^{2}}\epsilon_{\lambda\sigma\rho}\partial^{\sigma}J^{\rho} + \partial_{\lambda}\theta. \tag{1.74}$$

Looking at Eq. (1.73), we notice that the $a_{\lambda} - \partial_{\lambda}\theta$ is proportional to the magnetic field across the sample, $a_{\lambda} = -\left(c/8\pi\right)\epsilon_{\lambda\sigma\rho}F^{\sigma\rho} + \partial_{\lambda}\theta$. Furthermore, from the definition of the vortex current and the equation above, we can see that

$$j_{\mu} = \frac{4\pi}{c}a_{\mu} + \epsilon_{\mu\nu\lambda}\partial^{\nu}A^{\lambda}. \tag{1.75}$$

Finally, we substitute Eqs. (1.69), (1.71), (1.73) and (1.75) into Eq. (1.66):

$$\mathcal{L} = \frac{m^{*}}{2e^{*2}\left|\phi\right|^{2}}f_{\mu\nu}f^{\mu\nu} - \frac{1}{2c}a_{\mu}\left(j^{\mu} - \epsilon^{\mu\nu\lambda}\partial_{\nu}A_{\lambda}\right), \tag{1.76}$$

where $f_{\mu\nu} = \partial_{\mu}a_{\nu} - \partial_{\nu}a_{\nu}$ and we have dropped $\partial^{\mu}\theta$. If we formally vary Eq. (1.76) by a^{μ}, we will recover the same equation on vortex current as one that is derived after substituting Eqs.(1.74), (1.71) into Eq. (1.75). This means that our theory is self-consistent.

To the contrary, we could start with conventional definition of Maxwell's field ten-

sor $F^{\mu\nu}$ instead of Eq. (1.67). Then the vortex current term $(-\epsilon_{\mu\nu\lambda}j_\lambda)$ would appear in Eq. (1.70). Moreover, Eq. (1.74) would contain an additional term $-(c/4\pi)j_\lambda$ and this equation would become the replacement for Eq. (1.75). However, this additional term would not be recovered after varying the new Lagrangian by a^μ, which means that one would have to add a term $(1/2c)j_\mu a^\mu$ to the Lagrangian so that the theory would be self-consistent. The latter correction is equivalent to re-defining $F^{\mu\nu}$ as in Eq. (1.67).

Thus, we have re-interpreted the model of a system in the superconducting state in terms of vortex currents. As we can see, this Langrangian Eq. (1.76) resembles the original model Eq. (1.66), but the signs are opposite. This is related to the fact that in the superconducting state the density of vortices is zero because vortex condensate is unstable.

The disordered state corresponds to the opposite regime. During the disordering transition the vortices condense and in this case the vortex current should be characterized by its own bosonic field Φ and the dual gauge field a^μ,

$$j_\lambda = 2\mathrm{Im}\left[\Phi^*\left(\partial^\mu - ia^\mu\right)\Phi\right]. \tag{1.77}$$

Then the dual Lagrangian can be written as following [54]:

$$\mathcal{L}_{\mathrm{dual}} = \left|\left(\partial^\mu - ia^\mu\right)\Phi\right|^2 - V\left(|\Phi|\right) - \frac{1}{4}f_{\mu\nu}f^{\mu\nu} - \kappa\epsilon_{\mu\nu\lambda}a^\mu\partial^\nu A^\lambda. \tag{1.78}$$

For this model the equations involving the superconducting order parameter $|\phi|^2$ are no longer applicable and Eq. (1.71) becomes the definition of the electrical current.

Chapter 2 Odd-Frequency Density Waves

2.1 Introduction

Many attempts to uncover non-Fermi-liquid metallic behavior in strongly-correlated electron systems have focused on enhanced scattering mechanisms which might lead to anomalous behavior in the electron Green function. In this chapter we attempt a different tack and focus on metallic states with a conventional Fermi surface which can be distinguished from Fermi liquids by an *order parameter* [55]. In order to preserve the Fermi surface, the order parameter is taken to be *odd in frequency*.[1] When the order parameter breaks a continuous symmetry, the low-energy spectrum must also include Goldstone modes. As a result, odd-frequency ordering results in a set of low-energy excitations which is larger than that of a Fermi liquid (so that they are no longer in one-to-one correspondence with those of a free Fermi gas), leading to a manifestly non-Fermi liquid state.

A number of authors have considered superconducting states with order parameters $\langle c_\alpha(k,\omega)\, c_\beta(-k,-\omega)\rangle$ which are odd in frequency [56, 57, 58, 59, 60, 61, 62, 63, 64]. The energetic advantage of such a state is that it would enable the electrons to avoid instantaneous Coulomb repulsion while still benefitting from pairing. The odd-frequency dependence of the order parameter is due to the unusual frequency dependence of interaction. The latter could be linear in ω and ω' [57, 58, 59], proportional to ω^{-1} and ω'^{-1} [60], or even have $\log|(\omega-\omega')\,/\,(\omega+\omega')|$ dependence [61]. Some exactly soluble one-dimensional models, such as the one-dimensional Kondo

[1] A frequency-independent order parameter may have Fermi pockets, but these are to be contrasted with the large true Fermi surface of a Fermi liquid. An odd-frequency ordered state has a Fermi surface of the latter variety.

lattice, have a tendency towards such ordering as well [65, 66]. However, there are claims that the simplest models of odd-frequency superconducting states suffer from pathologies which make them unstable [62, 63, 64, 67].

We will consider the analogous states in the particle-hole channels. These are metallic states — unlike the corresponding superconducting states — with normal Fermi surfaces. We find that simple models of odd-frequency density wave states do not suffer from any pathologies (and we comment briefly on the supposed pathologies of odd-frequency superconducting states as well). Odd-frequency states can exhibit a number of interesting non-Fermi liquid properties including the Goldstone modes mentioned above, a range of states above the Fermi surface with finite lifetimes even in the limit of vanishing frequency and temperature $\epsilon, T \to 0$, and a non-mean-field-like temperature-dependent order parameter.

However, the question of their detection is nontrivial and cuts to the heart of attempts to experimentally distinguish non-Fermi liquids from Fermi liquids. While an odd-frequency superconducting state is, first and foremost, a superconducting state, which would be identified by its vanishing resistivity, Meissner effect, etc., an odd-frequency density wave state can masquerade as a Fermi liquid since the order parameter vanishes at zero frequency. There will be signatures in thermodynamic and transport measurements, but they can easily be mistakenly attributed to other effects, as we discuss below.

2.2 Order parameters and symmetries

An odd-frequency charge-density wave state is defined by the anomalous correlation function

$$\left\langle c^{\alpha\dagger}\left(k,\epsilon_n\right) c_\alpha\left(k+Q,\epsilon_n\right)\right\rangle = F\left(k,\epsilon_n\right), \tag{2.1}$$

where $F(k,\epsilon_n)$ is an odd function of frequency,

$$F(k,-\epsilon_n) = -F(k,\epsilon_n). \tag{2.2}$$

To find an equal-time correlation function which serves as an order-parameter, we Fourier transform (2.1):

$$\left\langle T_\tau \left(c^{\alpha\dagger}(k,\tau)\, c_\alpha(k+Q,0) \right) \right\rangle = \tilde{F}(k,\tau), \tag{2.3}$$

where $\tilde{F}(k,\tau)$ is odd in τ. Since its Fourier transform is odd, $\tilde{F}(k,\tau)$ is imaginary. Thus, we can use the time-derivative as an order parameter:

$$\left\langle T_\tau \left(\partial_\tau c^{\alpha\dagger}(k,\tau)\; c_\alpha(k+Q,0) \right) \right\rangle_{\tau=0} = \partial_\tau \tilde{F}(k,0). \tag{2.4}$$

The state defined by these order parameters, (2.1) or (2.4), breaks translational symmetry. Time-reversal symmetry is not broken. This is most easily seen by considering (2.3). Taking the complex conjugate of both sides of (2.3) gives

$$\begin{aligned} \left\langle T_\tau \left(c^{\alpha\dagger}(k+Q,0)\, c_\alpha(k,\tau) \right) \right\rangle &= \left(\tilde{F}(k,\tau) \right)^* \\ &= -\tilde{F}(k,\tau). \end{aligned} \tag{2.5}$$

Meanwhile, (2.3) is transformed under time-reversal, $\mathcal{T}$, into:

$$\begin{aligned} &\left\langle T_\tau \left(\mathcal{T} \left(c^{\alpha\dagger}(k,\tau)\, c_\alpha(k+Q,0) \right) \right) \right\rangle \\ &\quad = \left\langle T_\tau \left(c^{\alpha\dagger}(k+Q,0)\, c_\alpha(k,-\tau) \right) \right\rangle \\ &\quad = -\tilde{F}(k,-\tau) \\ &\quad = \tilde{F}(k,\tau) \\ &\quad = \left\langle T_\tau \left(c^{\alpha\dagger}(k,\tau)\, c_\alpha(k+Q,0) \right) \right\rangle, \end{aligned} \tag{2.6}$$

and, hence, the order parameter does not break time-reversal symmetry. In going from the first equality to the second, we have used (2.5).

An odd-frequency spin-density wave is defined by

$$\left\langle c^{\alpha\dagger}\left(k,\epsilon_n\right)c_\beta\left(k+Q,\epsilon_n\right)\right\rangle = \vec{n}\cdot\vec{\sigma}^\alpha_\beta F\left(k,\epsilon_n\right), \tag{2.7}$$

where $F\left(k,\epsilon_n\right)$ is again an odd function of frequency and $\vec{n}$ is the direction chosen spontaneously by the ordered state. This state breaks translational symmetry and spin-rotational symmetry, which is broken to the $U(1)$ subgroup of rotations about $\vec{n}$. Again, time-reversal is preserved. Such a state will exhibit a nonzero expectations value and anomalous correlations of the spin nematic order parameter, $S_iS_j-\delta_{ij}S^2/3$, such as those discussed for spin-only models in Ref. [68].

2.3 Model interaction

We now consider a simple two-dimensional model which admits an odd-frequency charge-density-wave state at the mean-field level. The model contains a nonsingular four-fermion interaction which can be generated by the exchange of phonons or some gapped electronic collective mode. For simplicity, we focus on the charge-density-wave case; the spin-density-wave is analogous.

We consider an effective action which consists of a kinetic term

$$S_0 = \int d\tau \int_k c^{\alpha\dagger}(k,\tau)\left(\partial_\tau - \left(\epsilon(k)-\mu\right)\right)c_\alpha(k,\tau) \tag{2.8}$$

and an interaction term

$$S_{\rm int} = \frac{1}{\Omega_c^2} \int d\tau \int_{k,k'} \left[c^{\alpha\dagger}(k+Q,\tau) \partial_\tau c_\alpha(k,\tau) \right]_c V_{kk'} \times \left[c^{\beta\dagger}(k',\tau) \partial_\tau c_\beta(k',\tau) \right]_c . \tag{2.9}$$

To avoid clutter, the $\int_{k,k'}$ is used as shorthand for the integrals over k, k': $\int_k \equiv \int d^2k/(2\pi)^2$. The subscript c indicates that the terms in brackets are actually defined with a frequency cutoff, Ω_c:

$$\left[c^{\alpha\dagger}(k+Q,\tau) \partial_\tau c_\alpha(k,\tau) \right]_c \equiv T \sum_{|\epsilon_n|<\Omega_c} i\epsilon_n \, c^{\alpha\dagger}(k+Q,\epsilon_n) \, c_\alpha(k,\epsilon_n). \tag{2.10}$$

For simplicity, we take $V_{kk'}$ independent of k, k', $V_{kk'} = \lambda$. For simplicity, we also take $Q = (\pi,\pi)$ and $\epsilon(k) = -2t(\cos k_x + \cos k_y)$, corresponding to commensurate order for a system of electrons on a square lattice with nearest-neighbor hopping. The generalization to incommensurate order and other band structures is straightforward.

The interaction term $S_{\rm int}$ is long-ranged in precisely the same way as the BCS reduced interaction. A more realistic short-ranged interaction would be of the form

$$\tilde{S}_{\rm int} = \int_{k,k',q} \left[c^{\alpha\dagger}(k+q,\tau) \partial_\tau c_\alpha(k,\tau) \right]_c V^q_{kk'} \times \left[c^{\beta\dagger}(k',\tau) \partial_\tau c_\beta(k'+q,\tau) \right]_c , \tag{2.11}$$

which includes (2.9) as one term in the sum over q. Such an interaction could arise from the diagram of figure 2.1 if the collective mode has a propagator of the form

$$\lambda \, \frac{\Omega_c^2}{\Omega_c^2 + v^2(k-k')^2 + (\epsilon_n - \epsilon_{n'})^2}. \tag{2.12}$$

If v is small, then we can expand the collective mode propagator to obtain $V_{kk'} = \lambda$, for $|\epsilon_n|, |\epsilon_{n'}| \leq \Omega_c$. Other terms will also be generated which could drive the formation of even-frequency order, but they appear to be weaker.

A collective mode or phonon at finite frequency, Ω_c will mediate an interaction which grows as the mode frequency is approached but decreases at higher frequencies. At low frequencies, we can use the expansion suggested below (2.12) to extract the odd-frequency kernel. We model the decay of the interaction at high frequencies by introducing a cutoff at Ω_c. Later, we will model it more realistically by allowing this cutoff to be smooth.

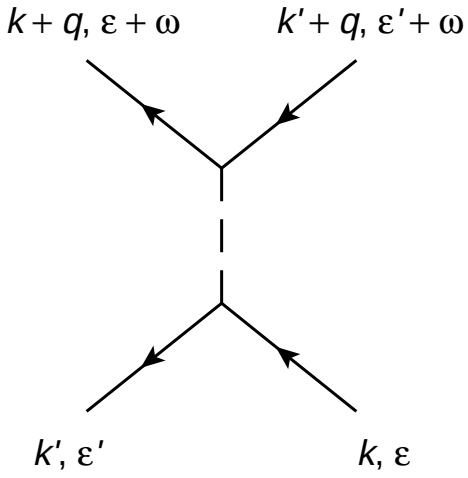

Figure 2.1: A diagram which can lead to an interaction favorable for odd-frequency density-wave ordering. The dashed line represents a collective mode which mediates the interaction.

We assume an order parameter of the form:

$$\alpha \equiv \frac{\lambda}{\Omega_c^2} \int_k \left\langle c^{\alpha\dagger}(k+Q,\tau)\, i\partial_\tau c_\alpha(k,\tau) \right\rangle_c. \tag{2.13}$$

According to our previous observations, α is real. Then the mean-field action takes

the form

$$S_{\rm MF} = T\sum_n \int_k c^{\alpha\dagger}(k,\epsilon_n)\left(i\epsilon_n - (\epsilon(k)-\mu)\right) c_\alpha(k,\epsilon_n) \\ - T\sum_n \int_k \alpha\epsilon_n\, c^{\alpha\dagger}(k,\epsilon_n) c_\alpha(k+Q,\epsilon_n). \tag{2.14}$$

The equation of motion following from the mean-field action is:

$$\left(i\epsilon_n - \epsilon(k) + \mu\right) c_\alpha(k,\epsilon_n) - \alpha\epsilon_n c_\alpha(k+Q,\epsilon_n) = 0. \tag{2.15}$$

We multiply the equation of motion by $c^\dagger_\alpha(k,\epsilon_n)$ and take the imaginary time-ordered expectation value. We see that the ordinary and anomalous Green functions satisfy the equation:

$$\left(i\epsilon_n - \epsilon(k) + \mu\right) G(k,\epsilon_n) - \alpha\epsilon_n F(k,\epsilon_n) = 1. \tag{2.16}$$

The right-hand-side results from the time-derivative (i.e., $i\epsilon_n$) acting on the time-ordering symbol.[2] If we make the replacement $k \to k+Q$ in (2.15), then we can derive a second equation in the same way,

$$\left(i\epsilon_n + \epsilon(k) + \mu\right) F(k,\epsilon_n) - \alpha\epsilon_n G(k,\epsilon_n) = 0, \tag{2.17}$$

and the Green function and anomalous Green function for $|\epsilon_n| \le \Omega_c$ take the form:

$$G\left(k,\epsilon_n\right) = \frac{i\epsilon_n + \mu + \epsilon(k)}{\left(i\epsilon_n+\mu\right)^2 - \left(\epsilon(k)\right)^2 - \alpha^2\epsilon_n^2}\,, \tag{2.18a}$$

$$F\left(k,\epsilon_n\right) = \frac{\alpha\epsilon_n}{\left(i\epsilon_n+\mu\right)^2 - \left(\epsilon(k)\right)^2 - \alpha^2\epsilon_n^2}\,. \tag{2.18b}$$

[2]Some care is required since both the kinetic *and* interaction terms in the mean-field action contain a single time-derivative. As a result, the commutations relations are modified. However, the resulting equations for G and F are of the same form as one would obtain by ignoring this fact and ignoring the time-derivative arising from the frequency dependence of the gap in (2.15), i.e., by making two compensating errors.

One might naively think that equation (2.17) could be obtained by inspection from (2.16) by replacing $\Delta(\epsilon_n)$ by $\Delta^*(-\epsilon_n)$ as one usually does in the case of an even-frequency gap. In this case, this would amount to the replacement of $\alpha\epsilon_n$ by $-\alpha\epsilon_n$, as was done in Ref. [62, 63, 64, 67]. However, in the case of an odd-frequency gap, this simple substitution only works for *real* frequencies. Since the gap is linear in frequency and the squared modulus of the gap appears in the Green functions, the Green functions are no longer analytic in the frequency. As a result, the analytic continuation from real to Matsubara frequencies is subtle. The safe route is to derive both (2.16) and (2.17) directly from the mean-field action, as we have done. The naive, incorrect form of (2.17) would lead to a negative superfluid density in the case of odd-gap superconductors. On the other hand, the correct analogue of (2.17) for a superconducting action would lead to a stable odd-frequency superconducting state. Such a Green function was used in the context of an odd-frequency superconducting state induced by disorder [61]. We derive the Green functions for odd-frequency superconductivity in Appendix B.

For $|\epsilon_n| > \Omega_c$, F vanishes and G returns to its normal state form. In principle, we should also allow for a quasiparticle renormalization Z resulting from the interaction, but this does not qualitatively modify our results, so we drop this correction for simplicity.

From these Green functions, we see that, at $\mu = 0$, the odd-frequency charge-density-wave order parameter modifies the quasiparticle spectrum to:

$$E(k) \equiv \frac{\epsilon(k)}{\sqrt{1+\alpha^2}}, \tag{2.19}$$

i.e., it renormalizes the effective mass. For $\mu \neq 0$, the effect is more complicated. As

a result of the odd-frequency charge-density-wave, $\epsilon(k) - \mu$ is replaced with

$$E(k) \equiv \frac{-\mu \pm \sqrt{(1+\alpha^2)\,\epsilon^2\,(k) - \alpha^2\mu^2}}{1+\alpha^2}. \tag{2.20}$$

From (2.20), we see that the Fermi surface is unmoved, i.e., $E(k) = 0$ when $\epsilon(k) = \mu$, as we expect, since the order parameter vanishes at zero frequency.

Furthermore, there is a range of k values above the Fermi surface, $|\epsilon(k)| < \left|\alpha\mu/\sqrt{1+\alpha^2}\right|$, where $E(k)$ has an imaginary part, so that quasiparticles in this region have a finite lifetime. However, these states have zero occupation number, as the corresponding poles in the Green functions turn out to be lying outside of the integration contour. This gives rise to a possibility of the ground state in which some of the quasiparticles are in levels which are in disconnected from the rest of the Fermi sea.

2.4 Gap equation

We must now impose a self-consistency condition on $F\,(k, \epsilon_n)$, which is the gap equation. To derive this equation, we substitute (2.1) and (2.18b) into (2.13). We will also impose a condition on the particle number, thereby implicitly fixing the chemical potential. These conditions read

$$-\frac{\lambda}{\Omega_c^2} 2T \sum_n{}' \int_k \frac{\epsilon_n^2}{(i\epsilon_n + \mu)^2 - (\epsilon(k))^2 - \alpha^2\epsilon_n^2} = 1, \tag{2.21a}$$

$$T \sum_n{}' \int_k \frac{i\epsilon_n + \mu + \epsilon(k)}{(i\epsilon_n + \mu)^2 - (\epsilon(k))^2 - \alpha^2\epsilon_n^2} = n. \tag{2.21b}$$

For simplicity, we consider the case of half-filling, $n = 1$. We have repeated our calculations at nonzero doping and found similar results.

The prime on the Matsubara summations in (2.21a), (2.21b) indicate that they

are done with $\alpha = 0$ for $|\epsilon_n| > \Omega_c$ and $\alpha \neq 0$ only for $|\epsilon_n| \leq \Omega_c$. A more realistic model replaces the interaction with one that has a "smooth" cutoff $s_\eta(\epsilon_n)\, s_\eta(\epsilon_{n'})$ and α by $\alpha\, s_\eta(\epsilon_n)$, with $s_\eta(\epsilon) = 1$ for $\epsilon \ll \Omega_c$ and $s_\eta(\epsilon) = 0$ for $\epsilon \gg \Omega_c$. We can vary η between the limit $\eta \to \infty$, which corresponds to a sharp cutoff, and $\eta \to 0$ which corresponds to the absence of a cutoff. For computational simplicity, we take $s_\eta(\epsilon) = n_F(|\epsilon| - \Omega_c; \beta = \eta)$.

We now discuss the analysis of (2.21a), (2.21b). Let us first consider the case of a sharp cutoff. The left-hand side of the gap equation vanishes if the temperature is above

$$T_c^{\max} = \frac{\Omega_c}{\pi}. \tag{2.22}$$

$T_c^{\max}$ is the highest possible transition temperature for this system. Just below this temperature there is only one pair of terms in the Matsubara sum which is allowed by the cutoff Ω_c. As the temperature is decreased, more Matsubara frequencies begin to contribute, resulting in minor steps in the phase diagram.

For large λ, $T_c = T_c^{\max}$. Decreasing λ, we enter a regime, $\lambda_{c2} < \lambda < \lambda_{c1}$, in which the system is in the odd-frequency density-wave phase for an intermediate range of temperatures $T_{c2} < T < T_{c1}$. λ_{c1} is the location of the quantum phase transition at which the odd-frequency density-wave order first appears at zero temperature. It is obtained from (2.21a) by setting $\mu = 0$ and $\alpha = 0$ and converting the Matsubara sum into an integral:

$$\int_k \left[\Omega_c - \epsilon\,(k) \arctan \frac{\Omega_c}{\epsilon\,(k)}\right] = \frac{\pi \Omega_c^2}{\lambda_{c1}}. \tag{2.23}$$

The integrand is approximately Ω_c for small $\epsilon\,(k)$ and $\Omega_c^3/3\epsilon^2\,(k)$ for $|\epsilon\,(k)| \gg \Omega_c$.

As λ is further decreased, T_{c2} increases and finally reaches $T_c^{\max}$ at λ_{c2}. To find λ_{c2}, we again set $\mu = 0$ and $\alpha = 0$, but now we retain only the pair of terms in the

Matsubara sum corresponding to the frequencies $\pm\Omega_c$:

$$\int_k \frac{T_c^{\max}}{\Omega_c^2 + \epsilon^2(k)} = \frac{1}{\lambda_{c2}}. \tag{2.24}$$

Comparing expressions (2.23) and (2.24), we find that the latter is larger by a factor of 3 for large $\epsilon(k)$; hence, $\lambda_{c2} < \lambda_{c1}$. For $\lambda > \lambda_{c2}$, α jumps discontinuously at $T_c^{\max}$. Finally, for $0 < \lambda < \lambda_{c2}$, there are no odd-frequency charge-density-wave solutions. As a result, the phase diagram has the shape shown in Fig. 2.2 (dashed line) with re-entrant transitions for $\lambda_{c2} < \lambda < \lambda_{c1}$.

Let us now consider how this picture is modified when we make the cutoff smooth, as it must be in a physical system. The sharpness of the steps which separate the re-entrant transitions depends on the details of the high-frequency cutoff; they disappear in the limit when the cutoff is very smooth. When the cutoff is relatively sharp, more re-entrant transitions are possible, and there will be several temperature regions in which an odd-frequency charge-density wave occurs. However, for a smooth cutoff, there is typically only one such region. The transition at $T_c^{\max}$ is replaced with a smooth curve $T_{c1}(\lambda)$, at which a second-order transition takes place. The corresponding phase boundary is depicted by the solid line in Fig. 2.2.

Below $T_{c1}(\lambda)$, α increases as shown in Fig. 2.3. Note that for a smooth cutoff all transitions are of second order, even though the rise of α at T_{c1} is very steep for large values of λ and may give a false impression of a first-order transition. It is also noteworthy that even for large λ the order parameter α rapidly attains its maximum as T is decreased below T_c and then decreases as $T \to 0$ to some nonzero asymptotic value. This has a significant impact on experimentally measurable parameters, as we describe in the following section.

The unusual temperature dependence of the order parameter, which is reflected in the re-entrant phase diagram and (as we will see in the next section) the condensa-

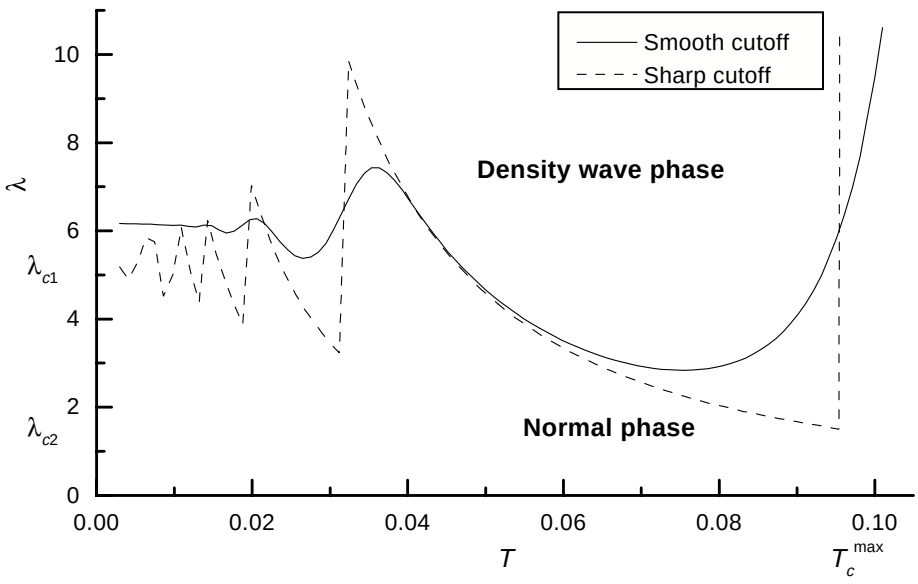

Figure 2.2: Phase diagram at half-filling for "smooth" and "sharp" cutoffs at $\Omega = 0.3$. The energy scale is set by the width of the band $W = 2$.

tion energy, is a consequence of the frequency-dependence of the gap. In an ordinary, frequency-independent (or weakly-dependent) ordered state, the condensation energy at weak-coupling comes primarily from states near the Fermi energy. At high temperatures, these states are thermally excited, so there is little condensation energy to be gained, and the order parameter decreases as the temperature is increased. In the case of odd-frequency ordered states, there is very little condensation energy to be gained from the particles near the Fermi surface because their energy is low (and, hence, they interact weakly with the order parameter). As a result, the order parameter and condensation energy decrease as the temperature is decreased.

In fact, there is a second solution to the gap equation in which it is favorable to have a disconnected Fermi sea in which some electrons are excited to a strip in momentum space above the Fermi surface which is diconnected from the rest of the Fermi sea, which is centered about $\mathbf{k} = 0$. When this occurs, the occupation number does not increase monotonically with $\epsilon(k)$. However, this solution is higher in energy, so it does not occur.

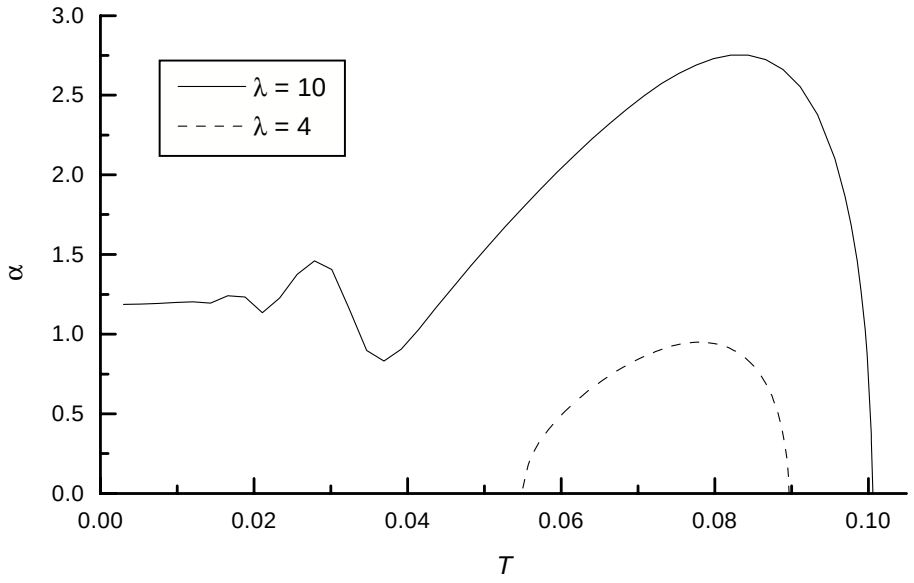

Figure 2.3: Order parameter for different values of the interaction strength, λ, with a "smooth" cutoff at $\Omega = 0.3$.

2.5 Experimental signatures

At T_c, there will be the usual thermodynamic signatures of a second-order phase transition. The condensation energy associated with this transition is the difference between the free energy of the odd-frequency charge-density-wave state and corresponding free energy of the normal state at the same temperature. At $\mu = 0$ and with a sharp cutoff,

$$\Delta E\left(T\right) = \frac{\Omega_c^2}{\lambda}\,\alpha^2 + 2T \sum_{n=-n_c-1}^{n_c} \int_k \ln\left(\frac{\epsilon(k)^2 + \epsilon_n^2}{\left(1+\alpha^2\right)\epsilon_n^2 + \epsilon(k)^2}\right), \tag{2.25}$$

where $n_c = \left(\Omega_c/\pi T - 1\right)/2$. This equation is obtained by using α as a Hubbard-Stratonovich field to decouple (2.9), resulting in the first term in (2.25). The electronic action is then the mean-field action (2.14), so that the partition function may be evaluated to give the second term in (2.25). At zero temperature, the integrals may

be evaluated analytically:

$$\begin{aligned}\Delta E\,(0) = \frac{\Omega_c^2}{\lambda}\,\alpha^2 \; &+ \frac{2}{\pi}\int_k \epsilon(k)\,\arctan\left(\frac{\Omega_c}{\epsilon(k)}\right) \\ &- \frac{2}{\pi}\int_k \frac{\epsilon(k)}{\sqrt{1+\alpha^2}}\,\arctan\left(\frac{\Omega_c\sqrt{1+\alpha^2}}{\epsilon(k)}\right) \\ &+ \Omega_c\,\frac{2}{\pi}\int_k \ln\left(\frac{\Omega_c^2+\epsilon^2(k)}{(1+\alpha^2)\,\Omega_c^2+\epsilon^2(k)}\right).\end{aligned} \tag{2.26}$$

The last term is overwhelmingly negative, as may be seen in various limits (e.g., $\alpha \ll 1$ or $\Omega_c \to \infty$). Note that the energetic gain comes not from the terms in the frequency sum (2.25) with small Matsubara frequency, which actually increase energy, but from the terms near the cutoff — in a complete reversal of the situation for a frequency-independent gap.[3]

Again, for a smooth cutoff the Matsubara frequency sum becomes infinite and α should be replaced with $s_\eta(\epsilon_n)\alpha$. For smooth cutoff and finite temperature, the condensation energy must be evaluated numerically. The dependence of the condensation energy ΔE on temperature is shown in Fig. 2.4. Unlike in even-frequency phases, where $|\Delta E|$ slowly increases as the system cools down and attains its maximum at zero temperature, in our model it rapidly reaches a maximum and decreases to a constant asymptotic value as $T \to 0$. As may be seen in figure 2.4, the condensation energy is of order of $N_F T_{c1}^2$ at the maximum, which is comparable to the maximum condensation energy attained in even-frequency phases.

The DC conductivity can be computed from the Kubo formula. We assume a model in which impurities give rise to a lifetime, τ. The resulting conductivity is given by

$$\sigma = \frac{1}{1+\alpha^2}\int_k \left(\frac{\partial\epsilon(k)}{\partial k_x}\right)^2 \frac{\tau}{4T}\frac{1}{\cosh\left(\frac{E(k)}{2T}\right)^2}, \tag{2.27}$$

[3]The derivation of the "anomalous" last term in (2.26) is straightforward from the partition function using the path integral formalism. It is much more difficult, if at all possible, to explain its presence within classical thermodynamics. It is manifestly a quantum phenomenon.

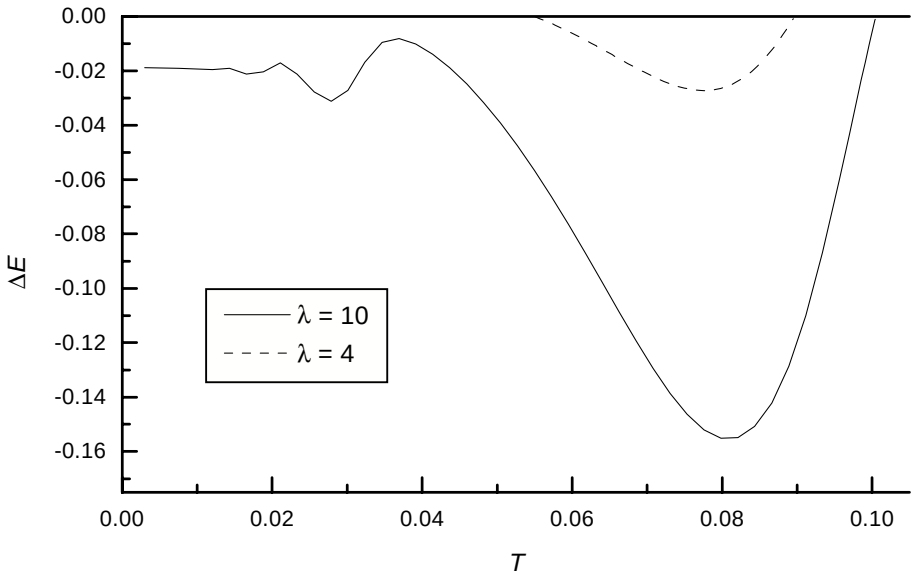

Figure 2.4: Condensation energy as a function of temperature in model (2.9) with a "smooth" cutoff at $\Omega = 0.3$.

where $E(k)$ is given in (2.20). For small μ, the modification of the quasiparticle spectrum in the odd-frequency charge-density-wave phase reduces to the rescaling of the electron mass near the Fermi surface, so that the new effective mass is $m^* = m\sqrt{1+\alpha^2}$. This mass enhancement leads to a noticeable increase of the resistivity, as shown in Fig. 2.5. Of course, outside of the the region $T_{c2}(\lambda) < T < T_{c1}(\lambda)$ the resistivity is that of the normal phase.

2.6 Discussion

In this work we have considered a model with an odd-frequency charge-density-wave solution. The transition to this state is signaled by a second-order phase transition with a jump in the specific heat. For strong interactions, the model is in an odd-frequency charge-density-wave phase for all temperatures $T < T_c$. For moderately weak interactions, the model is in such a phase for an intermediate temperature regime $T_{c1} < T < T_{c2}$. There is a quantum phase transition at $\lambda = \lambda_{c1}$; for weaker

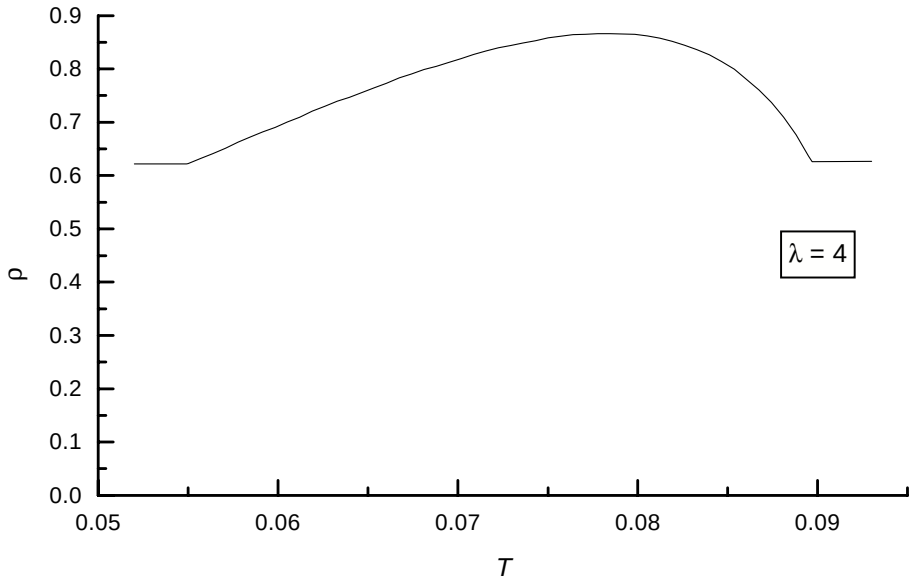

Figure 2.5: Resistivity as a function of temperature in the model of Eq. (2.9) with a "smooth" cutoff at $\Omega = 0.3$ and interaction strength $\lambda = 4$.

interactions, the system is not ordered at $T = 0$.

A similar model admits an odd-frequency spin-density-wave ground state. Such a state will have, in addition to its Fermi-liquid-like quasiparticles, Goldstone boson excitations. As a result $S_i S_j - \delta_{ij} S^2/3$, has a nonzero expectation value, and its correlation functions have Goldstone poles.

The method that we used to derive the Green functions of the odd-frequency density wave can be applied to the analysis of odd-frequency superconductivity as well, with some modification. The corresponding mean field theory should describe a stable state with positive superfluid density.

Odd-frequency charge-density wave order results in mass enhancement. This affects *transport properties*; in the density-wave state the resistivity is considerably larger than in the normal state. The effect is largest at intermediate temperatures due to the form of interaction, which attains its maximum value near the high-frequency cutoff. At low temperatures, the system is either in the normal state (for $\lambda < \lambda_{c1}$) or in an ordered state (for $\lambda \geq \lambda_{c1}$) with some asymptotic value of the order param-

eter. This type of non-monotonic resistivity curve has been observed in a number of strongly-correlated electron systems. In layered materials, such as the cuprates and ruthenates, it has been observed in c-axis transport [69, 70]. In 2DEGs, this type of behavior has been observed in the vicinity of a putative metal-insulator transition [71, 72, 73, 74, 75]. It would be premature to suggest that odd-frequency order is developing in any of these experiments, but it is noteworthy that it does provide a natural explanation of otherwise puzzling behavior.

Odd-frequency density wave ordering is also manifested in *thermodynamics*. Unlike in even-frequency states, where the condensation energy $|\Delta E|$ is small near the phase transition and reaches a maximum at zero temperature, in odd-frequency states the maximum of $|\Delta E|$ is located near the upper critical temperature. Consequently, there is strong variation of all thermodynamic quantities with temperature just below T_c. Again, at lower temperatures these phenomena disappear.

The model that we have introduced is certainly simplified, as it ignores the possible proximity of other phases. However, we believe that odd-frequency density-wave order can result when a tendency towards ordinary even-frequency density-wave order is frustrated by some interaction. Without such interaction, since the condensation energy in the odd-frequency phase is the largest at high temperatures, one should expect to find it *above* the even-frequency state. The final resolution of the competition will depend on the scales at which the various interactions act, essentially, Ω_c in our model. In particular, one can imagine a scenario in which an ordinary even-frequency density wave is favorable at higher temperatures, but below a certain temperature, the system undergoes a transition into an odd-frequency state.

More generally, the density-wave models with interaction that depends on frequency and whose maximum is attained at some finite frequency Ω_c would have similar thermodynamic and kinetic properties at intermediate temperatures as our model. This is because the thermally excited fermion quasiparticles would "sense"

such an interaction the strongest near temperature Ω_c/π. However, at low temperatures the pure odd-frequency phase would have distinguishibly different properties, since it would remain metallic at $T = 0$.

Chapter 3 Competing orders

The interactions that have high symmetry are of significant interest in the condensed-matter theory. When the symmetry is broken, the system undergoes a phase transition. The higher the symmetry is, the more possible phases can exist or coexist on the phase diagram. Each kind of order is associated with its own condensation energy, which causes them to compete with each other. The mean-field theory allows one to predict the phase diagram qualitatively, to determine the regions of possible phase coexistence and to locate the quantum critical points.

A realistic model usually includes a lot of other interactions in addition to one with high symmetry. However, often the overall symmetry of the problem is still quite high and is broken spontaneously. This means that in two dimensions (2-D), the mean-field critical temperature only predicts the formation of the local order and globally the system may remain normal (metallic) even below this temperature. The proximity of the quantum critical points may substantially affect the properties of the locally ordered phases as well, since they strongly enhance the quantum fluctuations. Conversely, the weak interlayer coupling suppresses the fluctuations and at sufficiently low temperature begins to act as an interaction in the third dimension, which drives the system through a global phase transition. Even in absence of such interlayer coupling, the transition can be of Kosterlitz-Thouless type, when no symmetry breaking actually takes place. Finally, there are cases when the broken symmetries are discrete (such as in the case of charge-density wave), in which the mean-field theory predicts the actual critical temperature.

We will illustrate it on a simple example of a 2-D bilayer bipartite lattice (Fig. 3.1), in which electrons on the two layers tend to bind into pairs due to an attractive

interaction between the electrons on different layers [76]. To make this model more realistic, consider each site on the lattice as a small *capacitor* formed by two layers. (It is actually possible to synthesize such systems and explore them experimentally [77].) If a is the lattice spacing and $b \ll a$ is the spacing between the layers, then the energies of interlayer Coulomb interaction and of the capacitor can be estimated, respectively, as $n^{(1)}n^{(2)}/b$ and $(2\pi b/a^2)\left(n^{(1)} - n^{(2)}\right)^2$, where $n^{(\lambda)}$ is the number of electrons on the layer λ at given site. Thus, it appears that the Coulomb interaction dominates over capacitance in this limit, hence this interaction becomes important only when $b \gg a$.

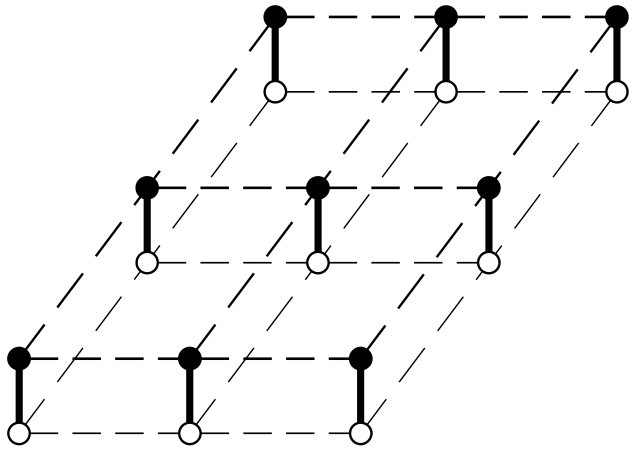

Figure 3.1: Two-dimensional bilayer lattice.

As we will show later, the capacitance term has a very high symmetry, $SU(4)$. One should expect the phase diagram resulting from such interaction to have a lot of phases in close proximity from each other. This is not necessarily a drawback, since, in fact, among the properties of the high-T_c cuprates that have long defied explanation is the proximity of the antiferromagnetic (AF) and d-wave superconducting (DSC) phases below the critical temperature. A recently proposed concept of an $SO(5)$ symmetry between AF and DSC phases [78] actually aimed to explain the former as well as the resonance mode observed in spin-flip neutron scattering on YBCO [79]. Several groups [80, 81, 82, 83, 84, 85] have constructed microscopic models with

exact $SO\,(5)$ symmetry, and it has been argued [86] that the 2-D Hubbard model has approximate $SO\,(5)$ symmetry. At first sight, this model seems to be artificial since it implies similar properties of the collective modes in different phases, while the properties of charge modes are dramatically different in the observed AF and DSC phases. In a recent modification of the theory [87, 88], Gutzwiller constraint was implemented exactly so that charge collective mode acquired a finite mass while magnon and hole-pair modes remained massless.

However, $SU\,(4)$ is a higher symmetry than $SO\,(5)$ and actually includes the latter as a subgroup. In Refs. [89, 90], the large-n limit of $SU\,(n)$ model has been studied by using the $1/n$ expansion. It has been found that in the strong coupling limit the ground state breaks translational symmetry and represents a density wave in which each site forms a dimer with one of its nearest neighbors. As the doping increases, a "kite" state with charge-density wave and no charge gaps forms. In the weak interaction limit, the flux state with full translational symmetry and gap vanishing at discrete points in momentum space was predicted. However, it was shown that at large n the ground state does not have off-diagonal long range order.

A real system that appears to have an $SU(4)$ symmetry is a quantum spin-1/2 antiferromagnet with twofold degenerate orbitals [91]. Such systems can be described by an $SU(4)$-symmetric Heisenberg model. Although Schwinger boson mean-field theory predicts long-range order in this model [92], it appears that the system is more likely to be a plaquette solid with alternating strong and weak correlations between the sites [93].

The algebra of $SU\,(4)$ is isomorphic to that of $SO\,(6)$. In Ref. [94] an $SO\,(6)$ model has been suggested, in which AF, DSC, and flux phases are unified. This and the subsequent work [95] have shown that the pinning of the Fermi level near a Van Hove singularity can explain the observed stripe phases [96] in cuprate superconductors. The essential difference between $SU\,(4)$ and $SO\,(6)$ is that a theory with $SO\,(6)$

symmetry assumes the presence of a 6-component vector (*superspin*) that transforms according to the adjoint representation. In case of the $SU(4)$ symmetry, there is no such vector, as one can only define the 5-component superspin for the $SO(5)$ subgroup.

In our model there are six possible phases that correspond to 15 generators of the $SU(4)$ algebra. The chemical potential reduces symmetry to $SO(4) \times U(1)$. This forced symmetry breaking leads to two phases and a quantum critical point between them, one phase unifying various density-wave states and the other unifying superconducting states. Although initially both phases have equal "rights" and one should expect the corresponding critical temperatures to be close, we will show that actually the density-wave phase requires stronger interaction than superconducting phase, at least in the weak-coupling regime.

3.1 Model

As it has been mentioned in the introduction, we will assume that the two-layer lattice is bipartite. In order to make the $SU(4)$ symmetry of the Hamiltonian explicit, let us group the fermion operators on a site into a 4-component operator

$$\Psi_j^\dagger = \left(\begin{array}{cccc} c_{j\uparrow}^{(1)\dagger}, & c_{j\downarrow}^{(1)\dagger}, & (-1)^j c_{j\uparrow}^{(2)}, & (-1)^j c_{j\downarrow}^{(2)} \end{array} \right). \tag{3.1}$$

Here $c_{j\sigma}^{(\lambda)\dagger}$ denotes a creation operator for the particle on site j of layer λ with spin σ. The terms that include only the scalar products of Ψ_j-operators are $SU(4)$-invariant. Those that involve the antisymmetric inner product $\Psi_{j\alpha}^\dagger E_{\alpha\beta} \Psi_{j\beta}^\dagger$ reduce the symmetry of the group to $Sp(4)$, or equivalently, $SO(5)$. As we will see below, such terms bring about interlayer hopping within the site.

We will study the model

$$\mathcal{H} = \mathcal{H}_{\text{kin}} + \mathcal{H}_{\text{int}} + \mathcal{H}_C + \mathcal{H}_{\text{chem}} \tag{3.2}$$

Here the kinetic (hopping) and the scalar interaction terms are $SU(4)$-invariant:

$$\mathcal{H}_{\text{kin}} = -t \sum_{\langle i,j\rangle \lambda\sigma} c_{i\sigma}^{(\lambda)\dagger} c_{j\sigma}^{(\lambda)} = -t \sum_{\langle i,j\rangle} \Psi_i^\dagger \Psi_j \tag{3.3}$$

$$\mathcal{H}_{\text{int}} = g \sum_j Y_j^2 = g \sum_j \left(\Psi_j^\dagger \Psi_j - 2\right)^2, \tag{3.4}$$

where the *hypercharge* operator $Y_j = n_j^{(1)} - n_j^{(2)} = \Psi_j^\dagger \Psi_j - 2$ and $n_j^{(\lambda)} = \sum_\sigma c_{j\sigma}^{(\lambda)\dagger} c_{j\sigma}^{(\lambda)}$. Thus, different layers have opposite hypercharge. Also note that the kinetic term is invariant only globally, since it contains scalar products of the operators on different rungs, while the interaction term is locally invariant as well. For the given kinetic term, the free energy spectrum of the fermions is $\varepsilon(k) = -2t(\cos k_x + \cos k_y)$. However, one can add $\varepsilon'(k) = -4t' \cos k_x \cos k_y$ to this expression to take into account next-nearest-neighbor hopping.

The $SU(4) \to SO(4) \times U(1)$ breaking terms are chemical potential and Coulomb interaction. The latter can be regarded also as superconductivity–antiferromagnetism anisotropy, as it can be expressed in terms of the square of the local spin operator:

$$\mathcal{H}_{\text{chem}} = -\mu \sum_j n_j, \tag{3.5}$$

$$\begin{aligned} \mathcal{H}_C &= -U \sum_j \left[\left(n_j^{(1)} - 1\right)^2 + \left(n_j^{(2)} - 1\right)^2 - 2\right] \\ &= -\frac{4U}{3} \sum_j \left(\left|\mathbf{S}_j^{(1)}\right|^2 + \left|\mathbf{S}_j^{(2)}\right|^2 + n_j\right). \end{aligned} \tag{3.6}$$

Here $n_j = n_j^{(1)} + n_j^{(2)}$. One can also introduce other symmetry breaking terms. For example the interlayer hopping has $SO(5)$ symmetry, therefore, its combination with

Eqs. (3.5,3.6) should reduce the symmetry to $SO(3) \times U(1)$:

$$\begin{aligned} \mathcal{H}_{\text{hop}} &= -t_\perp \sum_{j\sigma} c_{j\sigma}^{(1)\dagger} c_{j\sigma}^{(2)} + h.\ c. \\ &= -t_\perp \sum_{j\sigma} \Psi_j^\dagger E \Psi_j^\dagger + h.\ c., \end{aligned} \tag{3.7}$$

In the absence of interlayer hopping Eq. (3.7), the total hypercharge of the system $\sum_j Y_j$ is a conserved quantity.

Near the Fermi surface the lattice model Eq. (3.2) can be studied by using the continuum approximation. In the nodal $(\pi/2, \pi/2)$ direction the resulting Hamiltonian becomes very similar to that of Luttinger-Thirring [10, 97]. First, we replace the electron representation of the second layer with the hole one. In this case the operator $\Psi^\dagger$ will combine only creation operators, for electrons in the first layer and for holes in the second layer:

$$\Psi_j^\dagger = \left(\begin{array}{cccc} c_{j\uparrow}^{(1)\dagger}, & c_{j\downarrow}^{(1)\dagger}, & h_{j\uparrow}^{\dagger(2)}, & h_{j\downarrow}^{\dagger(2)} \end{array} \right). \tag{3.8}$$

Second, we introduce the 4-by-4 "Dirac" matrices

$$\gamma^0 = \left(\begin{array}{cc} 0 & 1 \\ 1 & 0 \end{array} \right), \quad \gamma^1 = \left(\begin{array}{cc} 0 & -1 \\ 1 & 0 \end{array} \right) \tag{3.9}$$

and the notation $\bar{\Psi} = \Psi^\dagger \gamma^0$. Finally, the linearized model in the $(\pi/2, \pi/2)$ direction becomes one-dimensional and "relativistic":

$$\mathcal{L} = \int dx\, \bar{\psi} \gamma^\mu p_\mu \psi + \mu \bar{\psi} \gamma^1 \psi + g' \left(\bar{\psi} \psi \right)^2. \tag{3.10}$$

In this formula $p_\mu = (i\partial_t, i\partial_x)$ is momentum, $\psi = (t/a)^{1/2} \Psi$ are the continuum fields,

and $g' = (a/t)\, g$ is Gross-Neveu coupling constant. The "mass" term

$$m\bar{\psi}\psi \to m\left(c_j^{(1)\dagger} h_j^{(2)} + h_j^{\dagger(2)} c_j^{(1)}\right) \tag{3.11}$$

actually does not conserve charge and must be zero. The chemical potential acts as magnetic field, which is consistent with the detailed analysis of interaction below (μ couples to one of the generators of the algebra, just like magnetic field couples to angular momentum). The conservation law for the current $\bar{\psi}\gamma^1\psi$ has physical meaning of charge conservation and for $\bar{\psi}\gamma^0\psi$ it is the conservation of hypercharge Y. These conservation laws imply that $\bar{\psi}\gamma^\mu\psi = \epsilon^{\mu\nu}\partial_\nu\phi$ with ϕ being a bosonic field [98]. Thus, along (π, π) direction, the behavior of the model can be expressed in terms of Schwinger bosons.

As it has been mentioned before, the interaction term in Eq. (3.2) can be interpreted as the contribution of the capacitor at site j formed by the layers. It can be written as a sum of 15 generators of $SO\,(6) \cong SU\,(4)$ so that $\mathcal{H}_{\text{int}}$ becomes $\sum_j \hat{\mathcal{H}}_{\text{int},j}$ with

$$\begin{aligned}\hat{\mathcal{H}}_{\text{int},j} &= g\left[4 - \frac{1}{5}\sum_{a=0}^{5}\sum_{b=a+1}^{5}\left(\Psi_j^\dagger M_{ab}\Psi_j\right)^2\right] \\ &= 4g\left(1 - \frac{1}{5}\sum_{a=1}^{5}\mathcal{N}_{ja}^2 - \frac{1}{5}\sum_{a=1}^{5}\sum_{b=a+1}^{5}\mathcal{L}_{jab}^2\right).\end{aligned} \tag{3.12}$$

Here M_{ab} are the generators of the matrix representation of $SO\,(6)$ that acts on the space of 4-by-4 matrices by conjugation, $\mathcal{L}_{ab}$ are the generators of the representation of $SO\,(5)$ and $\mathcal{N}_a$ is the corresponding superspin:

$$M_{ab} = \frac{1}{2}\Psi^\dagger M_{ab}\Psi \quad \text{for } a, b = 1 \ldots 5, \tag{3.13a}$$

$$\mathcal{N}_a = \frac{1}{2}\Psi^\dagger M_{0a}\Psi \quad \text{for } a = 1 \ldots 5. \tag{3.13b}$$

It is convenient to choose the following representation for M_{ab} [80]:

$$
\begin{aligned}
M_{0a} &= \begin{pmatrix} \sigma_a & 0 \\ 0 & \sigma_a^T \end{pmatrix}, \ a = 1, 2, 3, \\
M_{04} &= \begin{pmatrix} 0 & -i\sigma_y \\ i\sigma_y & 0 \end{pmatrix}, \ M_{05} = \begin{pmatrix} 0 & \sigma_y \\ \sigma_y & 0 \end{pmatrix}, \\
M_{ab} &= -\frac{i}{2}\left[M_{0a}, M_{0b}\right], \ a, b = 1 \ldots 5.
\end{aligned}
\tag{3.14}
$$

The physical meaning of the components of $\mathcal{N}_a = (m_x, m_y, m_z, \mathrm{Re}\Delta_{\mathbf{Q}}, \mathrm{Im}\Delta_{\mathbf{Q}})^T$ is that $\mathbf{m} = \frac{1}{2}\left(\mathbf{S}^{(1)} - \mathbf{S}^{(2)}\right)$ is AF order parameter and $\Delta_{\mathbf{Q}} = \Delta \exp\left(-i\mathbf{Q}\cdot\mathbf{r}\right)$, where $\mathbf{Q} = (\pi, \pi)$, $\mathbf{S}^{(\lambda)} = \frac{1}{2}c^{(\lambda)\dagger}\boldsymbol{\sigma}c^{(\lambda)}$ and $\Delta = ic^{(1)}\sigma_y c^{(2)}$ is the superconducting order parameter. Similarly, $\mathcal{L}_{ab}$ incorporates spin operator $\mathbf{S} = \mathbf{S}^{(1)} + \mathbf{S}^{(2)}$, π–operator $\boldsymbol{\pi}^\dagger = -\frac{1}{2}c^\dagger\boldsymbol{\sigma}\sigma_y d^\dagger$, and electric charge density $Q = \frac{1}{2}\left(n^{(c)} + n^{(d)}\right) - 1$. In the absence of $SU\left(4\right)$ symmetry breaking, the components of $\mathcal{L}_{ab}$ can also evolve into order parameters, such as ferromagnetic order parameter and π-wave superconducting order parameter. The presence of the charge density Q among the generators of the algebra explains why the chemical potential is a symmetry-breaking term in this model. Also note that if we formally replace $c^{(2)}$- operators in $\Delta_{\mathbf{Q}}$ by $c^{(1)}$-operators, the result will coincide with the expression for the η-operator that generates $SO(3)$ pseudospin symmetry in the standard Hubbard model [99].

All 15 generators of $SU\left(4\right)$ algebra transform according to the adjoint representation of $SU\left(4\right)$. If it was an $SO(n)$ group, one would say that the generators form a 15-component superspin. However, this would be misleading in our case, as such a superspin would not be even an order parameter, since it is known from the theory of the 2-D standard Hubbard models on a bipartite lattice [100] that at half-filling below the transition the staggered-spin state has lower ground energy than the spatially homogeneous state. In such a state the $SU\left(4\right)$ generators will alternate the

sign at even and odd sites. Thus, charge-density wave (CDW), spin-density wave (SDW), and superconductivity (SC) are the only actually possible ordered phases at half-filling. In the *pure* $SU(4)$ theory there are totally six phases that can be classified by the type of order and the interlayer symmetry with respect to the exchange of $c^{(1)}$ and $c^{(2)}$-particles. The table below displays the $SU(4)$ generators that vary as $\cos(\mathbf{Q}\cdot\mathbf{r})$ for CDW and SDW states and the actual order parameters for the SC states, according to such a classification:

Order	CDW	SDW	SC
odd interlayer symmetry	$n^{(c)}-n^{(d)}$	$\mathbf{S}^{(c)}-\mathbf{S}^{(d)}$	$\Delta,\Delta^{\dagger}$
even interlayer symmetry	$n^{(c)}+n^{(d)}-2$	$\mathbf{S}^{(c)}+\mathbf{S}^{(d)}$	$\boldsymbol{\pi},\boldsymbol{\pi}^{\dagger}$

(3.15)

Note that the odd interlayer symmetry CDW phase takes place only when the coupling g is negative, while the rest only when it is positive.

In the BM states the generators vary as $\cos(\mathbf{Q}\cdot\mathbf{r})$, but due to the presence of $(-1)^j$ factor in Eq. (3.1), these generators (such as $\Delta_{\mathbf{Q}}$) become naturally related to the quantities that are constant everywhere in the SC state (such as Δ). The latter are the order parameters. In the case of CDW and SDW states, the order parameter is the amplitude of the variation of the corresponding generators between even and odd sites.

There are also 16 eigenstates of $\hat{\mathcal{H}}_{\text{int}}$ [Eq. (3.12)] that can be labeled by the eigenvalues of $\mathcal{N}^2=\sum_a\mathcal{N}_a^2$, $\mathcal{L}^2=\sum_a\sum_{b>a}\mathcal{L}_{ab}^2$, rung spin component S_z, charge density Q, and hypercharge Y (table 3.1). The ground state of $\hat{\mathcal{H}}_{\text{int}}$ is 6-fold degenerate, consisting of the singlet state $|\Omega\rangle=\frac{1}{\sqrt{2}}\left(c_{\uparrow}^{(1)\dagger}c_{\downarrow}^{(2)\dagger}-c_{\downarrow}^{(1)\dagger}c_{\uparrow}^{(2)\dagger}\right)|0\rangle$ and its five transformations by the components of the $SO(5)$ superspin, corresponding to the triplet magnetic and particle-hole pair states. Thus, in the ground state of the total interaction term $\mathcal{H}_{\text{int}}$, each site is occupied only by $c^{(1)}-c^{(2)}$ pairs.

In the strong coupling limit, the ground state is approximately one of $\mathcal{H}_{\text{int}}$ and we

state	$\mathcal{N}^2$	$\mathcal{L}^2$	Q	S_z	Y	$E_{\rm int}/U$
$\|\Omega\rangle$	20	0	0	0	0	0
$(N_1+iN_2)\|\Omega\rangle$	4	16	0	2	0	0
$(N_1-iN_2)\|\Omega\rangle$	4	16	0	-2	0	0
$N_3\|\Omega\rangle$	4	16	0	0	0	0
$(N_4+iN_5)\|\Omega\rangle$	4	16	2	0	0	0
$(N_4-iN_5)\|\Omega\rangle$	4	16	-2	0	0	0
$c_\uparrow\|\Omega\rangle$	5	10	1	-1	-1	1
$c_\downarrow\|\Omega\rangle$	5	10	1	1	-1	1
$d_\uparrow\|\Omega\rangle$	5	10	1	-1	1	1
$d_\downarrow\|\Omega\rangle$	5	10	1	1	1	1
$c_\uparrow^\dagger\|\Omega\rangle$	5	10	-1	1	1	1
$c_\downarrow^\dagger\|\Omega\rangle$	5	10	-1	-1	1	1
$d_\uparrow^\dagger\|\Omega\rangle$	5	10	-1	1	-1	1
$d_\downarrow^\dagger\|\Omega\rangle$	5	10	-1	-1	-1	1
$\Psi E\Psi\|\Omega\rangle$	0	0	0	0	-2	4
$\Psi^\dagger E\Psi^\dagger\|\Omega\rangle$	0	0	0	0	2	4

Table 3.1: Classification of the eigenstates of $\hat{\mathcal{H}}_{\rm int}$.

can derive the analog of the $t-J$ model by computing the second-order correction to the kinetic term (as zero and first orders vanish in the ground state). Using the identity $\mathbf{M}_{\alpha\beta}\cdot\mathbf{M}_{\gamma\delta} = 4\delta_{\alpha\delta}\delta_{\beta\gamma} - \delta_{\alpha\beta}\delta_{\gamma\delta}$ and taking into account that $Y_j = 0$ in the ground state of $\mathcal{H}_{\rm int}$, we find

$$\mathcal{H}_{t-J} = \mathcal{H}_{\rm kin} + J_g \sum_{\langle i,j\rangle} \left(\mathcal{M}_i \cdot \mathcal{M}_j - \mathbf{t}_i^\dagger \cdot \mathbf{t}_j \right), \tag{3.16}$$

where $J_g = t^2/g$, $\mathcal{M}_{j,ab} = \frac{1}{2}\Psi_j^\dagger M_{ab}\Psi_j$, and $\mathbf{t}_{j,ab} = \frac{1}{2}\Psi_j M_{ab}\Psi_j$. Note that in the given representation for M_{ab} some of the components of $\mathbf{t}_j$ vanish. The third term in Eq. (3.16) has a physical interpretation as pair hopping. The analysis of this model is complicated, since it is necessary to take into account the possibility that inlayer hopping may pass through a transition as well, so that $\left\langle \sum_{\langle i,j\rangle} c_i^{(\lambda)\dagger} c_j^{(\lambda)} \right\rangle \neq 0$. In such a case, the system will split into plaquettes [93].

3.2 Critical temperature in mean-field theory

The mean-field theory of Eq. (3.2) is a valuable source of information about the phase diagram of the model. First, we need to find the reduced form of the Hamiltonian and the corresponding values of the mean-field coupling constants. This can be done either by analyzing the behavior of interaction vertices under renormalization or by regrouping the terms in the Hamiltonian. The second approach is easier, but we will present both for completeness. Second, we will derive the eigenvalues of the reduced Hamiltonian and the free energy. Minimizing the free energy with respect to the order parameters gives the phase diagram.

We will allow U to take a small nonzero value. Then it is necessary to split $\mathcal{H}_{\rm int}$ in Eq. (3.4) into a sum of two terms so that one of them will be similar to the Coulomb term Eq. (3.6). Introduce two vectors $P^{(1)}$ and $P^{(2)}$ defined as follows: $P^{(1)}_\alpha = 1$ for $\alpha = 1, 2$ and 0 for $\alpha = 3, 4$ and $P^{(2)}_\alpha = 1 - P^{(1)}_\alpha$. Then each term in Eq. (3.12) can be represented as $\left(\Psi^\dagger_j M_{ab} \Psi_j\right)^2 = \tilde{h}^{(1)}_{j,ab} + \tilde{h}^{(2)}_{j,ab}$, where $\tilde{h}^{(1)}_{j,ab} = \mathcal{M}^{(1)2}_{j,ab} + \mathcal{M}^{(2)2}_{j,ab}$, $\tilde{h}^{(2)}_{j,ab} = 2\mathcal{M}^{(1)}_{j,ab}\mathcal{M}^{(2)}_{j,ab}$, $\mathcal{M}^{(i)}_{j,ab} = \Psi^\dagger_j M^{(i)}_{ab} \Psi_j$, and $M^{(i)}_{ab} \equiv M_{ab} \cdot P^{(i)}$. Thus,

$$\mathcal{H}_{\rm int} + \mathcal{H}_C = -\frac{1}{5}(4g + U) \sum_j \sum_{a>b} \left(\mathcal{M}^{(1)2}_{j,ab} + \mathcal{M}^{(2)2}_{j,ab}\right) - \frac{4g}{5} \sum_j \sum_{a>b} 2\mathcal{M}^{(1)}_{j,ab}\mathcal{M}^{(2)}_{j,ab}, \quad (3.17)$$

up to an additive constant. In the diagrammatic calculations, the vertices $\mathcal{T}^{(1)}$ and $\mathcal{T}^{(2)}$, corresponding to the first and the second terms in Eq. (3.17) respectively, satisfy the identities $\mathcal{T}^{(z)} = \mathcal{T} \circ \mathcal{U}^{(z)}$, $z = 1, 2$, where $(A \circ B)^{(\gamma_1,\gamma_2;\gamma_3,\gamma_4)} \equiv \sum_{\beta_1\beta_2} A^{(\gamma_1,\gamma_2;\beta_1,\beta_2)} B^{(\beta_1,\beta_2;\gamma_3,\gamma_4)}$, and $\mathcal{U}^{(z)(\gamma_1,\gamma_2;\gamma_3,\gamma_4)}$ are antisymmetric with respect to

the interchange $\gamma_1 \leftrightarrow \gamma_2$ and $\gamma_3 \leftrightarrow \gamma_4$ and are defined by the components:

$$\begin{aligned}
\mathcal{U}^{(1)(12;12)} &= \frac{1}{2},\ \mathcal{U}^{(1)(34;34)} = \frac{1}{2}, \\
\mathcal{U}^{(2)(13;13)} &= \frac{1}{2},\ \mathcal{U}^{(2)(14;14)} = \frac{1}{2}, \\
\mathcal{U}^{(2)(23;23)} &= \frac{1}{2},\ \mathcal{U}^{(2)(24;24)} = \frac{1}{2}.
\end{aligned}$$

The rest of the components of $\mathcal{U}^{(z)}$ that remain undetermined after antisymmetrization are zero. Then it follows that $\mathcal{U}^{(z)}$ and $\mathcal{T}^{(z)}$ have the following properties: $\mathcal{U}^{(1)} \circ \mathcal{U}^{(2)} = 0$, $\mathcal{T}^{(z)} \circ \mathcal{U}^{(z)} = \mathcal{U}^{(z)} \circ \mathcal{T}^{(z)} = \mathcal{T}^{(z)}$, $\mathcal{T}^{(z)} \circ \mathcal{T}^{(z)} = \left(\Gamma^{(z)}\right)^2 \mathcal{U}^{(z)}$, where $\Gamma^{(1)} = g_{\mathrm{DW}}$, $\Gamma^{(2)} = g_{\mathrm{SC}}$ and

$$g_{\mathrm{DW}} = \frac{1}{5}\left(4g + U\right), \tag{3.18a}$$

$$g_{\mathrm{SC}} = \frac{4g}{5}. \tag{3.18b}$$

The alternative approach, regrouping terms in Eq. (3.2), immediately produces the reduced Hamiltonian with the same mean-field coupling constants as in Eq. (3.18):

$$\mathcal{H}_{\mathrm{red}} = \mathcal{H}_{\mathrm{kin}} - g_{\mathrm{DW}} \sum_j \left(|\mathbf{m}_j|^2 + |\mathbf{S}_j|^2\right) - g_{\mathrm{SC}} \sum_j \left(|\Delta_j|^2 + |\boldsymbol{\pi}_j|^2\right). \tag{3.19}$$

The eigenvalues of the reduced Hamiltonian are $\pm E\left(\mathbf{k}; s\right)$, where

$$E\left(\mathbf{k}; s\right) = \left\{ \left[s\sqrt{\varepsilon\left(k\right)^2 + M^2} + \epsilon'\left(k\right) - \mu \right]^2 + \Delta^2 \right\}^{1/2}, \quad s = \pm 1, \tag{3.20}$$

where m and Δ are density-wave and superconducting order parameters, respectively,

which turn nonzero at the phase transition. The free energy is

$$F(m,\Delta;T,\mu)=\frac{|m|^2}{g_{\mathrm{DW}}}+\frac{|\Delta|^2}{g_{\mathrm{SC}}}+\sum_{s=\pm1}\int_{\substack{k_x>0\\k_y>k_x}}\left(s\left|\varepsilon(\mathbf{k})\right|-\varepsilon'(\mathbf{k})-\mu\right.$$
$$\left.-2T\ln\left\{2\cosh\left[\frac{1}{2T}E(\mathbf{k};s)\right]\right\}\right). \quad (3.21)$$

Expanding this formula in terms of m and Δ up to the fourth order leads to the analog of the Ginzburg-Landau theory. The term of order of $|m|^2|\Delta|^2$ turns out to be positive, therefore, the phases do not tend to coexist with each other.

Minimizing the free energy with respect to the order parameters leads to the gap equations. In particular, the equations on critical temperatures (assuming the absence of the other order) are

$$1=\frac{g_{\mathrm{DW}}}{2}\int\frac{d^2k}{(2\pi)^2}\frac{1}{\varepsilon(\mathbf{k})}\tanh\left(\frac{\varepsilon(\mathbf{k})+\varepsilon'(\mathbf{k})-\mu}{2k_BT_{\mathrm{DW}}}\right), \quad (3.22)$$

$$1=\frac{g_{\mathrm{SC}}}{2}\int\frac{d^2k}{(2\pi)^2}\left[\frac{1}{\varepsilon(\mathbf{k})+\varepsilon'(\mathbf{k})-\mu}\tanh\left(\frac{\varepsilon(\mathbf{k})+\varepsilon'(k)-\mu}{2k_BT_{\mathrm{SC}}}\right)\right]. \quad (3.23)$$

Apparently, in case of nonzero $\varepsilon'(\mathbf{k})$, the integral of Eq. (3.22) is smaller than the integral of Eq. (3.23), since the former includes parts near the Fermi surface that cancel each other, while the expression in the latter always stays positive. Consequently, for the same values of g_{DW} and g_{SC}, the critical temperature of density-wave transition T_{DW} will be smaller that one for superconducting state T_{SC}. The integrals can be evaluated for weak interaction and $\varepsilon'(\mathbf{k})=0$ (see Appendix C), which gives

the following value of the critical temperature:

$$k_B T_c \simeq 2tD \exp\left(-\frac{\pi^2}{\ln\left(\frac{2t}{|\mu|}\right)}\frac{2t}{g_{\mathrm{DW}}}\right), \quad \frac{k_B T_c}{2t} \ll \frac{|\mu|}{2t} \ll 1, \tag{3.24a}$$

$$\simeq 2tD\left(\frac{|\mu|}{2t}\right)^{3/8}, \qquad \frac{|\mu|}{2t} \ll \frac{k_B T_c}{2t} \ll 1, \tag{3.24b}$$

where $D = \gamma 2^{1/4}/\pi^{1/2} \approx 0.387$ and $\gamma \approx 0.577$ is Euler's constant.

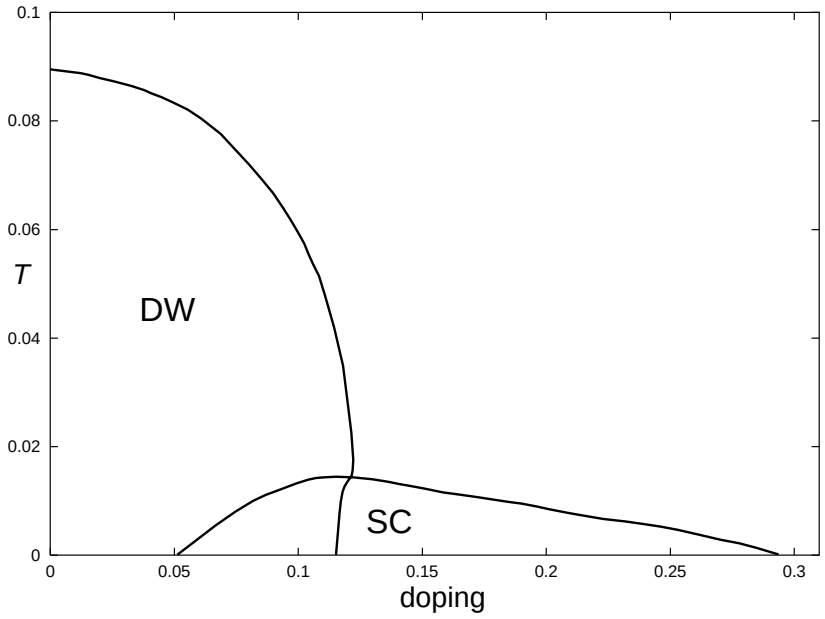

Figure 3.2: Phase diagram for $2t = 1$ eV, $t' = -0.05$ eV, $g_{\mathrm{DW}} = 0.1$ eV and $g_{\mathrm{SC}} = 0.05$ eV.

This agrees with the phase diagram Fig. 3.2, on which $g_{\mathrm{DW}} > g_{\mathrm{SC}}$ so that density-wave transition has higher critical temperature at half-filling, but away from half-filling the density-wave phase does not survive at all and we can only see the superconducting phase there, although at low temperatures due to small g_{SC}. (See Appendix D for the computation details.) However, one ought to remember that it corresponds

to the calculation in the weak-interaction regime. In the case of strong interaction, one must use Eq. (3.16) instead and both superconducting and density-wave states will have the same energy.

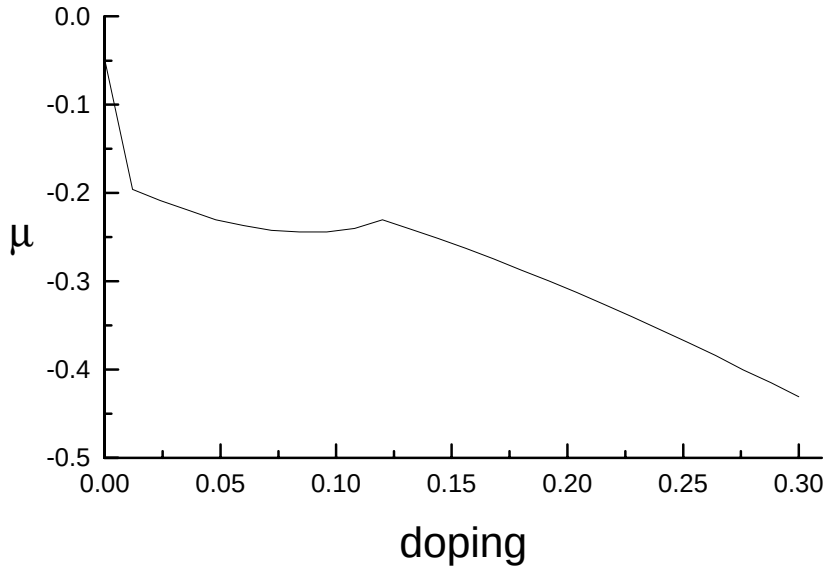

Figure 3.3: Chemical potential for $2t = 1$ eV, $t' = -0.05$ eV, $g_{\rm DW} = 0.1$ eV and $g_{\rm SC} = 0.05$ eV at $T = 0.006$ eV.

Note that the chemical potential μ no longer vanishes at half-filling due to $t' \neq 0$, instead it vanishes approximately at doping $x = -0.11$ and $\mu \simeq -0.13$ at doping $x = 0$. The dependence of μ on doping is nonmonotonic (Fig. 3.3), which is due to the fact that mean-field theory does not take into account fluctuations. The fluctuational corrections restore the thermodynamic inequality $\partial\mu/\partial x < 0$, but it is possible to correct the dependence approximately by using the analog of Maxwell's construction.

The figure 3.2 also includes a region of coexistence of the phases. If this corresponded to true long-range order, it would mean that both order parameters are nonzero so that the system is superconducting, but the translational and rotational symmetries are broken. However, the proximity of two quantum critical points should immediately alert us, as the region of coexistence is likely to be equally affected by both thermal and quantum effects. In this case the physics at length scales less than

$\lambda\!\!\!^{-}_T = \hbar/\sqrt{mT}$ and time scales less than $\hbar/T$ retains most of the features of quantum critical behavior and thermal effects begin to dominate only in the opposite limits.

3.3 Discussion

We have studied a simple model on a 2-D bipartite bilayer lattice, which includes an interaction of the fermions between the layers. This interaction can be interpreted as energy of the capacitor formed by the layers at each site of the lattice. In this model the interaction term in the Hamiltonian has very high $SU\,(4)$ symmerty. The symmetry breaking factors include chemical potential and Coulomb interaction, but the remaining symmetry should be broken spontaneously at the transition. This occurs at temperatures that is probably lower that the mean-field critical temperature, with transition being of Kosterlitz-Thouless type with additional elements of a 3-D phase transition due to interlayer coupling. Between the mean-field critical temperature and the temperature of the global phase transition, the system remains almost normal (metallic), but develops several non-Fermi-liquid features when the local order becomes superconducting. The fermions that belong to different layers have opposite "hypercharge," which becomes a symmetry-related quantum number. In the presence of interlayer hopping the total hypercharge of the system is no longer conserved, which significantly reduces the symmetry.

Although the symmetry of the model is even higher than $SO(5)$, the physical meaning of the components of the order parameter is slightly different from those given in Ref. [78], as the ground state of the "antiferromagnetic" phase is actually a density wave with varying local Néel vector. In the strong $SU\,(4)$ interaction limit, the Hamiltonian resembles one of $t-J$ model, but also includes a pair hopping term with operators similar to those introduced in Ref. [101].

The condition on the phase transition has been evaluated in weak interaction

limit in mean-field theory. We have found that in this case the superconducting phases dominate over the density-wave states. Even if due to Coulomb interaction the density-wave phase has higher transition temperature than the superconducting phase at half-filling, the situation becomes the opposite away from half-filling, where the density-wave eventually disappears. The region of coexistence of the density-wave and superconducting order is likely to be affected by the proximity of two quantum critical points.

Chapter 4 $d_{x^2-y^2}$ Density Wave Order

4.1 Introduction

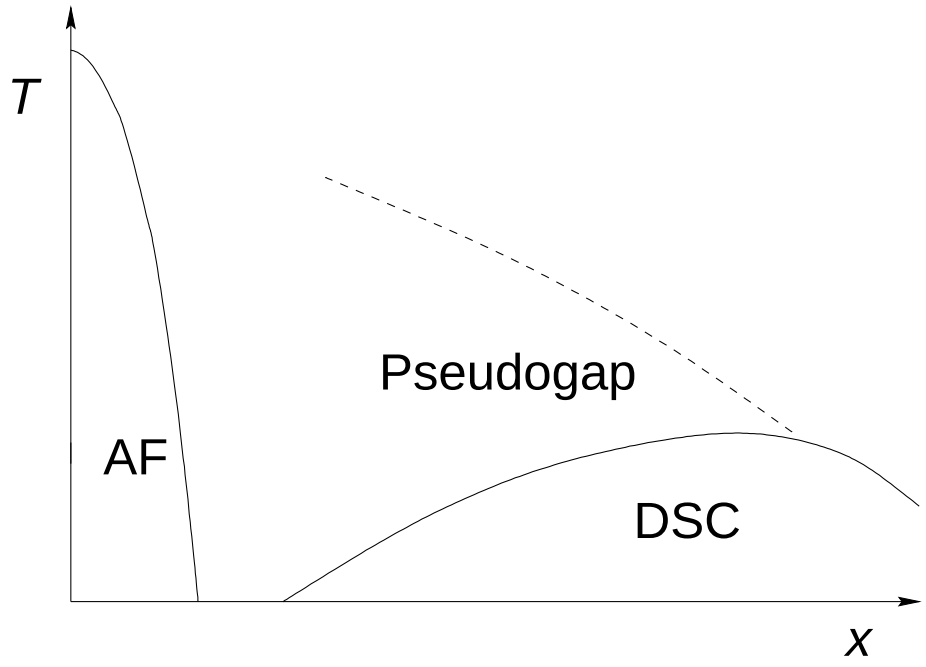

Figure 4.1: The sketch of the experimentally observed phase diagram in High-T_c cuprates.

The phase diagrams of high-T_c cuprates have many common features, some of which are shown schematically on Fig. 4.1. One of such features is the decrease of critical temperature of the superconducting transition T_c with underdoping. It is natural to explain it by the competition of superconducting order with some other orders. The latter could be long-range, such as antiferromagnetic order, which is already residing in the phase diagram in the low-doping region, or it could local order.

Another kind of peculiar behavior that the high-T_c cuprates exhibit when underdoped is that the density of states is depleted at low energies, as if some of the degrees of freedom of the system were developing a gap. This behavior, observed in optical conductivity [102, 103], NMR [104, 105], angle-resolved photoemission [106, 107], c-axis tunneling [108], and specific heat measurements [109], was dubbed the "pseudogap." The emergence of the pseudogap mimics somewhat the impoverishment of the low-energy excitation spectrum which accompanies the development of $d_{x^2-y^2}$ superconductivity and resembles, more generally, the type of gap formation which is concomitant with a large class of order parameters. However, it does not — at first glance — appear to be connected with the formation of an ordered state. Consequently, it was initially believed that the pseudogap was a crossover phenomenon and the attempts to describe it depended on various approximate methods of treating states with local, fluctuating order [29, 31, 110, 111, 112]. These theories have a common difficulty related to the fact that a fluctuating order would normally have to have a soft mode associated with it, which has not yet been observed experimentally.

However, it has recently been proposed that the 'pseudogap' state *is* actually a broken-symmetry ordered state, and that the signatures of the order are subtle enough that the state was able to appear incognito [113, 114, 115]. The absence of a static charge order at intermediate and high temperatures observed in X-ray and electronic-transport experiments eliminates the possibility of a charge-density wave order. Also, the angular resolved photoemission experiments [116, 117] suggest that the pseudogap has $d_{x^2-y^2}$-wave symmetry — just like the order in the superconducting phase. In Ref. [113], the $d_{x^2-y^2}$ density-wave (DDW) state [118, 119, 120, 121] was advanced as a candidate order.

DDW is a particle-hole condensate characterized by the following correlation func-

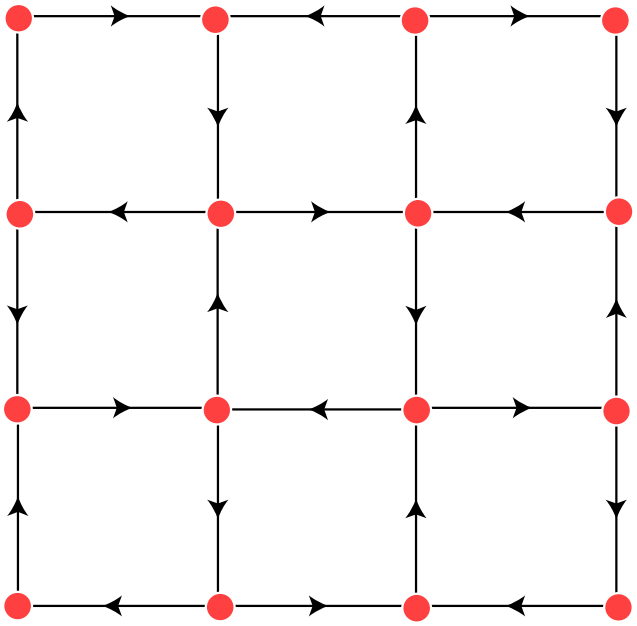

Figure 4.2: Orbital currents in $d_{x^2-y^2}$-density-wave phase.

tion taking a nonvanishing mean-field value:

$$\left\langle c^{\alpha\dagger}\left(k+Q,t\right)c_{\beta}\left(k,t\right)\right\rangle =\delta_{\beta}^{\alpha}\Phi f\left(k\right), \tag{4.1}$$

where $Q=(\pi/a,\pi/a)$, a is lattice spacing. This would be a charge density wave (CDW) for $f\left(k\right)=1$, but the DDW order is characterized by a different angular symmetry, $f\left(k\right)=\frac{1}{2}\left(\cos k_{x}a-\cos k_{y}a\right)$. Like CDW, DDW does not break any continuous symmetries, but it does break three discrete $\mathbb{Z}_2$ symmetries: time-reversal, translational, and rotational by $\pi/2$. This phase is described phenomenologically by a pattern of the alternating orbital currents (Fig. 4.2), which has to be associated with a staggered magnetic field of order of 10 gauss [113, 122, 123, 124].

The realization that pseudogap being a DDW state is a realistic possibility has led to a re-examination of the experimental circumstances. Recent *elastic* neutron scattering experiments, which directly probe the symmetries broken by DDW order — time-reversal and translation by one lattice spacing — appear to have observed

it [125]. A number of other experiments are consistent with the proposal [113], especially measurements of the superfluid density as a function of doping [28].

The results of the experiment by Mook et al. [125] have been analyzed theoretically in Ref. [126].[1] The observed Bragg scattering rods from small momenta at the in-plane vector $Q = (\pi/a, \pi/a)$ indicate the presence of a two-dimendional (2-D) static order, which breaks time-reversal and translational symmetries. In principle, this picture could certainly agree not only with DDW, but also with other orders, notebly, antiferromagnetic one. However, the magnitude of observed magnetic moments was 50 times smaller than in the undoped antiferromagnet, therefore, if it was in fact an antiferromagentic phase, it would not agree with high temperature T^* (about 190 K) at which the pseudogap state begins to evolve. The scattering intensity decreased rapidly with scattering wavevector q_z, which implies that the size of magnetic moments was large, i.e., it was of order of the current loops on Fig. 4.2 rather than of order of a single Cu atom. Finally, an antiferromagnetic order breaks continuous rotational symmetry, therefore, according to Mermin-Wagner-Coleman theorem, it should be three-dimensional (3-D). Instead, the order remained 2-D even at low temperatures and no Goldstone mode that would have been associated with spontaneous breaking of a continuous symmetry had been observed.

The experimental situation seems promising, which is strong incentive to reconsider the theoretical state of affairs. If the 'pseudogap' state is, indeed, an ordered state, then we should be able to study it within mean-field theory, as we would study the antiferromagnetic state, superconducting state, or any other ordered state. Mean-field theory is unlikely to explain the detailed shape of the phase boundary, but one can hope that it will capture the broad features of the phase diagram, such as its topology and the basic temperature scales. Deep within any phase, with $T \to 0$ and far from any quantum phase transitions, the mean-field Hamiltonian should be the

[1] See also the earlier work by Hsu et al. [124].

correct Hamiltonian, although the parameters in it may need to be renormalized from their mean-field values. Thus, it seems natural to simultaneously study the antiferromagnetic (AF), $d_{x^2-y^2}$-wave superconducting (DSC), and DDW order parameters in mean-field theory. The interplay and possible coexistence of these orders should be qualitatively and semi-quantitatively explained by mean-field theory. Phase transitions, quantum or thermal, may not be accurately described in their asymptotic limits, but the AF, DDW, and DSC phases will, as will possible phases with coexisting AF, DDW, and DSC orders.

However, there is an immediate problem faced by such a program. What microscopic Hamiltonian should be used? In the early days of high-T_c, it was hoped that the important physics of strong local repulsion and superexchange, which is present in the simplest models, such as the Hubbard and $t-J$ models, would be sufficient to explain all of the interesting physics of the cuprates. This appears not to be the case. Monte Carlo studies have not found superconductivity in the Hubbard model [127, 128, 129], while Monte Carlo calculations, exact diagonalization, and density-matrix renormalization-group (DMRG) calculations give conflicting results for the $t-J$ model [130, 131, 132]. DMRG studies have found that the behavior of n-leg ladders depends sensitively on the strength of, for instance, second-neighbor hopping [133], as have Monte Carlo studies [134]. Indeed, some numerical results are sensitively dependent on boundary conditions [135], which is further indication of the instability of many of these models to relatively small changes in the parameters. Furthermore, the physics of charge-ordering is probably not correctly described by the $t-J$ model without near-neighbor (and possibly long-range) Coulomb repulsion [30, 136, 137, 138]. Indeed, it is also clear from experiments that relatively small changes — such as those associated with substituting Nd for La [96, 139], which is off the radar screen of the $t-J$ and Hubbard models — can radically change at least some aspects of the behavior of these materials. In short, the detailed form of the

underlying Hamiltonian matters.

Fortunately, we are not completely in the dark about the nature of the microscopic Hamiltonian. Local Coulomb repulsion, both on-site and near-neighbor, is clearly an important part of the physics. This is known from microscopic calculations of the Hubbard parameters t, U, and also from the fact that the undoped parent compounds are antiferromagnetic insulators. The other important clue, which derives entirely from experiments, is that the cuprates superconduct. The correct microscopic model (or models) must support d-wave superconductivity when doped away from half-filling. If the Hubbard and $t-J$ do not have this property — and it appears that they do not for t/U small — then they cannot describe the cuprates fully.

Our strategy will be to take a generalization of the Hubbard model which includes next-neighbor repulsion and, most importantly, pair-hopping (or correlated hopping). The pair-hopping term favors superconductivity. Even when it is relatively small, it stabilizes superconductivity in the Hubbard model, as we will see. There are a variety of ways in which such a term — or another term with similar effect — could arise, either from quantum chemistry [140, 141, 142] or in the passage to an effective description such as the $t-J$ model; in both cases, it is essentially a result of strong local Coulomb repulsion, as superexchange is. In any event, it appears that such physics is necessary to stabilize superconductivity, so we will incorporate it in our model. We will find that such a term also leads to DDW order.

Since the experiments suggest that the DDW order has an antisymmetric configuration with respect to the layers, we will study a bilayer model. Of course, the main reason why antisymmetric configuration has lower energy than symmetric one is because interlayer repulsive interactions renormalize the coupling constants so that the interaction that favors the DDW phase appears to be stronger for antisymmetric case and weaker for the symmetric one. We will also study the role of the interlayer tunneling.

To summarize, we consider a model which is chosen so that it incorporates the basic physics of strong local repulsion *and* so that will have a phase diagram which includes AF at half-filling and DSC at some finite doping. We find that it naturally supports DDW order. In mean-field theory, we find a phase diagram in the temperature-doping plane which resembles the experimental phase diagram of the cuprates, with the DDW phase boundary playing the role of the experimental pseudogap onset line. This DDW line continues into the DSC state, so that the underdoped superconducting state is characterized by both DSC and DDW orders. At low doping, there is also a region of coexistence between AF and DDW orders. We comment on the interpretation of experiments vis-à-vis our findings.[2]

4.2 Model Hamiltonian

We consider the following bilayer lattice model of interacting electrons [122]:

$$\mathcal{H} = \mathcal{H}_{\rm kin} + \mathcal{H}_{\rm int}, \tag{4.2}$$

where

$$\begin{aligned}\mathcal{H}_{\rm kin} = -t_{ij} \sum_{\langle i,j \rangle} \left(c_{i\sigma}^{(\lambda)\dagger} c_{j\sigma}^{(\lambda)} + \text{h.c.} \right) \\ + \frac{t_\perp}{16} \sum_i \Big(c_{i+\hat{x}+\hat{y},\sigma}^{(1)\dagger} c_{i\sigma}^{(2)} + c_{i+\hat{x}-\hat{y},\sigma}^{(1)\dagger} c_{i\sigma}^{(2)} \\ - c_{i\sigma}^{(1)\dagger} c_{i\sigma}^{(2)} - c_{i+2\hat{x},\sigma}^{(1)\dagger} c_{i\sigma}^{(2)} + x \to y + 1 \to 2 + \text{h.c.} \Big),\end{aligned} \tag{4.3}$$

and

$$\mathcal{H}_{\rm int} = U \sum_i n_{i\uparrow}^{(\lambda)} n_{j\downarrow}^{(\lambda)} + V \sum_{\langle i,j \rangle} n_i^{(\lambda)} n_j^{(\lambda)} - t_c \sum_{\substack{\langle i,j \rangle, \langle i',j \rangle \\ i \neq i'}} c_{i\sigma}^{(\lambda)\dagger} c_{j\sigma}^{(\lambda)} c_{j\sigma}^{(\lambda)\dagger} c_{i'\sigma}^{(\lambda)}. \tag{4.4}$$

[2] The following sections in this chapter are from Ref. [143].

In the formulas above, t_{ij} is hopping with $t_{ij} = t$ for nearest neighbors, $t_{ij} = t'$ for next nearest neighbors and $t_{ij} = 0$ otherwise. The other parameters are the tunneling $t_\perp$, the on-site repulsion U, the nearest-neighbor repulsion V, and next-nearest-neighbor correlated hopping t_c. The indices i, j correspond to a lattice site, σ to the spin, and λ to the layer.

The next-nearest-neighbor correlated hopping term is physically kinetic, but since it is also quartic, we are going to treat it as interaction. It hops an electron from i' to j when j is vacated by an electron hopping to i. These two hops are correlated by virtue of Coulomb interaction between the electrons. The presence of this term in the cuprates has been shown in band-structure calculations [141]. Correlated hopping has been discussed in Refs. [142, 144, 145, 146] as a possible mechanism of superconductivity, but it has also been found [122] that it favors DDW order as well.

The tunneling term is momentum conserving [146, 147]. We consider a CuO_2 bilayer because the pseudogap has been best characterized in bilayer materials such as YBCO and Bi2212.

To derive a mean-field theory, it is convenient to take the Fourier transform of Eq. (4.2) and regroup the terms. This task would be particularly simple if there were only one phase at a given set of parameters. For example, a DDW reduced Hamiltonian would look like

$$\mathcal{H}_{\mathrm{DDW}} = -g_{\mathrm{DDW}} \int_{k,k'} f(k)\, f(k')\, c^{(\lambda)\dagger}_{k+Q,\sigma} c^{(\lambda)}_{k\sigma} c^{(\lambda)\dagger}_{k'\sigma'} c^{(\lambda)}_{k'+Q,\sigma'}, \tag{4.5}$$

where $f(k) = \cos k_x - \cos k_y$ (the lattice spacing has been set to unit) and the DDW mean-field coupling constant is

$$g_{\mathrm{DDW}} = 8V + 24t_c. \tag{4.6a}$$

Similar values of the mean filed coupling constants can be derived for other phases as

well. Thus, for antiferromagnesm, d-wave superconductivity and (π, π) charge-density wave we derive:

$$g_{\mathrm{AF}} = 2U, \tag{4.6b}$$

$$g_{\mathrm{DSC}} = 12t_c - 8V, \tag{4.6c}$$

$$g_{\mathrm{CDW}} = 16V + 24t_c - 2U. \tag{4.6d}$$

In fact, the interaction part of the Hamiltonian Eq. (4.4) can be further generalized to include the *interlayer* Coulomb interactions:

$$\mathcal{H}'_{\mathrm{int}} = U' \sum_i n_i^{(\lambda)} n_j^{(\lambda')} + V' \sum_{\langle i,j \rangle} n_i^{(\lambda)} n_j^{(\lambda')}, \tag{4.7}$$

where $\lambda \neq \lambda'$. Then for the given interlayer configuration of the order parameters (antisymmetric for AF and DDW and symmetric for DSC), the mean field coupling constants become

$$g_{\mathrm{DDW}} = 8V + 8V' + 24t_c, \tag{4.8a}$$

$$g_{\mathrm{AF}} = 2U + 2U', \tag{4.8b}$$

$$g_{\mathrm{DSC}} = 12t_c - 8V + 8V'. \tag{4.8c}$$

For the opposite configuration (symmetric for AF and DDW and antisymmetric for DSC), the contributions of U', V' would be negative, which is the main reason why such configurations have generally higher energy and are not observed. On the other hand, the fact that five interaction terms produce only three phases means that we can have the same phase diagrams (corresponding to a given set of g_p's) for a range of values of the interaction constants. In the following section we will assume that $U' = V' = 0$, so that each phase diagram will correspond to a unique set of U, V, t_c.

The total Hamiltonian contains the reduced parts corresponding to these phases as well as the interactions between the order parameters. However, since we expect g_{CDW} to be negative so that the corresponding order parameter is always zero, we will ignore the term corresponding to this phase. The final form of the reduced Hamiltonian is

$$\begin{aligned}\mathcal{H}_{\mathrm{red}} = \int_k \epsilon_{k\lambda\lambda'} c_{k\sigma}^{(\lambda)\dagger} c_{k\sigma}^{(\lambda')} \\ - g_{\mathrm{AF}} \int_{k,k'} c_{k+Q,\sigma}^{(\lambda)\dagger} c_{k\sigma}^{(\lambda)} c_{k'\sigma'}^{(\lambda)\dagger} c_{k'+Q,\sigma'}^{(\lambda)} \\ - g_{\mathrm{DDW}} \int_{k,k'} f(k) f(k') c_{k+Q,\sigma}^{(\lambda)\dagger} c_{k\sigma}^{(\lambda)} c_{k'\sigma'}^{(\lambda)\dagger} c_{k'+Q,\sigma'}^{(\lambda)} \\ - g_{\mathrm{DSC}} \int_{k,k'} f(k) f(k') c_{k\uparrow}^{(\lambda)\dagger} c_{-k\downarrow}^{(\lambda)\dagger} c_{k'\uparrow}^{(\lambda)} c_{-k'\downarrow}^{(\lambda)}, \quad (4.9)\end{aligned}$$

where $\epsilon_{k11} = \epsilon_{k22} = \epsilon_k + \epsilon'_k$, $\epsilon_k = -2t(\cos k_x + \cos k_y)$, $\epsilon'_k = -4t' \cos k_x \cos k_y$, $\epsilon_{k12} = \epsilon_{k21} = \epsilon_{k\perp} = (t_\perp/4) f(k)^2$.

The standard Hubbard-Stratonovich mean-field-theoretical treatment of Eq. (4.9) is to assume the presence of a bosonic mean field, defined as an order parameter, neglect the fluctuations, find the eigenvalues of the Hamiltonian and finally, integrate out the fermion degrees of freedom to derive the free energy.

We define the order parameters of DDW, AF and DSC phases as follows:

$$\phi_\lambda = g_{\mathrm{DDW}} \int_k f(k) c_{k+Q,\sigma}^{(\lambda)\dagger} c_{k\sigma}^{(\lambda)}, \quad (4.10a)$$

$$M_\lambda = g_{\mathrm{AF}} \int_k c_{k+Q,\sigma}^{(\lambda)\dagger} c_{k\sigma}^{(\lambda)}, \quad (4.10b)$$

$$\Delta_\lambda = g_{\mathrm{DSC}} \int_k f(k) c_{k\uparrow}^{(\lambda)\dagger} c_{-k\downarrow}^{(\lambda)\dagger}. \quad (4.10c)$$

We assume that ϕ_λ and M_λ are anti-symmetric in the bilayer index. Then, the

free energy of the system is

$$f = \frac{|M|^2}{g_{\mathrm{AF}}} + \frac{|\phi|^2}{g_{\mathrm{DDW}}} + \frac{|\Delta|^2}{g_{\mathrm{DSC}}} + \sum_{s_1,s_2,s_3=\pm 1} \int_{\substack{k_x>0 \\ k_y>k_x}} \left[s_1\epsilon_k + \epsilon'_k + s_2\epsilon_{k\perp} - \mu \right.$$
$$- 2T \ln \left(2\cosh \left\{ \frac{1}{2T} \left[\left\{ f(k)\,\Delta \right\}^2 + \left(s_1 \left\{ \left[\epsilon_k + s_2\epsilon_{k\perp} \right]^2 \right. \right. \right. \right.$$
$$\left. \left. \left. \left. + \left[f(k)\,\phi + s_3 M \right]^2 \right\}^{1/2} + \epsilon'_k - \mu \right)^2 \right]^{1/2} \right\} \right) \Bigg] . \quad (4.11)$$

As we expand this expression for small values of the order parameters, we can construct a Ginzburg-Landau theory:

$$f(T) = f_0(T) + \sum_p a_p \left|\Phi_p\right|^2 + \sum_p b_p \left|\Phi_p\right|^4 + \sum_{p\neq p'} c_{pp'} \left|\Phi_p\right|^2 \left|\Phi_{p'}\right|^2 , \quad (4.12)$$

where p denotes the kind of the order parameter (AF, DDW or DSC) and Φ_p is the order parameter (M, ϕ or Δ, respectively). The a_p coefficients cross zero at the transitions so that $a_p = 0$ are the equations that determine critical temperature T_c:

$$a_p = \frac{1}{g_p} - \sum_{s_1,s_2,s_3=\pm 1} \int_{\substack{k_x>0 \\ k_y>k_x}} K_p(k) , \quad (4.13)$$

where

$$K_{\mathrm{AF}}(k) = \frac{1}{2\left|\bar{\epsilon}_k\right|} \tanh\left(\frac{\left|\bar{\xi}_k\right|}{2T} \right) , \quad (4.14a)$$

$$K_{\mathrm{DDW}}(k) = f(k)^2 K_{\mathrm{AF}}(k) , \quad (4.14b)$$

$$K_{\mathrm{DSC}}(k) = \frac{f(k)^2}{2\left|\bar{\xi}_k\right|} \tanh\left(\frac{\left|\bar{\xi}_k\right|}{2T} \right) . \quad (4.14c)$$

Here $\bar{\xi}_k = s_1\epsilon_k + s_2\epsilon_{k\perp} + \epsilon'_k - \mu$ and $\bar{\epsilon}_k = \epsilon_k + s_2\epsilon_{k\perp}$. The b_p coefficients are positive:

$$b_p = \sum_{s_1,s_2,s_3=\pm 1} \int_{\substack{k_x>0 \\ k_y>k_x}} K'_p(k) , \quad (4.15)$$

where

$$K'_{\mathrm{AF}}(k) = \frac{\eta_1(k)}{8\left|\bar{\epsilon}_k\right|^3}, \tag{4.16a}$$

$$K'_{\mathrm{DDW}}(k) = f(k)^4 K'_{\mathrm{AF}}(k), \tag{4.16b}$$

$$K'_{\mathrm{DSC}}(k) = \frac{f(k)^4 \eta_2(k)}{8\left|\bar{\xi}_k\right|^3}, \tag{4.16c}$$

where

$$\eta_1(k) = \tanh\left(\frac{\left|\bar{\xi}_k\right|}{2T}\right) - \frac{\left|\bar{\epsilon}_k\right|/2T}{\cosh\left(\frac{\left|\bar{\xi}_k\right|}{2T}\right)^2}, \tag{4.17a}$$

$$\eta_2(k) = \tanh\left(\frac{\left|\bar{\xi}_k\right|}{2T}\right) - \frac{\left|\bar{\xi}_k\right|/2T}{\cosh\left(\frac{\left|\bar{\xi}_k\right|}{2T}\right)^2}. \tag{4.17b}$$

Finally, the $c_{pp'}$ coefficients are

$$c_{pp'} = \sum_{s_1,s_2,s_3=\pm 1} \int_{\substack{k_x>0 \\ k_y>k_x}} K''_{pp'}(k), \tag{4.18}$$

where

$$K''_{\mathrm{AF,DSC}}(k) = \frac{f(k)^2}{4\left|\bar{\xi}_k\right|^2\left|\bar{\epsilon}_k\right|}\eta_2(k), \tag{4.19a}$$

$$K''_{\mathrm{DDW,DSC}} = f(k)^2 K''_{\mathrm{AF,DSC}}(k), \tag{4.19b}$$

$$K''_{\mathrm{AF,DDW}}(k) = \frac{3f(k)^2}{4\left|\bar{\epsilon}_k\right|^3}\eta_1(k). \tag{4.19c}$$

The fact that all $K''_{pp'} > 0$ implies that the phases compete with each other.

4.3 Phase diagram

The mean-field phase diagram can be derived by minimizing Eq. (4.11) at fixed doping.

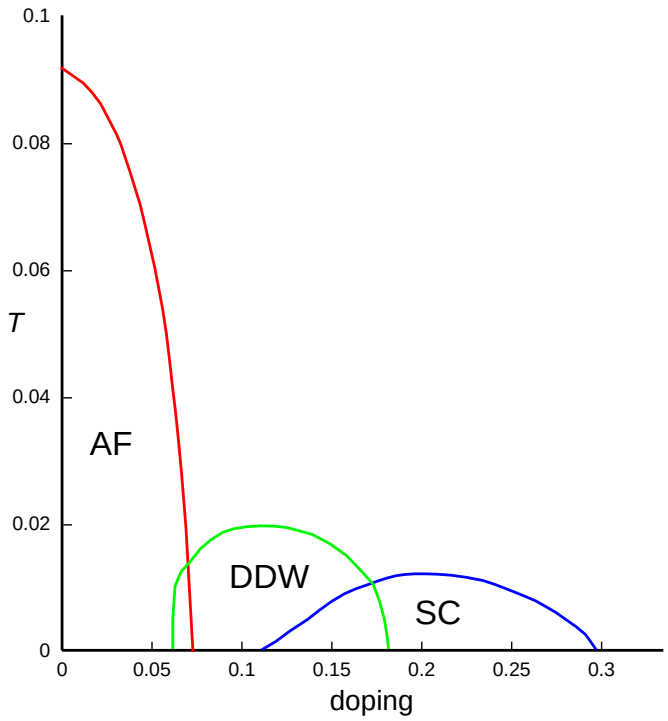

Figure 4.3: Phase diagram for $t = 0.5$ eV, $t' = -0.025$, $t_\perp = 0.05$ eV, $U \simeq 0.03$ eV, $V = 0$ eV, $t_c \simeq 0.8 \times 10^{-3}$ eV. ($g_{\rm AF} = 0.06$ eV, $g_{\rm DDW} = 0.02$ eV, $g_{\rm DSC} = 0.01$ eV.)

Since there is a large number of parameters in our model, there is substantial variety in the possible diagrams. One such diagram, generated with $t = 0.5$ eV, $t' = -0.025$ eV, $t_\perp = 0.05$ eV, $g_{\rm AF} = 0.06$ eV, $g_{\rm DDW} = 0.02$ eV, $g_{\rm DSC} = 0.01$ eV, is shown on the figure 4.3. The corresponding values of the interaction constants are $U \simeq 0.03$ eV, $V = 0$ eV, $t_c \simeq 0.8 \times 10^{-3}$ eV. Note that for these values of the constants, $g_{\rm CDW} = -0.04$ eV < 0, which is consistent with our assumption that a (π, π) charge-density wave is not energetically favorable.

Another diagram, shown on the figure 4.4, was generated with $t = 0.5$ eV, $t' = 0$, $t_\perp = 0.1$ eV, $g_{\rm AF} = 0.084$ eV, $g_{\rm DDW} = 0.038$ eV, and $g_{\rm DSC} = 0.017$ eV. The

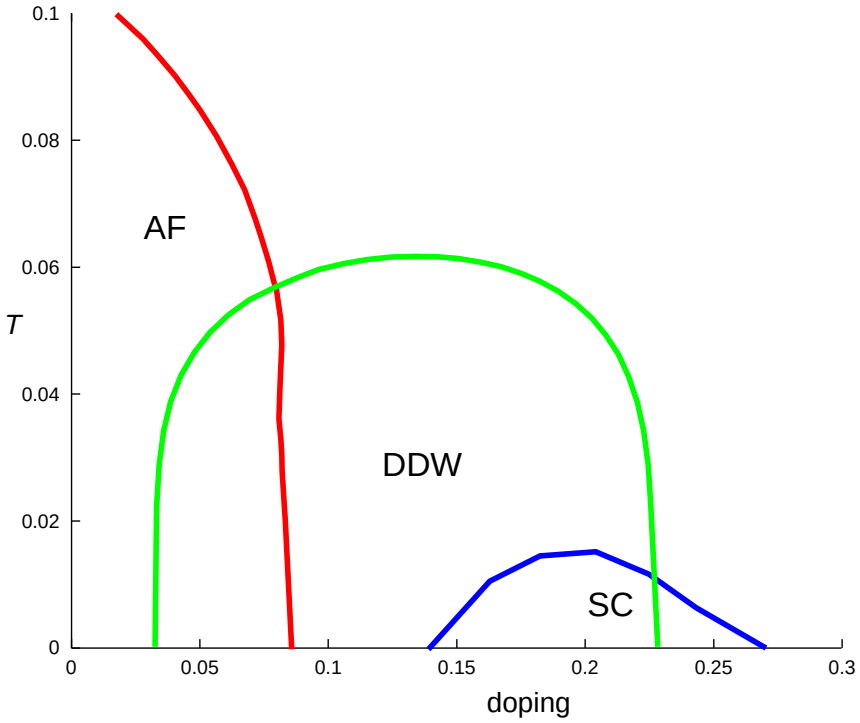

Figure 4.4: Phase diagram for $t = 0.5$ eV, $t' = 0$, $t_\perp = 0.1$ eV, $U \simeq 0.042$ eV, $V \simeq 1.7 \times 10^{-4}$ eV, $t_c \simeq 1.5 \times 10^{-3}$ eV. ($g_{\rm AF} = 0.084$ eV, $g_{\rm DDW} = 0.038$ eV, $g_{\rm DSC} = 0.017$ eV.)

corresponding values of the interaction constants are $U \simeq 0.042$ eV, $V \simeq 1.7 \times 10^{-4}$ eV, $t_c \simeq 1.5 \times 10^{-3}$ eV, and also $g_{\rm CDW} \simeq -0.045$ eV.

As we can see, in both diagrams the antiferromagnetic transition temperature at half-filling is close to 1000 K. This should be understood as the scale at which two-dimensional antiferromagnetic correlations develop locally. Due to the Mermin-Wagner-Coleman theorem, which states that a continuous symmetry cannot be broken spontaneously at finite-temperature in 2-D, the transition temperature is zero for a single bilayer. The coupling between different bilayers (which is not included in our single-bilayer calculation) stabilizes the antiferromagnetic phase with a transition temperature around 410 K. In lightly-doped cuprates, the presence of impurities causes the misalignment of locally ordered antiferromagnetic clusters, thereby forming a spin glass. Thus, if we interpret our T_N as the scale of local 2-D antiferromagnetic

order, which could become 3-D antiferromagnetic order or spin glass order, then the phase diagrams of Figs. 4.3 and 4.4 are very reasonable, indeed.

Experiments might lead us to expect that DDW order would occur in the range of doping between 0.07 and 0.19. This range is smaller than one shown on Fig. 4.4 and a bit larger than that shown in Fig. 4.3. The temperature scale for this phase on Fig. 4.3 is very reasonable; it is almost three times higher on Fig. 4.4. This change occurred primarily as a result of the increased value of t_c. If we further increase t_c to 1.9×10^{-3} eV, the DDW phase will begin to suppress the AF phase and will expand up to half-filling at finite temperatures. In general, varying the interaction constants by less that 20–30% does not change the phase diagram qualitatively. However, larger variations lead to completely different classes of phase diagrams, such as those with the AF phase suppressed or without a DDW phase at all. For example, Fig. 4.5 shows the case when due to the smaller value of correlation hopping, both DDW and DSC phases disappear and only AF phase remains in the diagram.

The DSC phase occupies a doping range away from half-filling primarily as a result of band structure effects associated with the bilayer splitting, i.e., by the fact that $t_\perp \neq 0$. In the absence of other orders, it would extend all the way to half-filling, but it is suppressed at low doping by DDW and AF order. In a more realistic calculation, superconductivity would be suppressed close to half-filling by no-double-occupancy constraint, i.e., by strong local Coulomb repulsion. However, the DSC phase never even makes it that close to half-filling because the DDW phase intervenes.

An important feature common to both diagrams is the existence of regions with two simultaneous kinds of order. Namely, there is a region with DDW+AF order and a region with DDW+DSC order. The system is an insulator in the AF state at half-filling, a metal in the DDW and DDW+AF states, and a superconductor in the DSC and DDW+DSC states.

All of the transitions are of second order at the mean-field level because of the

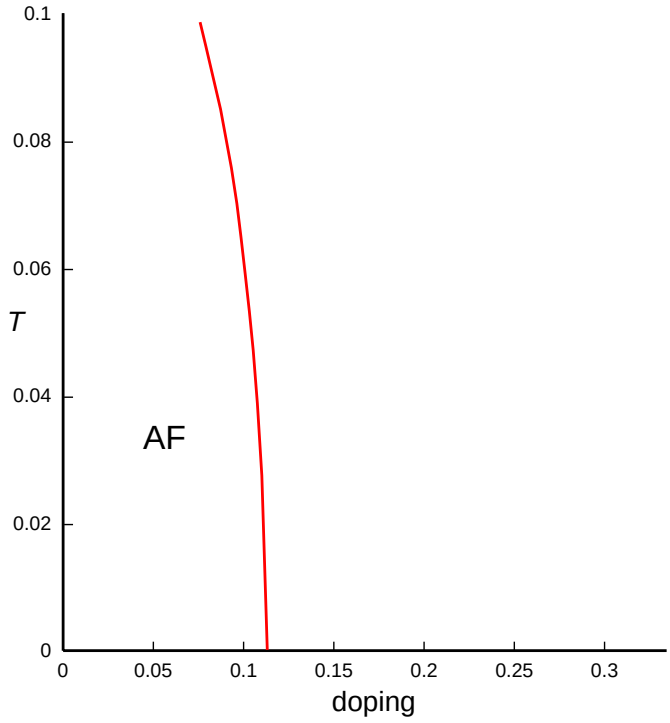

Figure 4.5: Phase diagram for $t = 0.5$ eV, $t' = -0.025$, $t_\perp = 0.05$ eV, $U = 0.05$ eV, $V = 0$ eV, $t_c \simeq 3.3 \times 10^{-4}$ eV. ($g_{\rm AF} = 0.1$ eV, $g_{\rm DDW} = 0.008$ eV, $g_{\rm DSC} = 0.004$ eV.)

signs of the $c_{pp'}$ couplings between the order parameters in the Ginzburg-Landau theory Eq. (4.12).

The calculated dependence of the chemical potential μ on the doping x inside the DDW phase and in its proximity is nonmonotonic. This is due to the rapid development of the DDW gap, which causes the chemical potential to be lower than in the normal state. The thermodynamic inequality $(\partial\mu/\partial x)_{T,V} \leq 0$ implies that when this is violated, mean-field theory should be corrected using Maxwell's construction, which signals that fluctuations drive the transitions first-order as a function of μ. Consequently, we would expect the underdoped side of the DSC phase to be characterized by a smaller than expected chemical shift, as has been observed [148]. A first-order phase transition as a function of chemical potential is manifested as phase separation in a two-phase coexistence region spanning a range of dopings when the doping is held fixed instead. It has been argued that such phase separation will be

precluded by Coulomb interactions, thereby leading to stripe formation [136, 137].

4.4 Conclusion

We have studied the phase diagram of a bilayer lattice model using mean field theory. Since we have focused on ordered phases, this should be a valid approximation. We found that for certain ranges of the values of the interaction constants the phase diagram agrees well with the experimentally observed phase diagram of YBCO if the 'pseudogap' is associated with DDW order. The diagram remains in qualitative agreement with the experimental data when the parameters of our model vary by less than 20 – 30% and becomes qualitatively different for larger variations. Clearly, such a phase diagram is reasonably robust, but is hardly inevitable. This is reassuring because high-temperature superconductivity is stable, but only appears in a special class of materials (to the best of our knowledge).

There are some systematic errors associated with mean-field theory, on which we now comment. It underestimates the effect of fluctuations. Thus, the Néel temperature is very large in mean-field theory, while it should actually be zero in any strictly two-dimensional system. However, the Néel temperature which we find should be regarded as the temperature below which a renormalized classical description is valid [149]. The Néel temperature observed in experiments is associated with the crossover from 2D to 3D. Mean-field theory also overestimates the coupling which drives antiferromagnetism, which it takes to be essentially U. For small U, this is correct, but for large U, it should be replaced by $J \sim t^2/U$. Indeed, the large-U limit is generally somewhat problematic near half-filling since the Gutwiller constraint is not enforced in mean-field theory. The $d_{x^2-y^2}$ symmetry of the DDW and DSC states lead one to the erroneous conclusion that they are completely unaffected by large U. This cannot, of course, really be true; clearly, mean-field theory underestimates the

tendency of large-U to push these ordered states away from half-filling. The seemingly small value of U taken in our calculation should be interpreted in light of these observations. Other mean-field treatments which incoporate strong local Coulomb repulsion more prominently have also found DDW order in a generalization of the $t-J$ model [150] and in the Hubbard model with nearest neighbor attraction [151].

We find that the scale associated with superconductivity is largely determined by the strength of correlated hopping. At the moment, this is rather *ad hoc*, but we had little choice but to introduce some term of this sort in order to have a phase diagram which includes superconductivity. It is possible that the superexchange coupling J plays a more important role than we have accorded it in setting T_c, but superexchange is beyond a mean-field treatment.

As we have seen, the very term which stabilizes superconductivity also supports the development of DDW order. One way of interpreting our results begins with the observation that the DDW order parameter, when combined with the real and imaginary parts of the DSC order parameter form a triplet under an $SU(2)$ group of transformations [122, 152]. If this 'pseudospin' $SU(2)$ is a symmetry of the Hamiltonian, then DDW and DSC orders will be equally favored. Thus, one can envision that the important order-producing term in the Hamiltonian is $SU(2)$-symmetric while small symmetry-breaking terms drive the system into either the DDW or DSC states. Our result shows that pair-hopping is of this form. Are all physically reasonable mechanisms for $d_{x^2-y^2}$ superconductivity similarly invariant under pseudospin $SU(2)$? This is an open problem; we have answered in the affirmative for one particular class of Hamiltonians.

Chapter 5 Conclusion

While the Fermi-liquid theory successfully agrees with experimental observations in the majority of metals, there is number of materials whose metallic behavior is associated with enigmatic non-Fermi-liquid peculiarities. These materials include certain heavy-fermion systems, high-T_c superconductors, and two-dimensional electron gas systems. In order to explain their properties, one has to classify the possible mechanisms in which the system develops non-Fermi-liquid features while remaining metallic. We have considered several examples of the scenario in which the non-Fermi-liquid behavior is induced by the presence of an order. In most of the known materials ordering is marked with a number of explicit and prominent changes of the physical properties, as a result of which the ordered phases become either insulating or superconducting. Therefore, the order has to be "hidden," i.e., not manifesting itself in a way common to usual phase transitions.

In the first example we have shown that odd-frequency (or, equivalently, odd-time) dependence of an order parameter falls into the "pattern" of a hidden-order scenario, indeed. The same-time correlation functions vanish, therefore, the system has a conventional Fermi surface and must be metallic at zero temperature. However, finite-frequency correlations are nonzero, therefore thermal excitations are able to "sense" them, leading to the development of order at intermediate finite temperatures. For odd-frequency density-wave, the resistivity of the system will increase in the ordered phase as if part of it became insulating.

The fact that the largest correlation functions are those with nonzero difference in imaginary time (i.e., finite temperature) implies that at zero temperature the system should have a peculiarity at a certain short-time scale. When the motion of electrons

is characterized by a similar time scale, they will develop the same features as at finite temperatures. Thus, one should expect strong frequency dependence of physical properties, such as conductivity, at low temperatures. The measurements should also depend on the magnetic field. For example, when the period of the cyclotron motion of the fermionic quasiparticles approaches the characteristic time scale, the T_1 lattice-relaxation time measured by NMR experiments should diverge, as it does in the case of ordinary density-wave or superconducting phase transitions.

Note that the frequency anomaly does not have to be associated with odd-frequency dependence of an order parameter. In fact, even-frequency order can achieve maximum at some finite characteristic frequency, too, leading to a short-time scale mentioned above. However, in this case the system is likely to be nonmetallic at $T = 0$.

The second example that we studied aimed to explain the non-Fermi-liquid features in the pseudogap phase of high-T_c cuprates. The $d_{x^2-y^2}$-density-wave order corresponds to a metallic state, because the gap vanishes at the nodes, where the quasiparticles can reach the Fermi surface. On the other hand, this order is not easy to detect, since it is not associated either with charge or spin order. This phase is characterized by a pattern of alternating circular currents and is associated with weak magnetic field induced by these currents.

An important result of our work is that we have shown that next-nearest-neighbor correlated hopping stabilized both d-density-wave and d-wave superconducting phases. As we have mentioned, the presence of this kinetic term has been shown in the band-structure calculations. Are there other interactions that lead to both phases? It has been long suspected that the mechanism of high-temperature superconductivity is related to the properties of the "normal" phase in the high-T_c cuprates. The d-density-wave model does not explain these properties on its own. However, there is a possibility that the underlying microscopic interaction that is responsible for the peculiarities in the normal phase and that induces the superconducting transition at

the same time favors the d-density-wave phase. Investigation of such a possibility is certainly the project of the future.

Although we have not devoted much space to third-order phase transitions, this is quite an interesting subject. In the presented model the behavior of the system is characterized by a long-range interaction and a short-scale coherence length (for the superconducting order). An obvious scenario that realized such a model is a model with strong long-range interaction. A more subtle scenario can take advantage of strong quantum fluctuations that suppress the coherence in the system, for example, due to the proximity of a quantum critical point. The associated third-order phase transition is not as explicit as the second- or first-order phase transitions and can be easily overlooked. It is important to investigate the role of thermal fluctuations, since they are likely to affect the substantial temperature region below the mean-field critical temperature. The system will likely remain normal (or metallic) at large scale, but it will develop non-Fermi-liquid features at short scales.

Appendix A Third-order phase transition

The existence of a phase transition is usually determined by the strength of the interaction of the quasiparticles near the Fermi level. In most of the well-studied cases such interaction is present in the slice around the Fermi surface that is much thicker than the critical temperature of the transition. Is it possible for the opposite case to take place, when interaction that favors particular phase exists in the region that is much smaller than critical temperature? We will show that such possibility exists, indeed.

For simplicity, consider a two-dimensional *isotropic* system with the following Hamiltonian at half filling:

$$\mathcal{H} = \int_k \epsilon_k c_k^\dagger c_k - \int_k \int_{k'} g \delta_{|k|,|k'|} c_{k+Q,\sigma}^\dagger c_{k\sigma} c_{k'\sigma'}^\dagger c_{k'+Q,\sigma'}. \tag{A.1}$$

This model corresponds to an extreme case, when interaction is allowed only between the particles with the same absolute value of momentum. As we will see later, in fact, this is a good approximation provided that such interaction is significant only in the region where $|\epsilon_k - \epsilon_{k'}| \ll g$, i.e., when it is long-ranged in real space.

The traditional order parameter in the mean-field theory could be defined as

$$\phi_k = \phi_{|k|} = g \int_{\hat{k}} c_{k+Q,\sigma}^\dagger c_{k\sigma}, \tag{A.2}$$

where $\int_{\hat{k}}$ denotes integration over all directions of k, while $|k|$ remains fixed. Note that order parameter explicitly depends on $|k|$, which makes it possible for $\phi_{|k|}$ to be nonzero near Fermi surface and zero away from Fermi surface. This is qualitatively different from the abovementioned case of short-ranged interaction, in which

transition occurs in entire Fermi-liquid so that $\phi_{|k|}$ becomes nonzero everywhere.

The difference between the free energy of the ordered state and that of disordered state, i.e., the condensation energy, is

$$\Delta F = \int_{|k|} \left[\frac{|\phi_k|^2}{g} - 2T \int_{\hat{k}} \ln \frac{\cosh\left(E_k/2T\right)}{\cosh\left(\epsilon_k/2T\right)} \right], \tag{A.3}$$

where $E_k = \left(\epsilon_k^2 + |\phi_k|^2\right)^{1/2}$. Varying this equation by ϕ_k, we derive the "gap equation":

$$\frac{1}{g} = \int_{\hat{k}} \frac{1}{2E_k} \tanh\left(\frac{E_k}{2T}\right). \tag{A.4}$$

This equation looks very similar to the gap equation for the CDW at half filling, with one essential exception: integration does not span over all values of $|k|$. As a result, there is only one solution for the energy of quasiparticles, if any:

$$E_k = \zeta(T). \tag{A.5}$$

The quantity $\zeta(T)$ is a true Ginzburg-Landau order parameter of the model and the mean field parameter introduced above is just $\phi_{|k|} = \left(\zeta(T)^2 - \epsilon_k^2\right)^{1/2}$ for $|\epsilon_k| < \zeta(T)$.

In BCS theory the coherence length at $T = 0$ is related to the order parameter as $\xi(T=0) = v_F/\left[\pi\Delta(0)\right]$, where $\Delta(T)$ is the single-particle excitation gap and is the order parameter. Therefore, we should expect the coherence length in our model to be $\xi(T=0) \sim v_F/\zeta(0) \sim v_F/g$. This is very short, indeed. We conclude that the model describes the superconductivity with short coherence length, specifically, with coherence length much smaller than the real-space range of interaction.

As we substitute the solution for $\zeta(T)$ back into free energy, we find that

$$\Delta F\left(T\right) = \int_0^{\zeta} d\epsilon N_{\epsilon} \left[2\pi \frac{\zeta^2 - \epsilon^2}{g} + 2T \ln \frac{\cosh\left(\epsilon/2T\right)}{\cosh\left(\zeta/2T\right)} \right], \tag{A.6}$$

where N_ϵ is density of states.

The critical temperature of the transition, at which $\phi_{|k|}$ becomes nonzero at Fermi surface (remaining zero for the rest of the phase space), is

$$T_c = \frac{\pi g}{2}. \tag{A.7}$$

Thus the transition takes place at relatively high temperature, compared to BCS theory, while condensation energy remains of the same order, $\Delta F(0) \sim N_F T_c^2$. However, the entire theory is valid only when interaction is limited to the area, where $|\epsilon_k - \epsilon_{k'}| \ll T_c \sim g$.

A very interesting consequence of this model is that transition is of *third order*. One can derive that directly from the expression for ΔF (taking into account that $\zeta > 0$) or by computing specific heat directly. The latter varies as $(T_c - T)^{1/2}$ at critical temperature. The reason is that phase transition initially involves only small part of the Fermi liquid and slowly expands as temperature goes down. If $\zeta(0) < \epsilon_F$, then even at zero temperature the low-energy part of the system remains normal. Of course the mean field theoretical description is only approximate, since it does not take into account fluctuations. The latter are substantial, since $|\Delta F(T)| < T$ in a large interval of temperatures, of order of $\Delta F(0)$ (Fig. A.1).

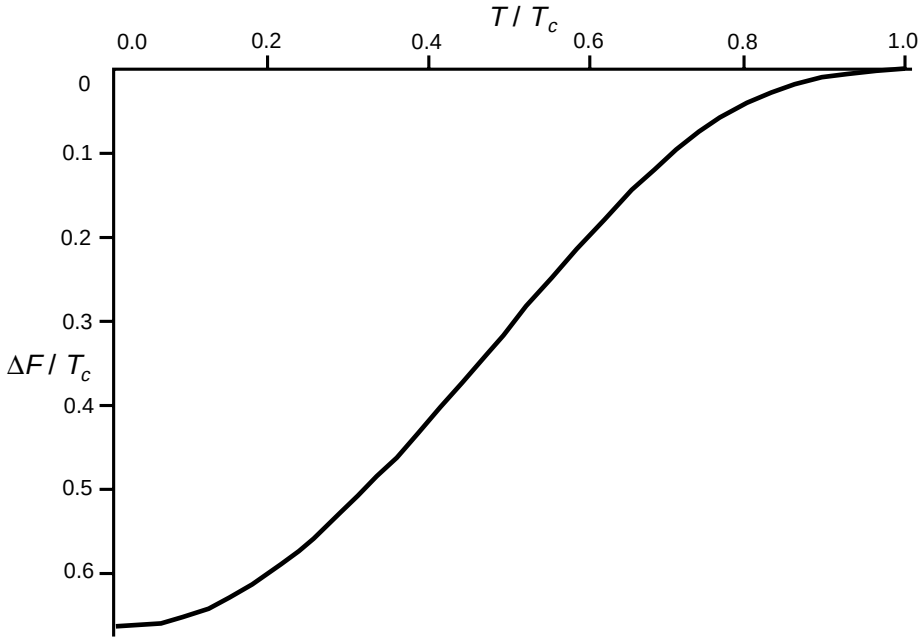

Figure A.1: Condensation energy for third-order phase transition.

Appendix B Odd-frequency superconductivity

The derivation of the Green functions for supreconductivity with odd-frequency dependence of the order parameter is similar to the derivation of Eq. (2.18). We start with the reduced action, in which the interaction term has already been factorized:

$$S = \int d\tau \left\{ \int_k \delta_{\alpha\beta} c^{\alpha\dagger}(k,\tau) \left(\partial_\tau - \epsilon_k + \mu\right) c^{\beta}(k,\tau) + \frac{\lambda}{\Omega_c^2} \int_k \left[c^{\alpha\dagger}(k,\tau)\, g_{\alpha\beta} \partial_\tau c^{\beta\dagger}(-k,\tau)\right]_c \left[c_\alpha(-k,\tau)\, g_{\alpha\beta} \partial_\tau c_\beta(k,\tau)\right]_c \right\}, \quad \text{(B.1)}$$

where

$$g_{\alpha\beta} = \begin{pmatrix} 0 & 1 \\ -1 & 0 \end{pmatrix} \quad \text{(B.2)}$$

and $[\ldots]_c$ assumes existence of a high-frequency cutoff Ω_c so that for high frequencies the interaction vanishes. We now introduce the order parameter α:

$$\frac{\lambda}{\Omega_c^2} \int_k \left[c_\alpha(k,\tau)\, i\partial_\tau c_\beta(-k,\tau)\right]_c = \alpha g_{\alpha\beta}. \quad \text{(B.3)}$$

This allows us to write the interaction part of the action as

$$S_{\mathrm{MF}} = T \sum_n \int_k \alpha \omega_n g_{\alpha\beta} c^{\alpha\dagger}(k,\omega_n)\, c^{\beta\dagger}(-k,\omega_n) + \int_k \alpha^* \omega_n g_{\alpha\beta} c^{\alpha}(-k,\omega_n)\, c^{\beta}(k,\omega_n). \quad \text{(B.4)}$$

The equation of motion for c follows by varying the action by $c^{\alpha\dagger}$:

$$\left(i\omega_n - \epsilon_k + \mu\right) c_\alpha(k,\omega_n) + \alpha \omega_n g_{\alpha\beta} c^{\beta\dagger}(-k,\omega_n) = 0. \quad \text{(B.5)}$$

This gives the first Eliashberg-like equation:

$$\left(i\omega_n - \epsilon_k + \mu\right) G\left(k, \omega_n\right) + \alpha\omega_n F^{\dagger}\left(k, \omega_n\right) = 1, \tag{B.6}$$

where the Green functions $G\left(k,\tau\right)$ and $F^{\dagger}\left(k,\tau\right)$ are defined as

$$\left\langle T c_{\alpha}\left(k,\tau\right) c^{\beta\dagger}\left(k,0\right)\right\rangle = G\left(k,\tau\right)\delta_{\alpha}^{\beta}, \tag{B.7}$$

$$g_{\alpha\gamma}\left\langle T c^{\gamma\dagger}\left(-k,\tau\right) c^{\beta\dagger}\left(k,0\right)\right\rangle = F^{\dagger}\left(k,\tau\right)\delta_{\alpha}^{\beta}. \tag{B.8}$$

Again, the right-hand side of Eq. (B.6) is 1 because of the time-ordering in the definition of $G\left(k,\omega_n\right)$.

Similarly, the equation of motion for $c^{\dagger}$ follows by varying the action by c^{α}:

$$\left(-i\omega_n - \epsilon_k + \mu\right) c_{\alpha}^{\dagger}\left(k,\omega_n\right) + \alpha^{*}\omega_n g_{\alpha\beta} c^{\beta}\left(-k,\omega_n\right) = 0. \tag{B.9}$$

Note that this equation could be derived from Eq. (B.5) just by taking complex conjugate. Thus, since $g_{\alpha\beta}g^{\alpha\gamma} = \delta_{\beta}^{\gamma}$, $g_{\alpha\beta} = -g_{\beta\alpha}$ and $\epsilon_k = \epsilon_{-k}$, we obtain the second Eliashberg-like equation:

$$\left(i\omega_n + \epsilon_k - \mu\right) F^{\dagger}\left(k,\omega_n\right) + \alpha^{*}\omega_n G\left(k,\omega_n\right) = 0. \tag{B.10}$$

As we can see, the sign in front of the second term in Eq. (B.10) has not changed. Naively, from our BCS experience, we could expect to see $\Delta\left(-\omega_n\right)^{*}$ there, therefore, it seems to contradict to the fact that for an odd-frequency-dependent gap, $\Delta\left(-\omega\right) = -\Delta\left(\omega\right)$. To understand what has happened, consider it at *real* frequencies: $\Delta\left(\omega\right) \sim i\omega$ is being replaced with $\Delta\left(-\omega\right)^{*} = -\Delta\left(\omega\right)^{*} \sim i\omega$. Thus, the sign has not changed at real frequencies. Since the equations are analytical in frequency, the same statement should hold for Matsubara frequencies ω_n, too. The mistake is the very expectation

to see the gap $\Delta\left(-\omega_n\right)^*$ in the second equation, because this function is not analytical in frequency (it depends on ω^*) and can not possibly appear in the odd-frequency case. It is order parameter α^* that appears.

As a result, we have obtained the Green functions:

$$G\left(k,\omega_n\right)=\frac{i\omega_n+\mu+\epsilon_k}{\left(i\omega_n\right)^2-\left(\epsilon_k-\mu\right)^2-\alpha^2\omega_n^2}, \tag{B.11a}$$

$$F^\dagger\left(k,\omega_n\right)=\frac{\alpha^*\omega_n}{\left(i\omega_n\right)^2-\left(\epsilon_k-\mu\right)^2-\alpha^2\omega_n^2}. \tag{B.11b}$$

The theory with these Green functions is free from contradicions discussed in Refs. [62, 63, 64, 67], in particular, the Meissner effect is positive.

Appendix C Integral evaluation

In this Appendix the integral that appears in the right-hand side of Eq. (3.22) is evaluated:

$$I = \int_0^{\pi} \frac{dk_x}{2\pi} \int_0^{\pi} \frac{dk_y}{2\pi} \frac{\tanh\left(\frac{\varepsilon(\mathbf{k})-\mu}{2k_BT}\right)}{\varepsilon\left(\mathbf{k}\right)-\mu}. \tag{C.1}$$

First, we make a substitution $k_+ = \left(k_x + k_y\right)/2$, $k_- = \left(k_x - k_y\right)/2$ and expand the energy in terms of k_+ about the Fermi level $\varepsilon\left(\mathbf{k}\right) = \mu$:

$$\begin{aligned} \varepsilon\left(\mathbf{k}\right) - \mu \simeq & -\sqrt{\left(4t\cos k_-\right)^2 - \mu} \\ & \times \left[k_+ - \arccos\left(\frac{\mu}{4t\cos k_-}\right)\right]. \end{aligned} \tag{C.2}$$

In the limit of $\mu/2t \to 0$, the integral I diverges logarithmically. The internal integral can be taken by parts, which results in a logarithmic part and a convergent integral. In the latter the limits can be replaced by $\pm\infty$. Then there will be a region of integration at $k_x = 0$, $k_y = \pi/2$ that will not be covered and a symmetric region that will be covered twice. However, the expression in the integral takes the same value in both regions, therefore the result remains unchanged and after the limit replacement no corrections will be necessary:

$$\begin{aligned} I = \frac{1}{\pi^2} \int_0^{\frac{1}{2}\arccos\left(\frac{\mu}{2t}-1\right)} & \frac{dk_-}{\sqrt{\left(4t\cos k_-\right)^2 - \mu}} \ln\left\{\left[\pi + \arccos\left(\frac{\mu}{4t\cos k_-}\right) - k_-\right]\right. \\ & \left. \times \left[\arccos\left(\frac{\mu}{4t\cos k_-}\right) - k_-\right]\left[\left(4t\cos k_-\right)^2 - \mu\right]\left(\frac{\gamma}{\pi}\frac{1}{k_BT}\right)^2\right\}. \end{aligned} \tag{C.3}$$

Here Euler's constant $\gamma \approx 0.577$ and μ is assumed to be positive. Furthermore,

Eq. (C.1) does not depend on the sign of μ, thus, we can replace μ by $|\mu|$. The asymptotic expansion at $|\mu|/2t \to 0$ is

$$I = \frac{1}{4\pi^2 t} \ln\left(\frac{2t}{|\mu|}\right) \ln\left(\frac{\gamma 2^{1/4}}{\pi^{1/2}} \frac{2t}{k_B T}\right) - \frac{3}{32\pi^2 t} \ln\left(\frac{2t}{|\mu|}\right)^2 + O\left[\left(\frac{|\mu|}{2t}\right)^0\right]. \qquad \text{(C.4)}$$

Appendix D Computation of the phase diagram in the $SU(4)$-symmetric model

The phase diagram corresponding to the free energy Eq. (3.21) has been computed numerically. The Fortran program listed below is based on Numerical Recipes [153]. The expression for the quasiparticle energy has been slightly generalized in order to take into account interlayer tunneling $\varepsilon_\perp$. For the antisymmetric configuration of order parameters between the layers, this energy becomes

$$E\left(k;s_1,s_2\right)=E\left(\mathbf{k};s\right)=\left(\left\{s_1\sqrt{\left[\varepsilon\left(k\right)+s_2\varepsilon_\perp\right]^2+M^2}+\epsilon'\left(k\right)-\mu\right\}^2+\Delta^2\right)^{1/2},$$
$$s_1,s_2=\pm1. \quad \text{(D.1)}$$

One can suggest ways to impose the constraint on the number of particles. One way is to minimize the free energy $F\left(m,\Delta;T,N\right)=F\left(m,\Delta;T,\mu\right)+\mu N$ with respect to the order parameters m and Δ only and enforce the constraint prior to each computation of $F\left(m,\Delta;T,N\right)$. The other way is to take advantage of the fact that

$$\frac{\partial}{\partial\mu}F\left(m,\Delta;T,\mu\right)=N. \quad \text{(D.2)}$$

Naively, to implement the second approach, one only needs to minimize $F\left(m,\Delta;T,N\right)$ formally as a function of μ. The problem is that $F\left(N\right)$ does not have a minimum when Eq. (D.2) is satisfied, it actually has a maximum there! In some cases, it is possible to use a trick, which is to take advantage of the Luttinger theorem to construct a new function with a minimum at the point Eq. (D.2) and which leads to the same gap equation when one varies m or Δ. Due to the theorem (or by direct verification),

Eq. (D.2) is valid for the same values of μ and N and any values of m and Δ. Thus, we can minimize

$$\tilde{F} = F(m, \Delta; T, N) - 2F(0, 0; T, N) - \mu N \tag{D.3}$$

with respect to m, Δ, μ and the corresponding Euler's equations will be the gap equations and the constraint on the particle number. The practical implementation of the second method in our problem shows, however, that it produces poor results and is not significantly faster than the first one. In our case, Luttinger's theorem is not valid either, therefore, we can not take advantage of this trick. Therefore, the code below is an implementation of the first approach.

```
! Source of the program pd.F
! Language: FORTRAN 77
#define NT 21
#define NX 21


      program PD
CU    USES powell
      double precision pi
      parameter (pi = 3.1415926535897932D0)
      parameter (NK = 262144)
      parameter (TOL = 1E-5)
      real x,mu,t,t0,tl,cosx(0:NK),p(2),xi(2,2),ftol,xmax,xmin
      real outp1(NX),outp2(NX),outp3(NX)
      real p1max,p2max
      integer n
      common mu,t,/cosdat/cosx,/g/g1,g2,/hop/t0,tl,tprime,/x/x
```

```
      data n,p1max,p2max/2,0.0,0.0/
      do 10, i=0,NK
        cosx(i) = cos(pi*i/(2*NK))
10    continue
        !Enter the values of the constants
      write (*,*) 'Calculation of order parameters (SC, DW)'
      t0 = 0.5
      write (*,*) 'Hopping is set to  t0 =', t0
      write (*,*) 't_perp = '
      read (*,*) tl
      write (*,*) 't^prime = '
      read (*,*) tprime
      write (*,*) 'g(SC) = '
      read (*,*) g1
      write (*,*) 'g(DW) = '
      read (*,*) g2
      write (*,*) 'doping (x) varies from'
      read (*,*) xmin
      if (xmin .LE. 0.0) xmin = 1.0E-5
      write (*,*) ' to'
      read (*,*) xmax
      write (*,*) 'T start = '
      read (*,*) tstart
      if (tstart .LE. 0.0) tstart= 1.0E-4
      write (*,*) 'T end = '
      read (*,*) tend
        !Beginning the main loop
```

```
      open (9, FILE='pd0.dat')
      open (10, FILE='pd1.dat')
      open (11, FILE='pd2.dat')
      open (12, FILE='pd3.dat')
      t = tstart
      ftol = TOL
      do 15, i=1,NX
        outp1(i) = g1**2
        outp2(i) = g2**2
15    continue
      do 30, j=1,NT
        x = xmin
        do 20, i=1,NX
            !Initial values of order parameters are inherited from
            !the previous computation at higher temperature.
          p(1) = outp1(i)
          p(2) = outp2(i)
          if (p(1).lt.1E-4) p(1)=g1**2
          if (p(2).lt.1E-4) p(2)=g2**2
          xi(1,1)=0.1
          xi(1,2)=0.0
          xi(2,1)=0.0
          xi(2,2)=0.1
          call POWELL(p,xi,n,n,ftol,iter,fret)
          if (p(1) .LT. 0.0) p(1)= -p(1)
          if (p(2) .LT. 0.0) p(2)= -p(2)
          outp1(i) = p(1)
```

```
          outp2(i) = p(2)
          outp3(i) = mu
          write(*,*) 'Finished x=',x,' after ',iter,' iterations',
     *    ' mu,p1,p2',mu,p(1),p(2)
          x = x + (xmax-xmin)/(NX-1)
20      continue
          !Saving the results of the computation at given T.
        write (9,40) (xmin+(i-1)*(xmax-xmin)/(NX-1), t, outp1(i),
     *   outp2(i),outp3(i), i=1,NX)
        write (9,*) ' '
        write (10,50) (outp1(i), i=1,NX)
        write (11,50) (outp2(i), i=1,NX)
        write (12,50) (outp3(i), i=1,NX)
        write (*,*) 'T = ',t,' finished'
        do 25, i=1,NX
          if (outp1(i) .GT. p1max) p1max = outp1(i)
          if (outp2(i) .GT. p2max) p2max = outp2(i)
25      continue
        t = t + (tend-tstart)/(NT-1)
30    continue
      close (9)
      close (10)
      close (11)
      close (12)
      write (*,*) 'The phase diagram has been generated'
      write (*,*) 'Maxima of the order parameters Delta,M:',
     *  p1max,p2max
```

```
      write (*,*) 'pd0.dat contains data in format
     * {x,T,Delta,M,mu}'
      write (*,*) 'pd1.dat is a',NX,' by',NT,' matrix of Delta(x,T)'
      write (*,*) 'pd2.dat is a',NX,' by',NT,' matrix of M(x,T)'
      write (*,*) 'pd3.dat is a',NX,' by',NT,' matrix of mu(x,T)'
      open (14, FILE='params.txt')
      write (14,60) 't_perp',tl,'t^prime',tprime,'xmax',xmax,
     * 'g_SC',g1,'g_DW',g2
      close (14)
40    format ((F5.3,F7.4,2F7.4,F8.4))
50    format (NX F7.4)
60    format ((A,' = ',F6.3))
      end

      real function FUNC(p)
        !Computes the free energy for given order parameters
CU    USES rtflsp, qgausx
      double precision pi
      parameter (pi = 3.1415926535897932D0)
      parameter (ftol = 1E-5)
      real p(2)
      real a,b,ss
      real F1
      real mumin,mumax,muacc,mu,t
      external F1,FNUM
      common mu,t,/g/g1,g2,/pnt/p1(2),/x/x,/hop/t0,tl,tprime
        !Determine mu
```

```
      p1(1) = p(1)
      p1(2) = p(2)
      mumax = -3*tprime
      mumin = -sqrt(4*x**2+2*p1(1)**2+p1(2)**2
     * +50*tprime**2)-0.02
      muacc = ftol
      mu = RTFLSP(FNUM,mumin,mumax,muacc)
      if (mu .EQ. 1E5) then
          !Something is wrong
        FUNC = 1E7
        write(*,*) '*** mu,p1,p2,FUNC',mu,p(1),p(2),FUNC
      else
         !Compute free energy
        a = 0.0
        b = pi/2.0
        call QGAUSX(F1,a,b,ss)
        FUNC = 2*((p(1)**2)/g1+(p(2)**2)/g2)+ss-mu*x/2*(2*pi)**2
      endif
      end

      real function F1 (kx)
        !Part of computation of free energy.
        !Computes and integral over ky for fixed kx.
CU    USES qgausy
      double precision pi
      parameter (pi = 3.1415926535897932D0)
      parameter (NK = 262144)
```

```
      real kx
      real a, b, ss
      external FREEEN
      integer ix
      common /ix/ix
      a = 0.0
      b = kx
      ix = kx/pi*(2*NK)
        !Above: ROUND rather than TRUNCATE assumed.
        !This depends on the compiler.
      call QGAUSY(FREEEN,a,b,ss)
      F1 = ss
      end

      real function FREEEN (ky)
        !Part of computation of free energy.
        !Computes the expression in the integral
CU    USES faux
      double precision pi
      parameter (pi = 3.1415926535897932D0)
      parameter (NK = 262144)
      real ky
      real cosx(0:NK), t0, tl, tp
      integer ix, iy
      common /cosdat/cosx,/ix/ix,/hop/t0,tl,tp
      iy = ky/pi*(2*NK)
        !Above: ROUND rather than TRUNCATE assumed.
```

```
        !This depends on the compiler.
      epsl = tl
      epsk1 = -2*t0*(cosx(ix)+cosx(iy))
      epspk1 = -4*tp*cosx(ix)*cosx(iy)
      aux1 = FAUX(epsk1,epspk1,epsl)
      epsk2 = -2*t0*(cosx(ix)-cosx(iy))
      epspk2 = +4*tp*cosx(ix)*cosx(iy)
      aux2 = FAUX(epsk2,epspk2,epsl)
      epsk3 = 2*t0*(cosx(ix)-cosx(iy))
      epspk3 = +4*tp*cosx(ix)*cosx(iy)
      aux3 = FAUX(epsk3,epspk3,epsl)
      epsk4 = 2*t0*(cosx(ix)+cosx(iy))
      epspk4 = -4*tp*cosx(ix)*cosx(iy)
      aux4 = FAUX(epsk4,epspk4,epsl)
        !Combining all four quadrants together
      FREEEN = aux1+aux2+aux3+aux4
      end

      real function FAUX (epsk,epspk,epsl)
        !Part of computation of free energy.
        !Computes the contribution of a single quadrant
CU    USES daux2
      real epsk, epspk, epsl
      real mu, t, dt, M
      double precision res1,res2,res3,res4
      double precision sr1, sr2
      double precision expr1,expr2,expr3,expr4
```

```
common mu,t,/pnt/dt,M,/x/x
double precision DAUX2
  !The auxiliary expression in the eigenvalues
sr1 = sqrt( (epsk + epsl)**2 + (M**2) )
sr2 = sqrt( (epsk - epsl)**2 + (M**2) )
  !The four eigenvalues
expr1 = sqrt( (sr1 + epspk - mu)**2 + (dt**2) )
expr2 = sqrt( (sr2 + epspk - mu)**2 + (dt**2) )
expr3 = sqrt( (-sr1 + epspk - mu)**2 + (dt**2) )
expr4 = sqrt( (-sr2 + epspk - mu)**2 + (dt**2) )
res1=DAUX2(expr1,t)
res2=DAUX2(expr2,t)
res3=DAUX2(expr3,t)
res4=DAUX2(expr4,t)
FAUX = - 2.0*t*(res1+res2+res3+res4)
end

double precision function DAUX2 (darg,t)
  !This function allows to compute the eigenvalues
  !at low temperatures when the expression
  !in the log() becomes very large.
real t
double precision darg, dmisc
dmisc = darg / (2.0*t)
if (dmisc .LT. 17.0) then
  DAUX2 = log( 2.0*cosh( dmisc ))
else
```

```
        DAUX2 = dmisc
      endif
      end

      real function FNUM(mu1)
        !Calculates the number of particles per volume
        !for given chemical potential mu1
CU    USES qgausx
      double precision pi
      parameter (pi = 3.1415926535897932D0)
      real mu1,mu,t
      real a,b,ss
      real F2
      external F2
      common mu,t,/x/x
      mu = mu1
      a = 0.0
      b = pi/2.0
      call QGAUSX(F2,a,b,ss)
        !We return the difference between the particle
        !number and what is expected from doping x.
      FNUM = ss / (2.0*pi)**2 - (1.0 - x)/2
      end

      real function F2 (kx)
        !Part of computation of particle number.
        !Evaluates the integral over ky for fixed kx.
```

```
CU    USES qgausy
      double precision pi
      parameter (pi = 3.1415926535897932D0)
      parameter (NK = 262144)
      real kx
      real a, b, ss
      external FN
      integer ix
      common /ix/ix
      a = 0.0
      b = kx
      ix = kx/pi*(2*NK)
        !Above: ROUND rather than TRUNCATE assumed.
        !This depends on the compiler.
      call QGAUSY(FN,a,b,ss)
      F2 = ss
      end

      real function FN (ky)
        !Part of computation of particle number.
        !Evaluates the expression in the integral.
CU    USES faux2
      double precision pi
      parameter (pi = 3.1415926535897932D0)
      parameter (NK = 262144)
      real ky
      real cosx(0:NK), t0, t1
```

```
      integer ix, iy
      common /cosdat/cosx,/ix/ix,/hop/t0,tl,tp
      iy = ky/pi*(2*NK)
        !Above: ROUND rather than TRUNCATE assumed.
        !This depends on the compiler.
      epsl = tl
      epsk1 = -2*t0*(cosx(ix)+cosx(iy))
      epspk1 = -4*tp*cosx(ix)*cosx(iy)
      aux1 = FAUX2(epsk1,epspk1,epsl)
      epsk2 = -2*t0*(cosx(ix)-cosx(iy))
      epspk2 = +4*tp*cosx(ix)*cosx(iy)
      aux2 = FAUX2(epsk2,epspk2,epsl)
      epsk3 = 2*t0*(cosx(ix)-cosx(iy))
      epspk3 = +4*tp*cosx(ix)*cosx(iy)
      aux3 = FAUX2(epsk3,epspk3,epsl)
      epsk4 = 2*t0*(cosx(ix)+cosx(iy))
      epspk4 = -4*tp*cosx(ix)*cosx(iy)
      aux4 = FAUX2(epsk4,epspk4,epsl)
         !Combining all four quadrants together
      FN = aux1+aux2+aux3+aux4
      end

      real function FAUX2 (epsk,epspk,epsl)
        !Part of computation of particle number.
        !Evaluates the contribution of a single quadrant.
CU    USES daux3
      real epsk, epspk, epsl
```

```
real mu, t, dt, M
double precision res1,res2,res3,res4
double precision sr, sr1, sr2, temp
double precision expr1,expr2,expr3,expr4
common mu,t,/pnt/dt,M
double precision DAUX3
  !Auxiliary expression
sr1 = sqrt( (epsk + epsl)**2 + (M**2) )
sr2 = sqrt( (epsk - epsl)**2 + (M**2) )
  !Contributions from four eigenstates
expr1 = sqrt( (sr1 + epspk - mu)**2 + (dt**2) )
expr2 = sqrt( (sr2 + epspk - mu)**2 + (dt**2) )
expr3 = sqrt( (-sr1 + epspk - mu)**2 + (dt**2) )
expr4 = sqrt( (-sr2 + epspk - mu)**2 + (dt**2) )
res1 = (sr1 + epspk - mu)*DAUX3(expr1,t)
res2 = (sr2 + epspk - mu)*DAUX3(expr2,t)
res3 = (-sr1 + epspk - mu)*DAUX3(expr3,t)
res4 = (-sr2 + epspk - mu)*DAUX3(expr4,t)
FAUX2 = 4.0 - (res1+res2+res3+res4)
end

double precision function DAUX3 (darg,t)
  !An auxiliary function
real t
double precision darg
DAUX3 = tanh(darg/(2.0*t))/darg
end
```

```
      block data
      parameter (NGAUS=16)
      real w(NGAUS),x(NGAUS)
      common /gaus/w,x
! Gauss-Chebyshev method of integration
C      data x/4.906768E-02, 0.1467305, 0.2429802, 0.3368899, 0.4275551,
C     * 0.5141028, 0.5956993, 0.6715590, 0.7409511, 0.8032075, 0.8577286,
C     * 0.9039893, 0.9415441, 0.9700313, 0.9891765, 0.9987954/
C      data w/9.805688E-02, 9.711254E-02, 9.523296E-02, 9.243622E-02,
C     * 8.874927E-02, 8.420762E-02, 7.885501E-02, 7.274298E-02,
C     * 6.593039E-02, 5.848286E-02, 5.047211E-02, 4.197527E-02,
C     * 3.307421E-02, 2.385461E-02, 1.440528E-02, 4.817239E-03/
! Gauss-Legendre method of integration
      data x/4.830766E-02, 0.1444720, 0.2392874, 0.3318686, 0.4213513,
     * 0.5068999, 0.5877157, 0.6630443, 0.7321821, 0.7944838, 0.8493676,
     * 0.8963212, 0.9349061, 0.9647623, 0.9856115, 0.9972638/
      data w/9.654000E-02, 9.563863E-02, 9.384431E-02, 9.117379E-02,
     * 8.765201E-02, 8.331185E-02, 7.819382E-02, 7.234573E-02,
     * 6.582216E-02, 5.868404E-02, 5.099801E-02, 4.283586E-02,
     * 3.427383E-02, 2.539204E-02, 1.627438E-02, 7.018603E-03/
      end

      SUBROUTINE qgausx(func,a,b,ss)
        !Gauss method of integration of the function func.
      parameter (NGAUS=16)
      REAL a,b,ss,func
```

```
      EXTERNAL func
      INTEGER j
      REAL dx,xm,xr
      COMMON /gaus/w(NGAUS),x(NGAUS)
      xm=0.5*(b+a)
      xr=0.5*(b-a)
      ss=0
      do 11 j=1,NGAUS
        dx=xr*x(j)
        ss=ss+w(j)*(func(xm+dx)+func(xm-dx))
11    continue
      ss=xr*ss
      return
      END

      SUBROUTINE qgausy(func,a,b,ss)
       !Gauss method of integration of the function func.
       !This subroutine is identical to qgausx
       !and is included to avoid recursion.
      parameter (NGAUS=16)
      REAL a,b,ss,func
      EXTERNAL func
      INTEGER j
      REAL dx,xm,xr
      COMMON /gaus/w(NGAUS),x(NGAUS)
      xm=0.5*(b+a)
      xr=0.5*(b-a)
```

```
      ss=0
      do 11 j=1,NGAUS
        dx=xr*x(j)
        ss=ss+w(j)*(func(xm+dx)+func(xm-dx))
11    continue
      ss=xr*ss
      return
      END

! The modules below are from Numerical Recipes in FORTRAN
      SUBROUTINE powell(p,xi,n,np,ftol,iter,fret)
        !Minimizes FUNC(p) (see above) by varying p(n).
      FUNCTION rtflsp(func,x1,x2,xacc)
        !Finds the root of func between x1 and x2.
      SUBROUTINE linmin(p,xi,n,fret)
      SUBROUTINE mnbrak(ax,bx,cx,fa,fb,fc,func)
      FUNCTION f1dim(x)
      FUNCTION brent(ax,bx,cx,f,tol,xmin)
```

Bibliography

[1] L. D. Landau, Zh. Eksperim. Teor. Fiz. **30**, 1058 (1956).

[2] L. D. Landau, Zh. Eksperim. Teor. Fiz. **32**, 59 (1957).

[3] R. Shankar, Rev. Mod. Phys. **66**, 129 (1994).

[4] A. A. Abrikosov, L. P. Gorkov, and I. E. Dzyaloshinski, *Quantum Field Theoretical Methods in Statistical Physics* (Pergamon Press, Oxford, 1965).

[5] E. M. Lifshitz and L. P. Pitaevskiĭ, *Statistical Physics. Part 2: Theory of the Condensed State*, vol. 9 of *Course of Theoretical Physics* (Butterworth-Heinemann, Oxford, 1980).

[6] C. M. Varma, P. Littewood, S. Schmitt-Rink, E. Abrahams, and A. E. Ruckenstein, Phys. Rev. Lett. **63**, 1996 (1989).

[7] L. B. Ioffe and G. Kotliar, Phys. Rev. B **42**, 10348 (1990).

[8] J. M. Luttinger, Phys. Rev. **119**, 1153 (1960).

[9] S.-I. Tomonaga, Prog. Theor. Phys. **5**, 544 (1950).

[10] J. M. Luttinger, J. Math. Phys. (N.Y.) **4**, 1154 (1963).

[11] D. C. Mattis and E. H. Lieb, J. Math. Phys. (N.Y.) **6**, 304 (1965).

[12] F. D. M. Haldane, J. Phys. C **14**, 2685 (1981).

[13] M. Yamanaka, M. Oshikawa, and I. Affleck, Phys. Rev. Lett. **79**, 1110 (1997).

[14] N. N. Bogoliubov, Zh. Eksperim. Teor. Fiz. **34**, 58 (1958), [Sov. Phys. – JETP **7**, 41 (1958)].

[15] O. Penrose and L. Onsagar, Phys. Rev. **104**, 576 (1956).

[16] S. Chakravarty and H.-Y. Kee, Phys. Rev. B **61**, 14821 (2000).

[17] P. Nozières and S. Schmitt-Rink, J. Low Temp. Phys. **81**, 195 (1985).

[18] L. Belkhir and M. Randeria, Phys. Rev. B **45**, 5087 (1992).

[19] A. J. Leggett, J. Phys. (Paris), Colloq. **41**, C7 (1980).

[20] V. B. Geshkenbein, L. B. Ioffe, and A. I. Larkin, Phys. Rev. B **55**, 3173 (1997).

[21] Q. Chen, I. Kosztin, B. Jankó, and K. Levin, Phys. Rev. Lett. **81**, 4708 (1999).

[22] I. Kosztin, Q. Chen, Y.-J. Kao, and K. Levin, Phys. Rev. B **61**, 11662 (2000).

[23] Y. J. Uemura, Physica C **282-287**, 194 (1997).

[24] A. Paramekanti, L. Balents, and M. P. A. Fisher, cond-mat/0203171.

[25] J. S. Langer and V. Ambegaokar, Phys. Rev **164**, 498 (1967).

[26] J. M. Kosterlitz and D. J. Thouless, J. Phys. C **6**, 1181 (1973).

[27] C. Dasgupta and B. I. Halperin, Phys. Rev. Lett. **47**, 1556 (1981).

[28] Y. J. Uemura et al., Phys. Rev. Lett. **62**, 2317 (1989).

[29] V. J. Emery and S. A. Kivelson, Nature (London) **374**, 434 (1995).

[30] V. J. Emery and S. A. Kivelson, Phys. Rev. Lett. **74**, 3253 (1995), and references therein.

[31] M. Franz and A. J. Millis, Phys. Rev. B **58**, 14572 (1998).

[32] J. Kondo, Prog. Theor. Phys. **32**, 37 (1964).

[33] K. Yosida, Phys. Rev. **147**, 223 (1966).

[34] P. Nozières, J. Low Temp. Phys. **17**, 31 (1974).

[35] P. W. Anderson, Phys. Rev. **124**, 41 (1961).

[36] A. C. Hewson, Phys. Rev. Lett. **70**, 4007 (1993).

[37] A. M. Tsvelick and P. B. Wiegmann, Adv. Phys. **32**, 453 (1983).

[38] K. G. Wilson, Rev. Mod. Phys. **47**, 773 (1975).

[39] N. Andrei, K. Furuya, and J. H. Lowenstein, Rev. Mod. Phys. **55**, 331 (1983).

[40] M. A. Ruderman and C. Kittel, Phys. Rev. **96**, 99 (1954).

[41] O. Sakai, Y. Shimizu, and T. Kasuya, Solid State Commun. **75**, 81 (1990).

[42] P. Coleman and A. M. Tsvelik, Phys. Rev. B **57**, 12757 (1998).

[43] P. Nozières and A. Blandin, J. Phys. (Paris) **41**, 193 (1980).

[44] P. Coleman and A. J. Schofield, Phys. Rev. Lett. **75**, 2184 (1995).

[45] A. W. W. Ludwig and I. Affleck, Phys. Rev. Lett. **67**, 3160 (1991).

[46] C. Nayak, *Lecture notes* (1998), unpublished.

[47] M. P. A. Fisher and L. I. Glazman, in *Mesoscopic Electron Transport*, edited by L. L. Sohn, L. P. Kouwenhoven, and G. Shön (Kluwer Academic Publishers, Dordrecht, 1997), vol. 345 of *NATO Science Series E*, p. 331.

[48] X.-G. Wen, Phys. Rev. B **42**, 6623 (1990).

[49] P. W. Anderson, *The Theory of Superconductivity in the High-T_c Cuprates* (Princeton University Press, Princeton, 1997).

[50] V. L. Ginzburg and L. D. Landau, Zh. Eksperim. Teor. Fiz. **20**, 1064 (1950).

[51] J. Bardeen, L. N. Cooper, and J. R. Schrieffer, Phys. Rev. **108**, 1175 (1957).

[52] L. P. Gor'kov, Zh. Eksperim. Teor. Fiz. **36**, 1918 (1959), [Sov. Phys. – JETP **9**, 1364 (1959)].

[53] L. P. Gor'kov and G. M. Eliashberg, Zh. Eksperim. Teor. Fiz. **54**, 612 (1968), [Sov. Phys. – JETP **27**, 328 (1968)].

[54] X.-G. Wen and A. Zee, Int. J. Mod. Phys. B **4**, 437 (1990).

[55] E. Pivovarov and C. Nayak, Phys. Rev. B **64**, 035107 (2001).

[56] V. L. Berezinskii, Pis'ma Zh. Eksp. Teor. Fiz. **20**, 628 (1974), [JETP Lett. **20**, 287 (1974)].

[57] A. Balatsky and E. Abrahams, Phys. Rev. B **45**, 13125 (1992).

[58] E. Abrahams, A. Balatsky, J. R. Schrieffer, and P. B. Allen, Phys. Rev. B **47**, 513 (1993).

[59] E. Abrahams, A. Balatsky, D. J. Scalapino, and J. R. Schrieffer, Phys. Rev. B **52**, 1271 (1995).

[60] P. Coleman, E. Miranda, and A. Tsvelik, Phys. Rev. Lett. **70**, 2960 (1993).

[61] D. Belitz and T. R. Kirkpatrick, Phys. Rev. B **60**, 3485 (1999), and references therein.

[62] P. Coleman, E. Miranda, and A. Tsvelik, Phys. Rev. B **49**, 8955 (1994).

[63] O. V. Dolgov and V. V. Losyakov, Phys. Lett. A **190**, 189 (1994).

[64] R. Heid, Z. Phys. B **99**, 15 (1995).

[65] O. Zachar, S. A. Kivelson, and V. J. Emery, Phys. Rev. Lett. **77**, 1342 (1996).

[66] P. Coleman, A. Georges, and A. Tsvelik, J. Phys.: Condens. Matter **79**, 345 (1997).

[67] S. Yip and A. J. Legget, unpublished.

[68] A. V. Balatsky and E. Abrahams, Phys. Rev. Lett. **74**, 1004 (1995).

[69] N. P. Ong, Physica C **235-240**, 221 (1994), and references therein.

[70] A. W. Tyler et al., Phys. Rev. B **58**, R10107 (1998).

[71] S. V. Kravchenko et al., Phys. Rev. B **51**, 7038 (1995).

[72] P. T. Coleridge et al., Phys. Rev. B **56**, R12764 (1997).

[73] S. J. Papadakis and M. Shayegan, Phys. Rev. B **57**, R15068 (1998).

[74] Y. Hanein et al., Nature (London) **400**, 735 (1999).

[75] M. Y. Simmons and A. R. Hamilton, Nature (London) **400**, 715 (1999).

[76] E. Pivovarov, CALT 68-2187, Caltech (1998), unpublished.

[77] E. Dagotto and T. M. Rice, Science **271**, 618 (1996).

[78] S.-C. Zhang, Science **275**, 1089 (1997).

[79] H. F. Fong et al., Phys. Rev. Lett. **75**, 316 (1995).

[80] D. Scalapino, S. C. Zhang, and W. Hanke, Phys. Rev. B **58**, 443 (1998).

[81] C. L. Henley, Phys. Rev. Lett. **61**, 11662 (2000).

[82] C. P. Burgess, J. M. Cline, R. MacKenzie, and R. Ray, Phys. Rev. B **57**, 8549 (1998).

[83] S. Rabello, H. Kohno, E. Demler, and S. C. Zhang, Phys. Rev. Lett. **80**, 3586 (1998).

[84] E. Arrigoni and W. Hanke, Phys. Rev. Lett. **82**, 2115 (1999).

[85] R. Eder et al., Phys. Rev. B **59**, 561 (1999).

[86] S. Meixner, W. Hanke, E. Demler, and S.-C. Zhang, Phys. Rev. Lett. **79**, 4902 (1997).

[87] S.-C. Zhang et al., Phys. Rev. B **60**, 13070 (1999).

[88] M. G. Zacher et al., Phys. Rev. Lett. **85**, 824 (2000).

[89] I. Affleck, Phys. Rev. Lett. **54**, 966 (1985).

[90] J. B. Marston and I. Affleck, Phys. Rev. B **39**, 11538 (1989).

[91] Y. Q. Li, M. Ma, D. N. Shi, and F. C. Zhang, Phys. Rev. Lett. **81**, 3527 (1998).

[92] G.-M. Zhang and S.-Q. Shen, Phys. Rev. Lett. **87**, 157201 (2001).

[93] A. Mishra, M. Ma, and F.-C. Zhang, cond-mat/0202132.

[94] R. S. Markiewicz and M. T. Vaughn, cond-mat/9709137.

[95] R. S. Markiewicz, C. Kusko, and M. T. Vaughn, cond-mat/9807067.

[96] J. M. Tranquada et al., Nature (London) **375**, 561 (1995).

[97] W. F. Thirring, Ann. Phys. (NY) **3**, 91 (1958).

[98] S. Mandelstam, Phys. Rev. D **11**, 3026 (1975).

[99] C. N. Yang and S. C. Zhang, Mod. Phys. Lett. B **4**, 759 (1990).

[100] E. Fradkin, *Field theories of condensed matter systems* (Addison-Wesley, New York, 1994).

[101] S. Sachdev and R. N. Bhatt, Phys. Rev. B **41**, 9323 (1990).

[102] J. Orenstein et al., Phys. Rev. B **42**, 6342 (1990).

[103] A. Puchkov et al., J. Phys. Cond. Matt. **8**, 10049 (1996).

[104] H. Yasuoka, T. Imai, and T. Shimizu, in *Strong Correlations and Superconductivity*, edited by H. Fukuyama, S. Maekawa, and A. P. Malozemoff (Springer-Verlag, 1989).

[105] N. J. Curro et al., Phys. Rev. Lett. **85**, 642 (2000).

[106] J. Harris et al., Nature (London) **382**, 51 (1996).

[107] M. R. Norman et al., Nature (London) **392**, 157 (1998).

[108] M. Kugler et al., Phys. Rev. Lett. **86**, 4911 (2001).

[109] J. L. Tallon and J. W. Loram, Physica C **349**, 53 (2001).

[110] M. Randeria, in *Proceedings of the Tenth International School of Physics "Enrico Fermi," Varenna, 1997*, edited by G. Iadonisi and J. R. Schrieffer (IOS Press, Amsterdam, 1998).

[111] A. V. Chubukov and J. Schmalian, Phys. Rev. B **57**, R11085 (1998).

[112] X.-G. Wen and P. A. Lee, Phys. Rev. Lett. **76**, 503 (1996).

[113] S. Chakravarty, R. B. Laughlin, D. K. Morr, and C. Nayak, Phys. Rev. B **63**, 094503 (2001).

[114] C. M. Varma, Phys. Rev. Lett. **83**, 3538 (1999).

[115] S. Kivelson, E. Fradkin, and V. Emery, Nature (London) **393**, 550 (1998).

[116] A. G. Loeser et al., Science **273**, 325 (1996).

[117] H. Ding et al., Nature (London) **382**, 51 (1996).

[118] H. J. Schulz, Phys. Rev. B **39**, 2940 (1989).

[119] I. Affleck and J. B. Marston, Phys. Rev. B **37**, 3774 (1988).

[120] G. Kotliar, Phys. Rev. B **37**, 3664 (1988).

[121] D. A. Ivanov, P. A. Lee, and X.-G. Wen, Phys. Rev. Lett. **84**, 3958 (2000).

[122] C. Nayak, Phys. Rev. B **62**, 4880 (2000).

[123] N. Shah, P. Chandra, P. Coleman, and J. A. Mydosh, Phys. Rev. B **61**, 564 (2000).

[124] T. C. Hsu, J. B. Marston, and I. Affleck, Phys. Rev. Lett. **43**, 2866 (1991).

[125] H. A. Mook, P. Dai, and F. Dogan, Phys. Rev. B **64**, 012502 (2001).

[126] S. Chakravarty, H.-Y. Kee, and C. Nayak, Int. J. Mod. Phys. **15**, 2901 (2001).

[127] E. Dagotto, Rev. Mod. Phys. **66**, 763 (1994).

[128] A. Moreo, Phys. Rev. B **45**, 5059 (1992).

[129] S. Zhang, J. Carlson, and J. E. Gubernatis, Phys. Rev. B **55**, 7464 (1997).

[130] T. Tohyama et al., Phys. Rev. B **59**, R11649 (1999).

[131] S. R. White and D. J. Scalapino, Phys. Rev. Lett. **80**, 1272 (1998).

[132] S. Sorella et al., Phys. Rev. Lett. **88**, 117002 (2002).

[133] S. R. White and D. J. Scalapino, Phys. Rev. B **60**, R753 (1999).

[134] D. Poilblanc et al., Phys. Rev. B **62**, R14633 (2000).

[135] C. S. Hellberg and E. Manousakis, Phys. Rev. Lett. **83**, 132 (1999).

[136] S. A. Kivelson and V. J. Emery, Synthetic Metals **80**, 151 (1996), and references therein.

[137] J. Zaanen, Physica C **317-318**, 217 (1999), and references therein.

[138] E. Arrigoni et al., Phys. Rev. B **65**, 134503 (2002).

[139] J. M. Tranquada et al., Phys. Rev. B **54**, 7489 (1996).

[140] O. Navarro and C. Wang, Sol. State Commun. **83**, 473 (1992).

[141] J. Appel, M. Grodzicki, and F. Paulsen, Phys. Rev. B **47**, 2812 (1993).

[142] J. E. Hirsch, Physica C **58**, 326 (1989).

[143] C. Nayak and E. Pivovarov, cond-mat/0203580.

[144] J. M. Wheatley, T. C. Hsu, and P. W. Anderson, Phys. Rev. B **37**, 5897 (1988).

[145] F. F. Assaad, M. Imada, and D. Scalapino, Phys. Rev. B **56**, 15001 (1997).

[146] S. Chakravarty, A. Sudbø, P. W. Anderson, and S. Strong, Science **261**, 337 (1993).

[147] O. K. Andersen, A. I. Liechtenstein, O. Jepsen, and F. Paulsen, J. Phys. Chem. Solids **56**, 1573 (1995).

[148] A. Ino et al., Phys. Rev. Lett. **79**, 2101 (1997).

[149] S. Chakravarty, B. I. Halperin, and D. R. Nelson, Phys. Rev. B **39**, 2344 (1989).

[150] E. Cappelluti and R. Zeyher, Phys. Rev. B **59**, 6475 (1999).

[151] T. D. Stanescu and P. Phillips, Phys. Rev. B **64**, 220509/1 (2001).

[152] C. Nayak, Phys. Rev. B **62**, R6135 (2000).

[153] W. H. Press, S. A. Teukolsky, W. T. Vetterling, and B. P. Flannery, *Numerical Recipes in Fortran* (Cambridge University Press, Cambridge, 1992), 2nd ed.